THE ROLE OF HUMAN BLOOD-VESSEL-DERIVED STEM CELLS IN TISSUE REPAIR AND REGENERATION

by

Chien-Wen (William) Chen

B. S. in Biology, Chung-Shan Medical University, Taichung, Taiwan, 1999

M. D. in Medicine, Chung-Shan Medical University, Taichung, Taiwan, 2003

M. B. in Biotechnology, University of Pennsylvania, PA, USA, 2006

Submitted to the Graduate Faculty of

Swanson School of Engineering in partial fulfillment

of the requirements for the degree of

Doctor of Philosophy in Bioengineering

University of Pittsburgh

2012

UNIVERSITY OF PITTSBURGH

SWANSON SCHOOL OF ENGINEERING

This dissertation was presented

by

Chien-Wen (William) Chen

It was defended on

March 29, 2012

and approved by

William Wagner, Ph.D., Professor, Departments of Bioengineering and Surgery

Stephen Badylak, D.V.M., Ph.D., M.D., Professor, Department of Surgery

David Vorp, Ph.D., Professor, Departments of Bioengineering and Surgery

Kimimasa Tobita, M.D., Assistant Professor, Department of Developmental Biology

Dissertation Co-Director: Bruno Péault, Ph.D., Professor, University of Edinburgh, UK

Dissertation Director: Johnny Huard, Ph.D., Professor, Department of Orthopedic Surgery

THE ROLE OF HUMAN BLOOD-VESSEL-DERIVED STEM CELLS IN TISSUE REPAIR AND REGENERATION

Chien-Wen (William) Chen, M.B., M.D., Ph.D.

University of Pittsburgh, 2012

Multipotent stem/progenitor cells have been identified in nearly all vascularized organs in the human body. Our research group recently discovered that human blood vessels harbor various stem/progenitor cell populace of mesodermal lineage, exhibiting common multi-lineage differentiation capacity and yet distinct cell lineage markers. Specifically, each of the three structural layers of blood vessels: intima, media, and adventitia, have been found to respectively include one of the three populations of precursor cells: myogenic endothelial cells (MECs), pericytes, and adventitial cells (ACs). Our studies have independently characterized each of "Three Musketeers" and evaluated their myogenic capacity. Nevertheless, the therapeutic potential of pericytes in cardiac repair remains unknown, and whether pericytes natively residing in human heart possess similar stem cell characteristics and multipotency has not been investigated. Moreover, none of our prior studies has directly compared the regenerative efficacy between subpopulations of blood-vessel-derived stem cells (BVSCs), nor did we explore any alternative source, other than fresh tissue biopsies, to isolate BVSCs.

My dissertation study aims to understand the role of subpopulations of BVSCs, pericytes in particular, and their relative efficiency in tissue repair/regeneration, with emphases in myocardial infarction and skeletal muscle injury. Specifically, my work has three independent yet related focuses: (I) to investigate the therapeutic efficacy of human pericyte transplantation and associated mechanisms of action in ischemic heart repair; (II) to characterize native human heart pericytes and examine whether tissue specificity exists between pericytes of different tissue origins; (III) to directly compare the myogenic potential between subpopulations of BVSCs and explore alternative source(s) of BVSCs that are more clinically accessible for skeletal muscle repair.

The results of my studies showed that transplantation of human skeletal muscle-derived pericytes (SkMPs) repair the infarcted hearts more effectively than control and myoblast groups with their multiple restorative effects under hypoxia, including angiogenesis, anti-fibrosis, and anti-inflammation. Resident human heart pericytes (HPs) shared common similarity with pericytes of other tissues, such as typical pericyte and MSC marker expression, cell growth pattern in culture, and certain mesodermal developmental potential. Nevertheless, HPs differ from SkMPs in the lack of skeletal myogenic potential and differential angiogenic response under hypoxia, tissue-specific phenomena that were not observed previously. Additionally, in terms of skeletal myogenesis, MECs demonstrated superior efficiency to pericytes in vitro and in vivo. Finally, MECs and pericytes purified from long-term cryopreserved primary human muscle culture by cell sorting exhibited similar myogenic potential in vivo to their counterparts isolated from fresh biopsies, indicating cryopreservation of unpurified cells may serve as an alternative source of therapeutic myogenic precursors.

TABLE OF CONTENTS

LIST OF TABLES

LIST OF FIGURES

ACKNOWLEDGEMENTS

It has been a wonderful pleasure to work with a team of world-renown scientists in stem cells and regenerative medicine for my dissertation research in the past five and half years. I would like to specially thank my advisor, Dr. Huard, and co-advisor, Dr. Péault, for their strong support and the independence that I have been given in my research. I would also like to thank Dr. Tobita for his great advice and mentorship to the specific aim 1 (Chapter 3) of my dissertation work. My sincere appreciations are due to the current and past members of SCRC for their kind assistance to my dissertation research. Most importantly, I am in great debt to my family members for their remarkable and generous support.

1.0 HUMAN BLOOD-VESSEL-DERIVED STEM CELLS AND THEIR POTENTIAL FOR TISSUE REPAIR AND REGENERATION

1.1 INTRODUCTION

To date, multipotent adult stem/progenitor cells have been identified in nearly all human organs and extensively investigated [1-6]. For example, the human bone marrow (BM) functions as a diverse reservoir for several stem/progenitor cell populations, including hematopoietic stem cells (HSCs), multipotent mesenchymal stem/stromal cells (MSCs), and endothelial progenitor cells (EPCs) [7, 8]. The human skeletal muscle contains committed myogenic precursors, skeletal myoblasts, as well as primitive myogenic stem cells, satellite cells [1]. On the other hand, the human fat harbors adipose progenitor cells and adipose-derived stem cells (ADSCs) which are functionally and phenotypically resembling the BM-MSCs [9, 10].

However, many of these stem/progenitor cell populations have been identified retrospectively in *ex vivo* tissue and organ cultures, such as multipotent adult progenitor cells (MAPCs), mesoangioblasts, and MSCs [10-13]. This obscures the origin and the native identity of these stem/progenitor cells *in vivo*. In order to fully utilize the developmental potentials and therapeutic potencies of the adult stem/progenitor cells, it is deemed important to understand whether these different populations of adult stem/progenitor cells are developmentally and/or hierarchically connected. Due to the phenotypical and functional similarities of several of these

stem/progenitor cell populations, we hypothesized the existence of a common source in the human body. In this review, we will discuss this newly emerged concept: blood vessel-derived mesodermal stem/progenitor cells and their therapeutic applications in the futuristic personalized regenerative medicine.

1.2 STEM/PROGENITOR CELL-BASED THERAPY

The use of stem/progenitor cells for cell-based therapy is deemed promising owing to not only their high proliferative capacity and multi-lineage differentiation potential but also their functionality in secretion of trophic molecules and anti-environmental stress to promote cell survival. Specifically, adult stem/progenitor cells from an abundant autologous origin have the additional advantages over other stem cell types: high availability, no immunogenicity, low tumorigeneity, with no associated ethical issues [14]. To efficiently repair/regenerate defective organs, the donor stem/progenitor cells are expected to possess desirable therapeutic properties, for example, minimal side effects, ability to integrate into host tissue, differentiation into desired cell lineages, paracrine effect, immunomodulation, regulation of tissue remodeling, and activation of endogenous repair/regeneration mechanisms [15-18].

The therapeutic potentials of adult stem/progenitor cells have been extensively investigated in the pre-clinical and clinical studies. For instance, MSCs have been widely explored in a number of phase I/II and phase III clinical trials for several indications such as cardiovascular disease, stroke, multiple sclerosis/amyotrophic lateral sclerosis, Crohn's disease, and osteogenesis imperfecta [19-21]. Many other recent and ongoing human studies have chosen bone marrow mononuclear cells (BM-MNCs), skeletal myoblasts, EPCs, or ADSCs as their

donor cell populations [16, 22-24]. Unfortunately, in some cases, donor stem/progenitor cells initially demonstrated encouraging outcome but later on showed uneven success in clinical trials, especially in the treatment of cardiovascular disease [16, 23]. Nevertheless, BM-MSCs, ADSCs, and other MSC-like mesodermal stem/progenitor cells still hold great promise for tissue repair and regeneration because of their multipotency, autologous availability, immune tolerance and regulation as well as robust paracrine secretion of trophic effectors.

1.3 BLOOD VESSELS AS A SOURCE OF STEM/PROGENITOR CELLS

The evidence of the vascular wall as a source of stem/progenitor cells has been demonstrated in the emerging hematopoietic system in the early development of human embryo and fetus [25]. The hematopoietic cells emerge in close vicinity to vascular endothelial cells in both intra- and extra-embryonic hematopoiesis. Specifically, a population of angiohematopoietic stem cells expressing flk-1 and angiotensin-converting enzyme (ACE) migrates from the para-aortic splanchnopleura into the ventral part of the aorta, where they give rise to hemogenic endothelial cells and subsequently hematopoietic cells [25]. Furthermore, hematopoietic cells also appear to develop from endothelium in the embryonic liver and fetal bone marrow, albeit at a much lower frequency.

The similarity between many human mesodermal stem/progenitor cell populations that are retrospectively discovered in tissue/organ cultures has made us hypothesize that there exists a common, systemic source of stem/progenitor cells in the adult human body [26]. Blood vessels, which consist of three structural layers: tunica intima, tunica media, and tunica adventitia, distribute throughout nearly all human organs where adult mesodermal stem/progenitor cells can

be identified [27]. Apart from tunica intima, in which the sub-endothelial zone has been suggested as one of the sources of endothelial progenitor cells (EPCs), the possibility that other structural layers of the blood vessels harbor stem/progenitor cells was recently demonstrated in tunicae media and adventitia [26, 28, 29].

Perivascular cells, often known as vascular mural cells, are the cells that surround tunica intima of the blood vessels and constitute a major component of the vascular wall [27, 30]. Microvascular pericytes, though similar but distinct from vascular smooth muscle cells, closely encircle endothelial cells in capillaries and microvessels (arterioles and venules) in most human tissues [30-32]. Pericytes are commonly regarded as a structural element of blood vessels that regulate vascular contractility and support the stability of blood vessels [33-35]. Intimate interactions between pericytes and endothelial cells tightly relates to the vascular growth, maturation and remodeling [30, 34-36]. In addition, pericytes have been implicated in a number of pathological conditions, making them the potential targets for therapeutic interventions [36, 37].

Historically, the outmost layer of arteries and veins, the tunica adventitia, has been considered as a mere structural bystander constituted by collagen and fibroblasts. A number of recent findings have led to the re-evaluation of the active role of tunica adventitia in cell trafficking, immune response mediation, and vascular remodeling [38]. The importance of the tunica adventitia in regenerative vascular medicine is highlighted by the numerous reports describing the presence of multipotent progenitors within the wall of arteries and veins [29, 39-42]. In a vascular remodeling setting following an injury, it has been shown that adventitial cells (ACs) start a process of proliferation, migration into the tunicae media and intima, and differentiation into smooth muscle cells [41, 43, 44].

We have previously investigated whether the blood vessels contribute to stem/progenitor cell lineages other than hematopoietic cells. Through immunohistochemistry and flow cytometry analyses, we documented evidences showing the existence of rare subsets of human blood vessel derived stem cells (hBVSCs) in multiple human tissues, including skeletal muscle, fat, and placenta.

1.4 THE THREE MUSKETEERS OF BLOOD VESSEL WALLS: MYOGENIC ENDOTHELIAL CELLS, PERICYTES, AND ADVENTITIAL CELLS

We and other laboratories recently reported the existence of three distinct subpopulations of mesodermal precursors within the human blood vessel walls through anatomic and molecular identifications. At least one precursor subset, i.e. myogenic endothelial cells (MECs), pericytes, and adventitial cells (ACs) (Figure 1), was contained in each of the three tunicae of blood vessels: intima, media, and adventitia, respectively [26, 40, 45-47].

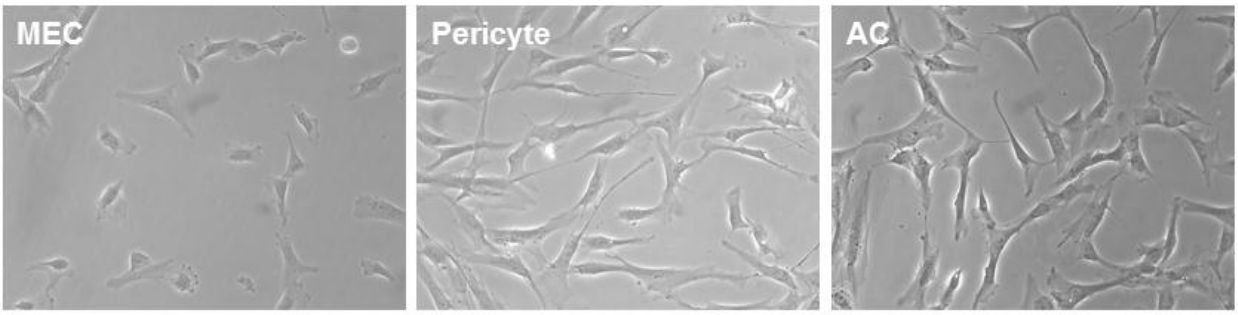

Figure 1: Morphology of hBVSCs

Distinct morphology of the three purified subpopulations of human blood vessel derived stem cells (hBVSCs) in culture. From left to right: myogenic endothelial cell (MEC), pericyte, and adventitial cell (AC) (100X).

Myogenic endothelial cells (MECs), which suggest a developmental relationship between endothelial and myogenic cells, have been identified within the vasculatures of human skeletal

muscle at a very low frequency (<0.5%) [45]. MECs uniquely co-expressed myogenic (CD56) and endothelial cell markers (CD34 and CD144) and were identified by immunohistochemistry and flow cytometry. Using fluorescent-activated cell sorting (FACS), we were able to purify these cells to homogeny [45]. MECs (CD56+CD34+CD144+CD45–) proliferate long term, retain a normal karyotype, survive better under oxidative stress than CD56+ myogenic cells, and are not tumorigenic [45]. Cultured MECs displayed mesenchymal developmental capacities, including myogenesis, osteogenesis, chondrogenesis, and adipogenesis, under appropriate inductive conditions *in vitro* [45]. Their stem cell characteristics were further confirmed by the expression of classic MSC markers and the mesodermal differentiations in culture from clonally derived MECs (Zheng et al., in revision). However, it is not clear yet whether MECs give rise to authentic MSCs in culture. Based on the phenotypic and functional similarities between MECs and the previously reported murine muscle derived stem cells (mMDSCs), we believe that MECs represent the human counterpart of mMDSCs (Zheng et al., in revision). In addition to MECs, which are primarily located in the intimal compartment of the blood vessels within human skeletal muscle, other distinct subsets of multipotent stem/progenitor cells were recently found in the perivascular compartment of the vasculature (tunicae media and adventitia), not only within the skeletal muscle but throughout the human body [26, 40, 46, 47].

Though microvascular pericytes have long been considered to possess mesenchymal plasticity, the lack of a proper purification method undermined the characterization of this potential precursor population [48-50]. Recently our group identified the native expression of classic MSC markers by microvascular pericytes and further discovered a collection of cell surface markers, i.e. CD146+CD34−CD45−CD56−, that enabled us to prospectively isolate homogenous pericyte populations by FACS from multiple human organs [26]. Purified pericytes

proliferate long term and express CD146, NG2, PDGFR-β, alkaline phosphatase (ALP), and α-smooth muscle actin (α-SMA), with the absence of endothelial cell markers, including von Willebrand factor (vWF), CD31, CD34, and CD144 [26, 46]. These cells can be efficiently expanded *in vitro* and demonstrate robust mesodermal developmental potentials, at the clonal level, by differentiating into osteogenic, chondrogenic, adipogenic, and myogenic lineages under suitable inductive conditions *in vitro* [26]. The MSC characteristics of these CD146+CD34−CD45−CD56− pericytes can be maintained for the long term in culture. Their myogenic and osteogenic capacities were further displayed by transplantation into the muscle pocket of immunodeficient mice. To date, no tumorigenicity of pericytes has been reported [26, 46]. We hypothesized that these cells are one of the developmental origins of MSCs [26].

In the past, fibroblasts that are capable of differentiating into myofibroblasts/smooth muscle cells (SMCs) following vascular injury have been regarded as the primary cellular component of the tunica adventitia [38, 51]. Recent studies have gradually uncovered the true identity of the cells residing in this outmost layer of the blood vessels [42]. Cells located at the interface between the tunica adventitia and media, the so-called "vasculogenic zone", have been identified as CD34+CD31- and described as progenitors endowed with the ability to differentiate into endothelial cells and participate in the blood vessel formation as well as the pathogenesis of atherosclerosis [29, 41, 51]. The concept that the tunica adventitia functions as a reservoir for stem/progenitor cells is highlighted by a recent study in which a population of CD34+CD31- progenitors residing in human saphenous vein was described [40]. These cells were localized in the tunica adventitia *in situ* and could be isolated and expanded at the clonal level *in vitro*. Our study also showed the stem cell characteristics of a CD34+CD31-CD146- non-pericyte perivascular cell population in the vasculature of human adipose and other tissues [47]. The

FACS-purified CD34+CD31-CD146- population exhibited the phenotype and developmental potentials of MSCs. Furthermore, immunohistochemistry revealed that CD34+CD31-CD146- cells reside in tunica adventitia of blood vessels in multiple human organs and similar to pericytes, natively express classic MSC surface markers.

1.4.1 Myogenic endothelial cells for skeletal muscle regeneration and cardiac repair

The therapeutic potential of myogenic endothelial cells (MECs) was first tested in the severe combined immunodeficiency (SCID) mouse model of cardiotoxin-injured skeletal muscle [45]. MECs (CD56+CD34+CD144+CD45–) isolated from fresh human muscle biopsies were shown to regenerate skeletal myofibers more effectively than skeletal myoblasts (SkMs, CD56+/CD34−/CD144−/CD45−), endothelial cells (ECs, CD34+/CD144+/CD56−/CD45−), and unpurified primary muscle cells, with or without *in vitro* expansion. Injection of MECs into skeletal muscle of mdx/SCID mice, a disease model of Duchenne muscular dystrophy (DMD), also displayed an efficient regeneration of human skeletal myofibers, indicated by positive staining of both dystrophin and human lamin A/C [45]. Furthermore, after expansion in culture, clonal MECs exhibited robust chondrogenesis and osteogenesis *in vivo* after implantation into the hind-limb muscle pocket of SCID mice (Zheng et al., submitted). These results suggest the feasibility of utilizing MECs to treat various musculoskeletal disorders.

The application of MECs in the cardiovascular disease was examined in an immune-deficient mouse model of acute myocardial infarction (AMI) [52]. Myocardial infarction was induced in SCID-non-obese diabetic (NOD/SCID) mice by ligation of left anterior descending coronary artery (LAD), and cells were immediately injected into the ischemic myocardium. Cardiac function was assessed by echocardiography. The results demonstrated a significant

improvement in cardiac contractility after intramyocardial injection of MECs when compared with injections of SkMs and ECs [52]. Transplanted MECs not only displayed robust engraftment within the infarcted myocardium but also stimulated angiogenesis, attenuated scar tissue formation, and promoted proliferation and survival of endogenous cardiomyocytes more effectively than the other two cell types [52]. This is presumably attributed to higher secretion of vascular endothelial growth factor (VEGF), a potent angiogenic factor, by MECs under hypoxia. Similar to mMDSCs, MECs regenerated significantly more fast-skeletal MHC-positive myofibers in the ischemic heart. A minor fraction of engrafted MECs differentiated into and/or fused with cardiomyocytes by expressing cardiomyocyte markers, cardiac troponin-T and –I [52]. These findings suggest that MECs represent a promising stem cell subset within human skeletal muscle, an accessible autologous tissue source, for cardiac repair and regeneration.

1.4.2 Pericytes for tissue repair and regeneration

The application of pericytes in regenerative medicine was first examined in SCID mouse models of injured and dystrophic skeletal muscle [26]. Microvascular pericytes freshly sorted by FACS from human skeletal muscle were injected into the hind-limb muscles of SCID-non-obese diabetic (NOD/SCID) mice that had been injured by intramuscular injection of cardiotoxin. The presence of regenerating human spectrin-positive myofibers was detected by immunohistochemistry and confirmed by fluorescence *in situ* hybridization of central human nuclei [26]. Quantification showed that freshly sorted or long-term cultured pericytes produced more human myofibers than purified SkMs and unpurified muscle cells, ruling out the possibility that the myogenic potential observed in pericytes resulted from a consequence of the contamination by myoblasts. Most importantly, this myogenic potential can be generalized to

pericytes residing in non-muscle tissues. Placenta-, white adipose tissue- and pancreas-derived pericytes also exhibited high myogenic potential in culture and *in vivo*, yielding human dystrophin- or spectrin-positive myofibers upon transplanted into mdx/SCID or cardiotoxin-treated NOD/SCID mouse muscles [26]. Dellavalle et al. also showed that pericytes sorted from healthy and dystrophic human skeletal muscles by ALP expression regenerate human myofibers in muscles of dystrophic immunodeficient mice [46]. Very recently, the same group demonstrated that pericytes residing in the postnatal skeletal muscle natively participate in the skeletal myofiber development and the satellite cell compartment and further contribute to the regeneration of injured/dystrophic skeletal muscle, using a transgenic label of inducible Alkaline Phosphatase CreERT2 [53]. These results indicate that pericytes play a role in muscle ontogeny and are endowed with robust myogenic potential that can be applied to skeletal muscle repair and regeneration.

With their inherent functions in the vascular physiology, pericytes seem to match the criteria of the ideal donor cell population for cardiovascular repair. Moreover, a human pericyte-based small-diameter vascular graft has been successfully engineered with high patency after long-term transplantation [54]. I investigated the hypothesis that transplantation of cultured pericytes benefits the ischemic heart, which is documented in detail in chapter 3 of this dissertation [55]. Briefly, long-term cultured human muscle pericytes were injected into acutely infarcted hearts of NOD/SCID mice. Echocardiography revealed a significant improvement of cardiac function in pericyte-injected hearts. Pericytes exhibited cardio-protective effects such as promotion of angiogenesis, reduction of scar formation, and inhibition of chronic inflammation (Chen et al. submitted). These data suggest that pericytes serve as a promising donor cell source for stem cell-based cardiovascular therapy.

1.4.3 Adventitial cells exhibit multi-lineage potential for blood vessel and tissue regeneration

The potential application of adventitial cells (ACs) in the clinical settings has thus far been focused on the cardiovascular repair and regeneration. Campagnolo et al. recently demonstrated that CD34+CD31- ACs interact with endothelial cells and promote the formation and stabilization of the capillary-like structures [40]. Most importantly, injection of adventitial in a hind-limb ischemia mouse model cells showed a significant pro-angiogenic effect as demonstrated by a full blood flow recovery as early as 7 days post-injection, indicating the therapeutic potential of ACs in angiogenesis/vasculogenesis [40]. Very recently, Katare et al. further reported that transplantation of ACs improves the repair of infarcted hearts through angiogenesis involving microRNA-132 [56]. Together these data indicate the therapeutic potential of ACs in ischemic tissue repair. Interestingly, the use of ACs derived from the umbilical artery, in conjunction with SMCs of the same source, in tissue-engineered small-caliber vessel constructs resulted in superior mechanical properties than the same constructs using cells derived from the umbilical vein, suggesting that ACs and SMCs originating from different sources may lead to distinct tissue characteristics in regenerative medicine [57].

The application of ACs is not limited to post-natal angiogenesis/vasculogenesis or cardiovascular repair. Though the myogenic potential of ACs remains to be determined, we and other authors have demonstrated that adventitial cells, regardless of their tissue of origin, display features typical of MSCs [40, 42, 47]. The ability of ACs to differentiate into major mesodermal cell lineages, including osteogenesis and chondrogenesis, suggests a likely contribution of these cells to the formation/regeneration of surrounding mesenchymal tissues after injury and further expands the potential clinical applications of this unique hBVSC subset into the field of

musculoskeletal diseases [47]. Altogether, these reports suggest that rather than a passive constituent of the vascular wall, the adventitia is a dynamic reservoir of stem/progenitor cells that participate in vascular remodeling and regeneration of surrounding tissues.

1.5 ONTOGENY AND HETEROGENEITY, INNATE FACTORS AFFECTING THE THERAPEUTIC POTENCY OF STEM/PROGENITOR CELLS?

MSCs represent a highly heterogeneous population of widely studied but poorly defined multipotent stem/progenitor cells [58]. Indeed, Guilak et al. have shown that only 52% of the clones obtained from cultured ADSCs retain the ability to differentiate into two or more mesodermal cell lineages [59]. The presence of subsets of cells with limited or no differentiation potential within the conventional stromal cultures may therefore hamper the clinical efficacy of these promising stem/progenitor cells. This raised the possibility that clinical trials based on the transplantations of the total SVF or unfractionated MNCs often showed uneven success because of the variable frequency of progenitors within the total stroma [16, 23]. Additionally, mesenchymal progenitors have mostly been selected by their plastic adherence and expanded long-term in culture with reagents originated from animals, which ultimately limits their clinical use due to FDA regulations.

The identification of pericytes as, at least in part, the ancestors of MSCs has represented a breakthrough in the search for the true identity of MSCs [26]. Though this has raised the possibility that most MSCs, if not all, are derived from pericytes, other subsets of stem/progenitor cells residing in the blood vessel walls may constitute part of the MSC entity as described above [60]. The question of whether all MSCs originate from microvascular pericytes

is partially answered by Tormin et al., who reported that, in bone marrow, MSCs can be derived not only from the subendothelial sinusoidal CD146+ cells, as previously demonstrated by Sacchetti et al., but also from the bone-lining CD146- cells [61, 62]. Furthermore, using the genetic lineage tracing, Feng et al. recently reported MSCs from both pericyte and non-pericyte origins differentiate into odontoblasts and participate in tooth growth and repair in mice, suggesting that the pericyte contribution to MSCs may vary in different tissues and possibly depend on the density of the local vascularity [63].

Another good example that different subsets of stem/progenitor cells contributing to the MSC entity is from the observation of the concurrent presence of two distinct subpopulations of perivascular multipotent progenitor cells, namely CD34-CD31-CD146+ microvascular pericytes and CD34+CD31-CD146- adventitial cells, in the adipose tissue [39, 47]. These two subpopulations of hBVSCs share *in situ* and *in vitro* expression of typical MSC surface markers, CD44, CD73, CD90 and CD105, but they are phenotypically and anatomically distinct [39, 47]. Pericytes are indeed defined as CD45-CD34-CD31-CD146+ cells tightly surrounding microvessels, whereas CD45-CD34+CD31-CD146- adventitial cells are located in the outmost layer of larger blood vessels in the human adipose, a literally unlimited tissue source. Both subpopulations of cells are endowed with multi-lineage mesenchymal differentiation capacity at the clonal level and represent ideal candidates for the treatment of musculoskeletal and vascular diseases [39, 40, 64]. Above all, both subpopulations are abundant in lipoaspirate; and with the definitive phenotypes of each hBVSC fraction, we can readily enrich both fractions by cell sorting in order to improve their therapeutic efficiency and safety [47]. Table 1 summarizes the basic characteristics and potential clinical applications of hBVSC subpopulations and BM-MSCs.

Table 1: Comparison of hBVSC subpopulations and bone marrow MSCs

	MEC	Pericyte	AC	BM-MSC
Native location	Intima	Media	Adventitia	Bone marrow
Surface marker profile for cell sorting	CD34+ CD45- CD56+ CD144+	CD34- CD45- CD56- CD146+	CD31- CD34+ CD45- CD146-	N/A
Classic MSC marker expression in culture	CD29+ CD44+ CD90+ CD105+	CD44+ CD73+ CD90+ CD105+	CD44+ CD73+ CD90+ CD105+	CD29+ CD44+ CD73+ CD90+ CD105+
Differentiation *in vitro*	Osteogenic (+) Chondrogenic (+) Adipogenic (ND) Myogenic (+)	Osteogenic (+) Chondrogenic(+) Adipogenic (+) Myogenic (+)	Osteogenic (+) Chondrogenic (+) Adipogenic (+) Myogenic (ND)	Osteogenic (+) Chondrogenic (+) Adipogenic (+) Myogenic (+)
Differentiation *in vivo*	Myogenesis	Myogenesis Osteogenesis	Vasculogenesis	Osteogenesis Chondrogenesis Adipogenesis Myogenesis Cardiomyogenesis Vasculogenesis
Potential Clinical Application	Skeletal muscle repair/regeneration; Cardiac repair	Skeletal muscle repair/regeneration; Vascular repair /regeneration	Vascular repair /regeneration; Cardiac repair	Bone repair; Cartilage repair; Tendon/ligament repair; Skeletal muscle repair; Vascular repair; Cardiac repair; Wound healing; Immunoregulation

MEC: myogenic endothelial cell; AC: adventitial cell; BM-MSC: bone marrow mesenchymal stem/stromal cells; N/A: not available; ND: not determined.

Nevertheless, while all, or at least part of, the three hBVSC subpopulations contributing to the MSC entity in culture is gradually becoming an accepted notion, whether the multi-lineage

potentials are natively present within hBVSC subsets and subsequently responsive to pathological stimulations *in vivo* remain to be investigated (Figure 2). Ultimately, the current therapeutic strategy based on the transplantation of unfractionated stromal cells may in the near future be replaced by the purification, combination, and direct re-infusion of the distinct subsets of hBVSCs, devoid of cells with none or a restricted regenerative potential.

1.6 CONCLUSION

In this chapter, I introduced the newly emerged concept of blood vessels as a systemic source of adult stem/progenitor cells. Three subpopulations of hBVSCs, i.e. MECs, pericytes, and ACs, have been respectively isolated from different layers of the blood vessels and examined in detail for their developmental capacities and therapeutic potentials in tissue repair and regeneration. Besides the fresh tissue biopsy, the cryogenically banked primary human skeletal muscle culture was shown to be an alternative source of myogenic subsets of hBVSCs, shedding new lights on the future of the personalized regenerative medicine. Finally, the identification of the precise phenotypes of distinct hBVSC subpopulations represents not only an important milestone for understanding the nature and origin of MSCs but also a crucial step toward the improvement of stem/progenitor cell based therapies.

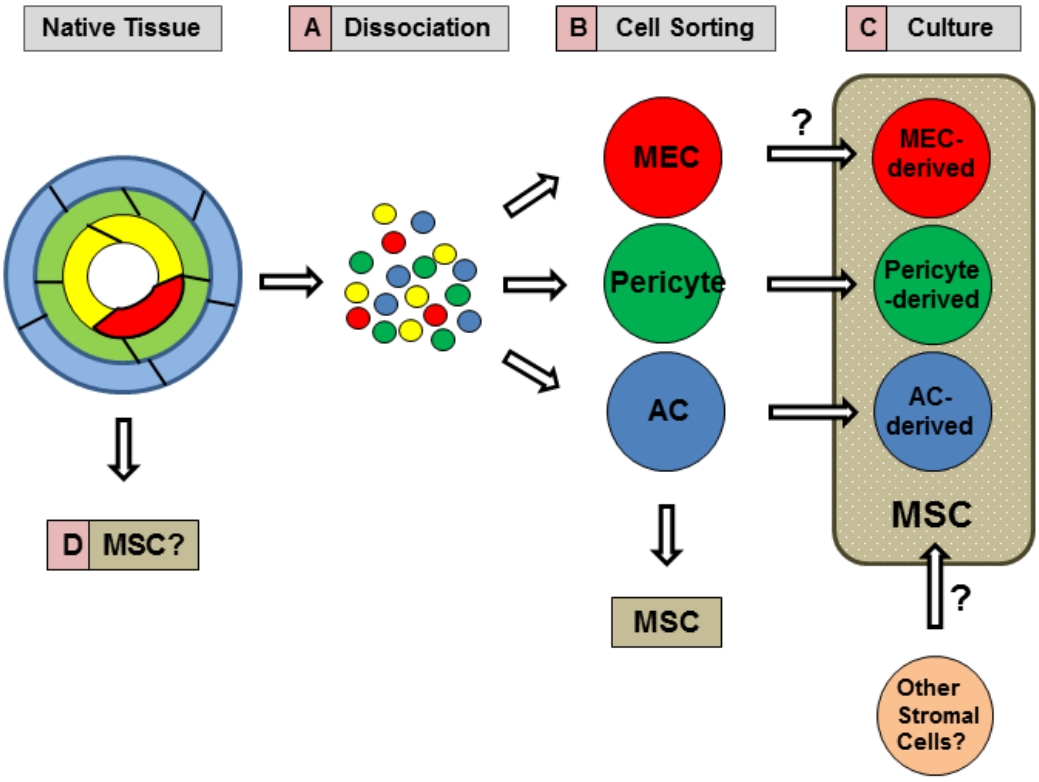

Figure 2: Schematic depiction of hBVSCs at the origin of mesenchymal stem/stromal cells (MSCs)

(A) hBVSCs, including myogenic endothelial cells (MECs, red), pericytes (green) and adventitial cells (AC, blue), are dissociated from fresh muscle biopsy and separated from endothelial cells (yellow) and other cell types. (B) Dissociated cells are purified to homogeneity by fluorescence-activated cell sorting (FACS), and newly sorted MECs, pericytes, and ACs already exhibit multi-lineage developmental potentials. (C) FACS-purified pericytes, ACs, and possibly MECs give rise to authentic MSCs in long-term culture. (D) Nevertheless, whether native hBVSCs serve as a source of MSCs *in situ* and participate in tissue repair and regeneration remains an open question.

2.0 MESODERMAL PRECURSOR CELLS FOR CARDIOVASCULAR REPAIR AND ASSOCIATED MECHANISMS

2.1 INTRODUCTION

In spite of recent advances in surgical and therapeutic interventions, cardiovascular diseases (CVD) remain the leading cause of death in the United States to date, accounting for 1 of every 2.9 deaths [65]. Coronary heart disease (CHD), affecting nearly 18 million American people, is caused by conditions that interfere with the coronary blood supply to the myocardium, such as atherosclerosis and thromboemboli [66]. Prolonged ischemia results in ischemic cardiomyopathy and myocardial infarction (MI), which in turn lead to heart failure (HF) or death due to a very limited capacity of the adult human heart to repair/regenerate its irreversibly damaged cardiac muscle [66]. Conventional therapeutic gold standards for patients who require treatments beyond interventional therapies include coronary artery bypass grafts (CABG) and heart transplantation, both limited by morbidity and availability. Stroke, peripheral artery disease (PAD), and other cardiovascular pathological conditions also claim millions of victims each year with high morbidity and mortality. The total cost of CVD and stroke in the United States alone reaches $500 billion annually, making it one of the most poignant clinical problems in modern medicine [65].

2.2 CARDIOVASCULAR REGENERATIVE MEDICINE

In the past decade, regenerative medicine has emerged as a futuristic option for treating CVD [67-69]. Among which, stem cell therapy is deemed promising due to the multiple advantages of stem/progenitor cells, such as differentiation capacity, high proliferation, self-renewal, resistance to stress, and trophic effect [70-72]. The recent discoveries of multipotent stem/progenitor cells residing in the adult human blood vessel walls further fuel the promise of this new approach in cardiovascular applications [1, 25, 26, 47]. Current stem cell-based therapies for CVD primarily involve the transplantation of exogenous stem/progenitor cells into the diseased/damaged organs [70]. Ideally, donor cell populations need to possess desirable properties for transplantation, for example, high availability and easy accessibility with minimal morbidity, high expansibility *in vitro* with no tumorigeneity, high efficiency to restore impaired organ structure and function, autologous origin to eliminate immunogenicity, ability to integrate into recipient tissue, minimal side effects, and no ethical controversy [15, 22, 73-76]. Consequently, autologous multipotent stem cells best match the definition of ideal donor cells and are of particular interest over other cell types. In the context of MI, a typical human infarct involves an irreversible loss of 1–1.5 billion cardiomyocytes (CMs) with a subsequent loss in myocardial cell mass [70]. Therefore, stem/progenitor cells that contribute to sustain the number of viable and functional CMs hold considerable clinical significance. Furthermore, given the vascular pathological nature of CHD, autologous stem cells that are capable of repairing host vascular networks and/or regenerating new blood vessels, in addition to other merits, would be ideal candidates [17].

Several types of adult stem/progenitor cells from multiple organs have been investigated not only in the laboratories and but also in the clinical trials. The bone marrow (BM) functions as

a reservoir for stem/progenitor cells, housing endothelial progenitor cells (EPCs) and hematopoietic stem cells (HSCs), other than BM mesenchymal stem/stromal cells (BM-MSCs). Adipose tissue throughout the body contains adipose-derived stem cells (ADSCs) that are phenotypically and functionally resembling BM-MSCs [77]. Skeletal muscle harbor committed myogenic precursors, skeletal myoblasts, as well as primitive stem/progenitor cells like satellite cells and muscle-derived stem cells (MDSCs) [1]. Most of these stem/progenitor cells have been demonstrated to be beneficial for treating CVD in the pre-clinical animal models. For example, HSCs were shown to occupy up to 68% of the infarcted region and integrate with the damaged host myocardium by forming connexin-43 gap junction in animal models [78]. EPCs have been successfully applied in cardiac repair for revascularization of the infarcted myocardium [79]. However, these precursor cells instead showed uneven success in early-phase human clinical trials [15, 16, 22, 23]. On the other hand, owing to their unique properties of high autologous availability, multi-lineage plasticity, efficient self-renewal, immune tolerance and regulation, paracrine effector release and trophic support, BM-MSCs and associated ADSCs as well as other MSC-like multipotent cells, including subpopulations of BVSCs described above, hold great promise for cardiovascular repair [72].

2.3 MULTI-LINEAGE MESODERMAL STEM/PROGENITOR CELLS FOR CARDIOVASCULAR REPAIR

Since the first discovery of mesenchymal stem/stromal cells (MSCs) in the stromal compartment of BM, MSCs or MSC-like multipotent stem/progenitor cells have been identified in many other tissues and organs that are available for therapeutic retrieval, such as fat, placenta, umbilical cord,

skin…etc. In brief, MSCs are initially defined as a BM stromal population of $CD45^{-}/CD34^{-}/CD133^{-}$ cells and selected by their adhesiveness to the surface of cell culture dishes [80]. MSCs have been shown to differentiate/transdifferentiate into various cell lineages, including osteoblasts, chondrocytes, adipocytes, skeletal and cardiac myocytes, smooth muscle cells (SMCs), tendon-ligament fibroblasts, marrow stromal cells, and other mesenchymal phenotypes [80]. MSCs have apparent immunoprivilege due to their low express level of MHC class II molecules, compared with MHC I, and B7 co-stimulatory molecules for MHC class I. MSCs also display local immunosuppressive properties, allowing successful transplantation into an allogenic setting and long-term engraftment [80]. Besides all these advantages, their easy isolation and fast expansion in culture make MSCs a highly desirable candidate for stem cell-based cardiac therapy (SCCT).

The use of MSCs for cardiovascular repair utterly matches the underlying objectives behind the cardiac regenerative therapy, which subsumes promoting angiogenesis and vascular perfusion in the ischemic myocardium, ameliorating cellular apoptosis and enhancing myocardial protection, reducing cardiac fibrosis and ventricular remodeling, and finally, regenerating the damaged myocardial structures by repopulating lost resident cells (e.g. endothelial cells, SMCs, cardiomyocytes, and stromal cells). Several studies have shown that injections of MSCs into the infarcted myocardium improve cardiac function. Animal studies showed that engrafted MSCs expressed cardiomyocyte markers after 4 weeks, aligned with host cardiomyocytes, and formed intercalated discs [81]. Overall, these preclinical studies have provided evidence for a beneficial effect of the MSC transplantation on the recovery of cardiac functions.

2.4 MECHANISMS OF MSC-MEDIATED CARDIOVASCULAR REPAIR

Following the ischemic insult, cardiomyocytes and the entire cardiac tissue within the affected area undergo apoptosis or necrosis if the blood supply is not quickly restored, leading to the chronic sequelae of cardiomyopathy and eventually congestive heart failure (CHF) [66]. The limited endogenous regenerative capacity of the adult human heart is unable to replenish such a substantial loss of myocardial tissue after incidents like AMI. As depicted previously, MSC-based cell therapies have been shown to significantly improve cardiac function and drastically attenuate post-infarction ventricular remodeling. The functional benefit observed after MSC transplantation has been attributed to a number of mechanisms: differentiation of MSCs into new cellular components; paracrine release of cardiogenic, cardioprotective and tissue remodeling agents from MSCs; stimulation of endogenous regeneration via circulatory or resident host cells; mechanical buttressing/passive girdling effect from locally increased myocardial thickness [15, 22, 74, 76]. Any one or a combination of these repair mechanisms directly or indirectly contribute to the overall functional recovery. Some of the established repair mechanisms are briefly discussed in this section.

2.4.1 Cardiomyogenesis

MSCs have been shown to differentiate into cardiac cells, though to a limited extent, under inductive conditions in culture and after transplantation *in vivo* [81]. This cardiomyogenic capacity sustains the high hope among investigators that engrafted MSCs regenerate lost cardiac tissue by differentiating into cardiomyocytes and integrating with the native myocardium in the damaged heart, resulting in a significant contribution to the functional restoration. However,

reports from Deb, Hocht-Zeisberg and Nygren demonstrated only a small fraction of bone marrow stem cells differentiated into cardiomyocytes in the infarcted hearts [79]. The number of newly regenerated cardiomyocytes is too low to fully explain the significant functional improvement. Additionally, it remains a daunting challenge to stably reproduce a functional cardiac phenotype in MSCs *in vitro* using physiological and nontoxic reagents. Cell fusion between donor cells with recipient cardiomyocytes, thereby preventing apoptosis and improving cellular performance, has been suggested to be another contributory factor, but its frequency is also debated [82]. In conclusion, regardless of whether cardiomyocyte trans-differentiation of MSCs is fusion-independent or not, the observed restoration of cardiac function can only be partially attributed to the cardiomyogenesis by MSCs.

2.4.2 Neovascularization

Vasculogenesis and neoangiogenesis in the recipient organ can result from trans-differentiation of implanted MSCs into endothelial cells (ECs) and vascular smooth muscle cells (VSMCs). Participation of MSCs in the formation of new blood vessels *ex vivo* and *in vivo* as VSMCs or perivascular cells has been displayed. Previous work revealed that bone marrow stem cells that integrated into the heart tissue participated more in angiogenesis than myogenesis [79]. Similar results were reported in a number of human clinical trials. Nevertheless, the same argument regarding the low number of donor cells trans-differentiating into vascular cells to entirely explain the increased vascularization stands. Our studies also showed that transplantation of MSC ancestors or other mesodermal lineage stem/progenitor cells significantly promote angiogenesis and consequently enhance myocardial perfusion in animal models [52, 55, 83]. The importance of neoangiogenesis in mesodermal stem cell-mediated cardiac repair was further

demonstrated by a linear relationship between angiogenic factors, angiogenesis and cardiac functional repair [84].

2.4.3 Paracrine effects

MSCs stimulate/mobilize/protect host cardiac cells by releasing an array of cardiogenic and cardioprotective molecules. It has been suggested that the favorable effects of MSC transplantation are primarily attributed to the paracrine effects of stem cells [85]. MSCs have the capacity to secrete angiogenic growth factors such as vascular endothelial growth factor (VEGF), basic fibroblast growth factor (bFGF), and platelet-derived growth factor (PDGF) as well as cell survival growth factors such as insulin-like growth factor-1 (IGF-1) and hepatocyte growth factor (HGF) [79]. MSCs also release multi-functional cytokines like interleukin (IL)-1, -6, -11 and molecules like transforming growth factor (TGF-β) and angiopoietins, which are related to vascular cell interactions and support vascular growth, stability, and remodeling [30]. MSCs are known to express matrix metalloproteinase (MMP)-1, -2, -9 and tissue inhibitor of metalloproteinase (TIMP)-1, -3 in addition to other proteinases/proteinase inhibitors. These trophic factors and cytokines secreted by transplanted MSCs may play multiple roles influencing neovascularization, myocardial protection, post-injury inflammation, cardiac remodeling, and/or host endogenous regeneration, ultimately leading to the improvement of cardiac function [70]. Moreover, many of these beneficial molecules were significantly upregulated in MSCs under hypoxia, suggesting the possibility that MSCs not only possess advantages for ischemic tissue repair but can be enhanced by hypoxic preconditioning [86].

2.5 CLINICAL APPLICATION OF MSC-BASED CARDIOVASCULAR THERAPY

The therapeutic application of MSCs and MSC-like precursor cells in the clinical setting is currently being explored in a number of phase I/II and phase III clinical trials for several indications, for instances, CVD, renal pathologies, multiple sclerosis/amyotrophic lateral sclerosis, Crohn's disease, and osteogenesis imperfecta [19, 20]. Due to their remarkable immunoregulatory capacities, the use of MSCs to reduce graft-versus-host disease (GvHD) and facilitate hematopoietic stem cell (HSC) engraftment has particularly been investigated in several studies. An early study (69 patients) reported that at 3 months follow-up, intracoronary injection of BM-MSCs significantly improved overall left ventricular function in MSC-treated patient who underwent primary percutaneous coronary interventions within 12 hours after the onset of AMI [87]. Perfusion defects, detected by positron emission tomography (PET), were significantly ameliorated after MSC treatment while electrocardiographic monitoring revealed lack of any occurrences of arrhythmia in the MSC-administered subjects [87]. In a recent double-blind study (53 patients), intravenous administration of allogeneic hMSCs (Prochymal, Osiris Therapeutics, Inc.) in reperfused MI patients, when compared to placebo, significantly reduced ventricular tachycardia episodes, increased forced expiratory volume in 1 second (FEV1), and improved global condition of patients at 6 months post-treatment [88]. hMSC-treated subjects had significantly better left ventricular ejection fraction (LVEF), measured by cardiac magnetic resonance imaging (MRI), in through the 12-month follow-up and exhibited evidence of reverse remodeling while the adverse event rates and laboratory indexes (renal, hepatic, and hematologic) remained no different between hMSC-treated and placebo groups [88]. An observer-blinded study (85 patients) utilizing intravenous transplantation of autologous *ex vivo* cultured BM-MSCs in patients with ischemic stroke reported improved functional outcomes, measured by

modified Rankin Scale (mRS), in a 5-year follow-up without significant side effects or higher co-morbidities like seizure [89]. A correlation between the serum level of stromal cell-derived factor-1α (SDF-1α) at the time of MSC-treatment and clinical improvement was observed within the MSC group, implicating the importance of chemokines in MSC recruitment and a potential biomarker for candidate patient selection [70, 89]. Novel MSC-based cell therapies for indications like insulin-dependent diabetes mellitus (IDDM), acute lung injury (ALI), and other diseases which broadly relate to CVD are also under intense investigation [90, 91]. Thus far most phase I/II trials reported that MSC administration is safe with absence of major adverse effects or associated toxicity, suggesting the feasibility to further pursue clinical translation of MSC-based cardiovascular therapies [19].

2.6 ENHANCEMENT OF MSC-BASED CARDIOVASCULAR CELL THERAPY

Despite the promising results of interventions with stem cells in animal disease models, until now, clinical studies have in general not been able to live up to the same expectations. Typical problems limiting the efficacy of MSC cell therapy in the cardiovascular milieu include: 1) poor viability of the transplanted grafts due to the hostile microenvironment; 2) low rate of engraftment and/or homing of donor cells; 3) lack of evidence on MSC behavior and differentiation in the recipient heart; 4) limited knowledge on the timing and modality of administration. Indeed, in most studies, only 1-5% of delivered cells successfully engrafted within the ischemic area for the long term. Hence there is an urgent need to overcome these limitations and enhance the therapeutic efficacy of MSCs. Several new strategies of *ex vivo* manipulation of MSCs have been applied successfully in the laboratories and in animal models

such as preconditioning of MSCs before transplantation to maximize cell survival, priming of MSCs to increase cell functionality and differentiation, and better delivery modality to minimize tissue damage [70]. A few of the most striking progresses will be reviewed in this section.

2.6.1 Improving MSC survival and engraftment

There are many causes of donor cell death in the ischemic myocardium. It may start with anoikis, the programmed cell death induced by loss of extracellular matrix (ECM) attachments, leading to cellular apoptosis [80]. Once MSCs are transplanted into the infarcted area, cells immediately encounter the harsh conditions (e.g. deprivation of nutrients and oxygen), deficiency of survival factors, and inflammation) coupled with excessive oxidative stress and apoptotic signals, all of which shorten the longevity of donor MSCs. Myocardial injury generates an inflammatory response mediated by neutrophils and macrophages, which produce inflammatory cytokines and reactive oxygen species (ROS) that may initiate apoptotic signaling pathways or lead to death of grafted cells [80]. The hostile recipient microenvironment further impedes physiological function and differentiation capacity of donor cells, resulting in low rate of homing, engraftment and regeneration.

In order to minimize the massive cell death after transplantation, measures were taken to promote engraftment and survival of donor cells via *ex vivo* preconditioning before transplantation [92]. These approaches include exposure of MSCs to physical treatments (i.e. hypoxia and heat shock) to stimulate cellular production of growth factors and internal survival signals, and treatment of pharmacological agents like anti-oxidants to enhance the capacity of cells against oxidative stress. Results from several studies demonstrated the effectiveness of *ex*

vivo preconditioning in increasing the engrafted cell number [80]. Drowley et al. reported that treating MDSCs with N-acetylcysteine (NAC) to increase cellular anti-oxidant level significantly enhance cell survival under inflammatory and oxidative stresses in culture and further improve post-infarction cardiac function after transplantation [71]. Erythropoietin, a hematopoietic cytokine, was shown to mobilize and stimulate the recruitment and survival of bone marrow–derived progenitor cells to the heart. Priming of MSCs with growth factors and genetic modification by over-expression of anti-apoptotic or pro-survival genes aim to achieve similar. MSCs that were genetically modified to overexpress Akt, SDF-1, or IGF-1 before transplantation are shown to survive and function better. These preconditioned or modified MSCs have yielded promising results and been proclaimed to stimulate the survival and cardioprotective pathways in the infarcted myocardium. However, to develop the ultimate strategy with maximal enhancement of engraftment, survival and function of MSCs in the ischemic heart may require a combination of approaches and remains a challenge for years to come.

2.6.2 Augmenting MSC cellular function

BM-derived cells isolated from patients with CHD risk factors exhibited a reduced capacity to promote neovascularization after ischemia [93], and several studies aimed to rescue the defective cellular properties. HMG-CoA reductase inhibitors, statins, were shown to increase the number of EPCs and enhance their migratory and survival capacity [92, 94]. Preconditioning of EPCs with statins increased their neovascularization-promoting effect. Mechanisms by which statins affect the functions of cells are not yet entirely clear but may involve the activation of PI3 kinase and Akt and subsequent activation of the endothelial nitric oxide (NO) synthase. Aging and cellular senescence also contribute to stem/progenitor cell dysfunction, causing decreased

restorative and regenerative capacities [95]. New evidence suggests that age-dependent functional impairment of stem/progenitor cells can be corrected by growth factors like IGF-1. Moreover, statins have been shown to partially antagonize progenitor cell senescence via activation of the PI3 kinase/Akt pathway. Therefore modulation of IGF-1 and/or Akt signaling system may be useful in regenerative therapies using MSCs isolated from elder or high risk patients.

2.6.3 Promoting cardiac regenerative capacity

Albeit recent studies provide convincing evidence that new cardiomyocytes can be generated in the human heart throughout the adult life [96], under severe pathological conditions in which larger numbers of cardiomyocytes are lost and/or malfunctioning, the endogenous regenerative system is insufficient to compensate the functional deficiency [94]. Due to their highly active paracrine capacity in the injured heart, transplantation of MSCs not only exert cardioprotective and neoangiogenic functions but may stimulate or reactivate the endogenous regeneration, e.g. by paracrine stimulation of resident cardiac stem cells or cardiomyocyte progenitor proliferation. Treatment of target tissue with FGF-2, IGF-1, or a combination of FGF-2, IGF-1 and bone morphogenetic protein-2 (BMP-2) were shown to improve cardiac function in animal models [92], all of which were part of the secretory portfolio of MSCs. These growth factors exhibit a wide range of influences (e.g. anti-apoptotic activity, pro-angiogenic effects…etc.) and may contribute to cardiac differentiation of stem cells. On the other hand, mixed results were reported regarding the engraftment and cardiac differentiation of various exogenous stem/progenitor cells in the injured heart [92, 94]. Though the number of implanted donor cells forming cardiomyocytes may not reach a functionally meaningful level, researchers continue pursuing

measures to drive adult stem/progenitor cells to acquire a cardiac fate. Wnt-11, required for cardiopoiesis in Xenopus, and other noncanonical members of the Wnt family such as Wnt-5a were reported to induce or enhance cardiac gene expression in adult progenitor cells and promote of cardiac differentiation. Over-expression of Wnt-11 increased the number of MDSCs or MSCs to differentiate toward cardiomyocytes in culture and *in vivo* [92, 97].

2.6.4 Changing cell delivery modality

Conventional delivery methods involve intramyocardial or intracoronary injections of MSCs into the ischemic myocardium, which often lead to substantial loss of cells and inadequate adhesion. Cell sheet technology, a new cell delivery modality based on the formation of sheet-like structures by culturing cells on a temperature-responsive poly(N-isopropylacrylamide) surface, has the advantage of maintaining cell-cell contact that promote cell survival and functionality [98]. Memon et al. found that myoblast cell sheets implanted with intact culture matrix onto the surface of infarcted rat hearts improved cardiac outcomes when compared with direct injection of myoblasts. This new approach not merely enhanced the survival of implanted cells but also diminished the arrhythmic events associated with the transplantation. Our recent study also suggested that MDSC cell sheets repair the infarcted hearts and reduce the arrhythmic events more efficiently than intramyocardial cell injections (Sekiya *et al.*, *in revision*). Additionally, successful engraftment of human embryonic stem cell (hESC)-derived cardiomyocytes was enhanced by co-delivery of stem cells with collagen matrices, including Gel Foam and Matrigel, a basement membrane preparation, indicating the importance of cell-ECM interaction [80].

2.6.5 Enhancing homing/recruiting signaling

Recruitment of stem/progenitor cells to the ischemic site requires activation and attraction by chemokines. Stromal derived factor-1 (SDF-1) and its receptor CXCR4 are well established to be essential for hematopoietic progenitor cell recruitment and angiogenesis [99]. The expression of CXCR4 receptor on EPCs and BMCs is stimulated by the up-regulation of SDF-1 during acute ischemia, thereby functioning as chemotactic and pro-migratory signals. Injection of cytokines to improve endogenous progenitor cell recruitment was demonstrated by local injections of SDF-1 in ischemic hind limbs which increased the recruitment of intravenously infused EPCs [92]. Activation/over-expression of the CXCR4 receptor may thus provide an option to enhance MSC recruitment. By increasing the extracellular calcium concentration, the transcription and surface expression of CXCR4 is stimulated, leading to enhanced recruitment of progenitor cells and augmented neovascularization. Reduction of SDF-1 cleavage by inhibition of CD26 dipeptidylpeptidase or mutation of the cleavage site showed increases in BM-derived progenitor cell recruitment and functional recovery after myocardial ischemia. MSCs that are genetically modified to over-express SDF-1 may further enhance both donor and host stem cell homing [92]. In addition, immune cells in the ischemic tissue release chemokines such as interleukins and monocyte chemoattractant protein-1 (MCP-1), which are involved in the homing of adult BM-MSCs to the ischemic hearts [100].

2.7 PERIVASCULAR ORIGIN OF MSCS

As development reaches the adult maturity, stem cells rarefy, and tissue growth and renewal become marginal, making it difficult to trace the anatomical locations of stem cells in the human body. MSCs [101], along with several other adult multi-lineage stem cells including multipotent adult progenitor cells (MAPCs) [102], muscle-derived stem cells (MDSCs) (reviewed in [1]) and adipose-derived stem cells (ADSCs) [103], were retrospectively identified in tissue cultures, leaving no clue to their native location and physiological role. Without apparent conformational traits of the stem cell niche, for example, crypts in the intestine, sarcolemma in skeletal muscle, and the bulge of hair follicles, it is nearly impossible to identify stem cells *in situ* within their natural microenvironment. Consequently, the true identity of these cells has remained elusive for many years, which in turn hinders further understanding of adult stem cell biology. Nonetheless, the omnipresence of MSCs and identification of multipotent stem cells with similar characteristics and developmental potentials in virtually all postnatal organs raised the possibility that a common source of supply may exist in the body.

As mesodermal stem/progenitor cells have been successfully extracted from most of the adult mouse and human organs such as bone marrow, fat, skin, skeletal muscle, dental pulp, placenta, umbilical cord and others, we hypothesized that a structure anatomically common to these organs represents the mysterious regenerative unit. Blood vessels present in all of these organs naturally stood out as the top candidate tissue. Indeed, blood vessels are known to contribute non-vascular cells such as hematopoietic cells [104] and myogenic cells [45] and has been applied to facilitate tissue repair in the clinical setting [105]. We and others recently reported evidences supporting the contention that perivascular cells constitute, at least in part, the

reservoir of multi-lineage mesodermal stem/progenitor cells distributing throughout the human body [26, 46].

Perivascular cells around capillaries and microvessels (arterioles and venules), namely pericytes, closely ensheath endothelial cells and are commonly regarded as the structural components of blood vessels that regulate vascular contractility and support the stability of blood vessels [30]. Through the selection of a combination of positive and negative cell lineage markers, pericytes ($CD146^{+}CD34^{-}CD45^{-}CD56^{-}$) can be prospectively purified to homology by fluorescence-activated cell sorting (FACS) from fresh biopsies of multiple human organ [26]. FACS-purified pericytes express perivascular surface antigens: CD146, NG2, PDGFR-β, alkaline phosphatase (ALP) [26, 46] with absence of hematopoietic cell marker CD45 and endothelial cell markers: CD31, CD34, CD144, vWF, and UEA-1 ligand. Most importantly, pericytes strongly express the classical MSC markers: CD44 CD73, CD90 and CD105, natively and in culture and possess osteo-, chondro-, adipo-, and myogenic differentiation competence [26]. These perivascular cells can be clonally expanded and long-term cultured with no alteration to their phenotypes and developmental potentials. The high repair/regenerative capacities of pericytes were not only demonstrated in injured and dystrophic skeletal muscles but also in infarcted hearts in mouse disease models [17, 26, 55]. Consequently, we postulated the developmental correlation between MSCs and pericytes, a ubiquitously distributed reserve of multi-lineage stem/progenitor cells, and concluded by the likely perivascular origin of MSCs.

Other tissue-specific stem/progenitor cells, for instance, osteogenic, odontoblastic, and adipogenic progenitors have been suggested to originate from perivascular niches *in vivo*, in agreement with the robust osteogenic and adipogenic properties of purified pericytes and the common origin from blood vessels [9, 61, 106]. Although it remains to be clarified whether these

tissue-specific stem/progenitor cells derive from or belong to one or more distinct vascular cell population(s), a tight connection between adult stem/progenitor cells and their vascular/perivascular niches has been established. Future investigations are required to elucidate the significance of this anatomical localization to the pathophysiology of tissue-specific stem/progenitor cells and their regenerative capacities.

2.8 CONCLUSION

In this chapter, I discussed therapeutic applications, repair mechanisms, and future strategies of MSCs and MSC-like precursor cells in CVD, with an emphasis on ischemic heart disease. Overall, multipotent mesodermal precursors represent a very promising and clinically available source of adult stem cells in cardiovascular applications, with their safety being demonstrated by recent clinical trials. Nevertheless, additional efforts will be required to further improve their salutary efficacy and delivery modality. With the fast advances in the mechanistic understanding of MSC-mediated tissue restoration, new approaches can be developed to maximize their sanative capacity in the cardiovascular milieu, including preconditioning and genetic modification of MSCs. The recent discovery of the likely perivascular origin of MSCs provides us with in-depth understanding of their native microenvironment and distributions as well as their physiological and pathological roles in the human body. The identification of multiple mesodermal stem/progenitor cell populations within the walls of blood vessels of all sizes further suggest the complexity of MSCs and stem cell biology as a whole. A continual joint effort by scientists and clinicians will be needed to pursue the futuristic personalized regenerative medicine using adult stem cells: a stem cell treatment plan tailored for individual patient.

3.0 HUMAN PERICYTES FOR ISCHEMIC HEART REPAIR

3.1 INTRODUCTION

Coronary heart disease (CHD) is the leading cause of death in the United States, affecting 16.3 million people and accounting for 1 of every 3 deaths in 2007 [107]. Prolonged pathological interference with the coronary blood supply, such as atherosclerosis and thromboemboli, results in ischemic cardiomyopathy and/or myocardial infarction (MI) [108]. MI often leads to heart failure (HF) due to the limited capacity of the human heart to repair/regenerate its damaged myocardium [108, 109]. Stem/progenitor cell-based cardiac therapy (SCCT), as an alternative to heart transplantation, is deemed promising for restoration of cardiac function and prevention of progressive HF because of manifold advantages [15, 109]. Specifically, human stem/progenitor cells, including skeletal myoblasts, bone marrow cells, endothelial progenitor cells, and endogenous cardiac progenitor cells, have been intensively investigated with uneven success in pre-clinical and clinical trials [15, 109-111]. Given the vascular origin of CHD pathology, stem/progenitor cells that are capable of reconstituting host vascular networks, in addition to other merits, will be ideal cell sources for SCCT.

Microvascular pericytes (aka mural cells) have recently been discovered to include stem/progenitor cells endowed with mesodermal differentiation potentials and suggested to be one of the several developmental origins of heterogeneous mesenchymal stem (aka stromal) cells

(MSCs) [26, 46, 47, 61-63, 112]. Multipotent pericytes isolated from human skeletal muscle, adipose, placenta, and pancreas repair and regenerate damaged/defective organs [26, 46, 112-114]. Owing to their wide distribution throughout the microvasculature, pericytes are regarded as a promising and attractive source of stem cells for regenerative medicine [17, 115]. Microvascular pericytes tightly encircle capillaries and microvessels (arterioles and venules) and regulate microvascular physiology [30]. Above all, due to their native vascular localization, pericytes may restore injured vascular networks more efficiently. We hypothesized that SCCT with pericytes is a suitable approach for the treatment of ischemic heart disease (IHD) [55].

Besides cardiomyogenesis, cardioprotective mechanisms, e.g. neovascularization, anti-fibrosis and anti-inflammation actions, play critical roles in SCCT-mediated cardiac repair following ischemic insults [72, 85]. To relieve the underlying cause of IHD, SCCT-based approaches toward myocardial revascularization have been extensively pursued [24, 116]. Pro-angiogenic signaling molecules released by stem/progenitor cells stimulate neovascularization in ischemic tissues [24]. Pericytes do secrete trophic factors associated with tissue repair and vascular growth/maturation/remodeling [17]. Nevertheless, cell-cell interaction between mural cells and endothelial cells was lately suggested to play essential roles in blood vessel remodeling and maturation [117-119]. It remains to be tested whether multiple angiogenic/vasculogenic mechanisms are involved in pericyte-mediated revascularization of the ischemic myocardium.

To prevent the progressive, pathological decline toward heart failure, favorable tissue remodeling after MI is deemed important. Mesodermal stem/progenitor cells reduce myocardial fibrosis and subsequently increase myocardial compliance and strength in the ischemic heart [120, 121]. This anti-fibrotic feature was attributed to increased collagen degradation by matrix metalloproteinases (MMPs), decreased collagen production, and inhibition of fibroblast

activation, possibly through a paracrine mechanism [122, 123]. Additionally, the immunosuppressive/anti-inflammatory capacity of MSCs has recently attracted clinical attention in organ transplantation and immune regulation [124, 125]. This immunoregulatory activity was primarily associated with secretion of interleukin (IL)-6, prostaglandin E_2 (PGE_2), leukemia inhibitory factor (LIF), and heme oxygenase-1 (HMOX-1) [124, 125]. Whether pericytes possess such an immunoregulatory capacity within the ischemic microenvironment remains to be addressed.

In the present study, we investigated the therapeutic potential of purified human skeletal muscle pericytes in IHD, using an acute MI (AMI) model in immunodeficient mice. Transplantation of pericytes not only reversed cardiac dilatation but also improved cardiac contractility. Four major healing mechanisms were investigated: promotion of angiogenesis, reduction of fibrosis, inhibition of chronic inflammation, and regeneration of the myocardium. We further describe putative mediators employed by pericytes in each mechanism. GFP-labeling was used to track the homing and lineage fate of engrafted pericytes. Our results demonstrate that the overall benefit of pericyte treatment is collectively attributed to multiple cardioprotective mechanisms that involve paracrine and direct cell-cell interactions.

3.2 METHODS

3.2.1 Human tissue biopsies

In total, 3 independent human skeletal muscle specimens (1 adult and 2 fetal) were used for cell isolation. The procurement of adult muscle biopsies from the National Disease Research

Interchange was approved by the Institutional Review Board (IRB) at the University of Pittsburgh Medical Center. Muscle biopsies (male subjects, 57 and 70 years old) were preserved in DMEM containing 1% antibiotics and transported to the laboratory on ice. Human fetal tissues (19-23 weeks of gestation) were obtained following voluntary pregnancy interruptions performed at Magee Womens Hospital, in compliance with IRB protocol 0506176. Informed consents for the use of fetal tissues were obtained from all patients.

3.2.2 Fluorescence-activated cell sorting (FACS) and flow cytometry analysis

Microvascular pericytes present in the adult and fetal skeletal muscles were purified by FACS as previously described[7]. Briefly, fresh muscle biopsies were minced and digested with collagenases I, II and IV (1 mg/mL, Sigma) at 37℃ for 1 hour. Cells were washed and sequentially filtered through 100- and 70-μm cell strainers (BD Falcon) to obtain single cell suspension. Cells (5-10x10^6) were incubated with one or all of the following directly conjugated mouse anti-human antibodies (all with 1:100 dilutions): anti-CD34-PE (DAKO), anti-CD45-APC-Cy7 (Santa Cruz), anti-CD56-PE-Cy7 and anti-CD146-FITC (both Serotec) at 4℃ for 20 min in the dark. As negative controls, isotype-matched mouse IgGs conjugated to PE (Chemicon), APC-Cy7 (Becton-Dickinson), PECy7 and FITC (Chemicon), were used. After washing, all labelled cells were incubated with 7-amino-actinomycin D (7-AAD) (BD, 1:100) for dead cell exclusion and subsequently sorted on a FACSAria flow cytometer (BD).

For quality control, flow cytometry was employed to examine the expression profile of cell lineage markers. Cultured pericytes at different passages were trypsinized and labelled with the following directly conjugated antibodies (all with 1:100 dilutions): anti-CD34-PE (BD), anti-CD44-PE (BD), anti-CD45-PE-Cy7 (Beckman Coulter), anti-CD56-PE (Chemicon), anti-CD73-

PE (BD), anti-CD90-APC (Chemicon), anti-CD105-PE (ImmunoTools) and anti-CD146-FITC (Serotec) for 20 min at 4℃ in the dark and subsequently analyzed on a FACSAria flow cytometer. For analysis of alkaline phosphatase (ALP) expression, cells were incubated with anti-human ALP (Biogenesis, 1:30) and then with donkey anti-sheep Ig-FITC (Serotec), each for 20 min at 4℃.

3.2.3 Cell culture and cell labelling

Sorted human microvascular pericytes were expanded and maintained in Dulbecco's modified eagle medium (DMEM) high glucose (Gibco) supplemented with 20% FBS and 1% Penicillin/Streptomycin (P/S) as previously described[7]. Cell morphology and the cell surface marker expression were monitored to ensure the quality of cells, using formerly published methods and criteria[7]. Single donor-derived human umbilical cord vein endothelial cells (HUVECs) were purchased from Lonza and cultured in endothelial cell growth medium 2 (EGM-2, Lonza), following the manufacturer's instructions.

For gene transfer of green fluorescence protein (GFP), cultured pericytes at passages 7-10 were detached with 0.25% trypsin-EDTA (Gibco) and seeded at a density of 10,000 cells per cm^2. After 24-48 hours, when the culture reached 60-70% confluence, the medium was replaced with transduction medium (α-MEM, 10% FBS, 1% P/S, and 8 μg/mL polybrene), and a lentivirus-based CMV-driven eGFP expression vector was added at a MOI of 10. Following incubation for 16-18 hours at 37℃, the transduction medium was removed and replenished by complete culture medium. Three days later, nearly 100% of cells expressed GFP. GFP-labeled cells were further expanded for 1-2 passages without significant adverse effect. For short-term *in vitro* experiments,

cells were labelled with cell membrane dye, PKH26 (Red) and PKH67 (Green) (Sigma-Aldrich), following the manufacturer's instructions. Dye-labelled cells were used for experiments immediately after labelling without further expansion.

3.2.4 Intramyocardial cell transplantation in acute myocardial infarction (AMI) model

The Institutional Animal Care and Use Committee at Children's Hospital of Pittsburgh of UPMC and University of Pittsburgh approved the animal usage and surgical procedures performed in this study (Protocol 37-04, 55-07, and 0901681A-5). A Total of 64 male NOD/SCID mice (Jackson Laboratory, Bar harbor, ME, USA) were used for this study.

After the induction of anesthesia, mice were intubated and inhalationally anesthetized with 2% isoflurane gas throughout the surgery. Myocardial infarction (MI) was induced by ligation of the left anterior descending coronary artery (LAD). Five minutes after the induction of infarction, $3x10^5$ cells in 30µl of PBS were injected into three sites (center and two borders of the infarct) of the myocardium. Control mice received either injection of 30µl PBS or no injection (MI sham) following AMI. The investigator creating the infarction injury and performing the injection was blinded to the content of the injectant, excluding the MI sham group.

3.2.5 Evaluation of cardiac function by echocardiography

Echocardiographic studies were performed by a blinded investigator repeatedly at 2 and 8 weeks after surgery to assess the cardiac function of anesthetized mice, as previously described[27]. End-systolic dimension (ESD) and end-diastolic dimension (EDD) were determined from the short

axis images of the LV and measured from at least six consecutive beats using the M-mode tracing. End-systolic area (ESA) and end-diastolic area (EDA) were measured from short-axis images of the LV. Fractional shortening (FS), an index of LV contractility, was calculated as FS (%) = [(EDD-ESD)/EDD] x 100. FAC (Fractional Area Change), another index of LV contractility, was calculated as FAC (%) = [(EDA-ESA)/EDA] x 100. Mice died or sacrificed for histological analysis prior to 8 weeks post-injection were not included in the echocardiographic study.

3.2.6 Histological and immunohistochemical analyses

Animals were sacrificed at 1, 2, and 8 weeks post-surgery. Hearts were arrested in diastole by intraventricular injection of 1M potassium chloride (KCl) and processed as formerly described[27]. Harvested hearts were flash frozen in 2-methylbutane (Sigma) pre-cooled in liquid nitrogen and serially cryosectioned at 6-8 μm thickness from apex to the ligation level (approximately 0.5 mm in length). Each series contains 21-24 heart sections, which are roughly 200 um apart originally and collected on one glass slide. Sections were fixed in a pre-cooled (-20℃) mixture of methanol and acetone (1:1) for 5 min or in 4% paraformaldehyde for 8 min prior to staining. Hematoxylin and eosin (H&E) staining was performed following the standard protocol. Non-specific antibody binding was blocked with 5% donkey or goat serum for 1 hour at room temperature (RT) and, if necessary, with the Mouse-on-Mouse (M.O.M.) antibody staining kit (Vector).

For homing and cell fate tracing, anti-GFP immunofluorescent staining was employed to detect GFP signals. Briefly, after fixation in paraformaldehyde and blocking, sections were permeabilized with 0.1% Triton in PBS and incubated at 37℃ for 1 hour with rabbit anti-GFP antibody (Abcam, 1:1000), followed by incubation with donkey anti-rabbit-Cy3 IgG (Jackson

Immunoresearch, 1:250) or donkey anti-rabbit-Alexa^{TM}488 IgG (1:250, Molecular Probes) for 1 hour at RT. To examine homing of donor cells, sections were then incubated overnight at 4°C with rat anti-mouse CD31 antibody (1:100, BD), followed by goat anti-rat-Alexa^{TM}488 IgG (Molecular Probes, 1:400) or donkey anti-rat-Alexa^{TM}555 IgG (Molecular Probes, 1:400). To examine expression of cardiomyocyte, smooth muscle cell, and endothelial cell markers as well as human $VEGF_{165}$, sections were first stained for GFP and then incubated overnight at 4°C with goat anti-cardiac troponin I (Abcam, 1:200), mouse anti-human SM-MHC (DAKO, 1:50), sheep anti-human CD31 (R&D systems, 1:50), or goat anti-human $VEGF_{165}$ (R&D systems, 1:50) primary antibody, followed respectively by donkey anti-goat Alexa^{TM}555 IgG, donkey anti-mouse Alexa^{TM}555 IgG, and rabbit anti-sheep Alexa^{TM}555 IgG (Molecular Probes, all 1:400). For evaluation of chronic inflammation, sections were incubated overnight at 4°C with rat anti-mouse CD68 primary antibody, followed by goat anti-rat-Alexa^{TM}488 IgG. Cell nuclei were stained by DAPI.

3.2.7 Quantification of donor cell engraftment and perivascular homing

To estimate the number of donor cells engrafted in the infarcted heart, quantification was performed on anti-GFP immunostained serial cryosections, using a digital image analyzer (Image J). The number of GFP-positive cells (nuclei identified by DAPI) present in each heart cryosection was computed. The total number of GFP-positive cells within each heart was extrapolated as the sum of the number of GFP-positive cells in all serial sections (21-24 sections) times the number of section series, corrected by a collection loss coefficient of 20%. The engraftment ratio was defined as the extrapolated total number of engrafted GFP-positive cells to the initial injection of $3x10^5$ cells. To estimate the number of donor cells that exhibited

perivascular homing, quantification was performed on anti-GFP and anti-mouse endothelial cell marker, CD31, dual-immunostained serial cryosections, using Image J. Perivascular homing was defined as GFP-positive cells juxtapose CD31-positive mouse endothelial cells. The number of perivascular homing GFP-positive cells in each heart cryosection was computed. The total number of perivascular homing GFP-positive cells within each heart was extrapolated using the same formula described above. The perivascular homing ratio was defined as the extrapolated number of perivascular homing GFP-positive cells to the extrapolated total number of engrafted cells.

3.2.8 Quantification of host angiogenesis and chronic inflammation

To quantify host angiogenesis in the heart, immunohistochemistry using anti-mouse endothelial cell marker, CD31, was performed on cryosections. The capillary density, represented by the number of CD31-positive capillary structures per mm^2, was subsequently computed from 6 representative images of the peri-infarct area or infarct region of each heart at the mid-infarct level, using Image J as described previously[27]. To evaluate chronic inflammation within the infarct region, we performed immunofluorescent staining of anti-mouse CD68 on cryosections and subsequently computed the infiltration index, represented by the number of CD68-positive host cells per mm^2, from 8-10 images covering the entire infarct region of each heart at the mid-infarct level, using Image J.

3.2.9 Measurement of Cardiac Fibrosis and Infarct Wall Thickness

Masson's trichrome staining kit (San Marcos) was used to stain collagen deposition on cryosections, following the manufacturer's instructions. The area of the collagen deposition, representing cardiac fibrosis, and the area of the entire cardiac tissue (excluding the void space in the chamber cavity) were measured using Image J. Fibrotic area fraction was estimated as the ratio of fibrotic tissue to the entire cross-sectional area of cardiac tissue and averaged from 6 representative sections per heart. Left ventricular wall thickness at the center of the infarct was estimated as the mean of 3 adjacent measurements (0.25mm apart) and was averaged from 6 representative sections per heart.

3.2.10 Hypoxia Assay

To assess the influence of the hypoxic microenvironment in human pericytes, we cultured cells under 2.5% O_2 hypoxic conditions *in vitro* as formerly described[27]. Concisely, pericytes were seeded in 6-well culture plates at 10,000 cells/cm^2 and allowed the cells to reach 80-90% confluence under normoxia. Upon the transition to low O_2 conditions, the complete culture medium was removed and cells were washed twice with PBS before defined, serum-free DMEM medium was added. Twenty-four hours later, cells were trypsinized and counted. The culture supernatant and cell pellets were collected for analysis. Cells cultured under normoxia with the serum-free medium served as controls.

3.2.11 Semi-quantitative RT-PCR and Real-time Quantitative PCR (real-time qPCR)

3.2.11.1 Semi-quantitative RT-PCR

For semi-quantitative RT-PCR (sqRT-PCR), cells were lysed with RLT-plus lysis buffer supplemented with beta-mecaptoethanol. Total RNA (N=3) were extracted with the Qiagen RNeasy plus-mini-kits. RNA concentration was measured using TECAN plate reader system with the NanoQuant measurement program. From each sample, 500ng of total RNA were reverse transcribed with SuperScript^{TM} III cDNA synthesis kits (Invitrogen) in 20 µl reactions. PCR was performed in 25 µl reaction with Promega Gotaq system and reacted in Vapo.Protect PCR machine (Eppendorf) using the following program: 3 minutes for the initial denature, 32 cycles at (94℃ for 30 seconds, 55℃ for 30 seconds, 72℃ for 45 seconds) and final extension for 6 minutes. PCR products were verified by 1% agarose gel electrophoresis. Images were captured using the GelDoc system with Quantify One 4.6.2 software. The intensities of the target gene bands were quantified using the same software, and normalized to those of the house keeping gene β-actin.

3.2.11.2 Real-time qPCR

For real-time qPCR, total RNA (N=6) was extracted from $1x10^5$ cells using the Nucleospin RNA kit (Clontech). cDNA was synthesized with SuperScript^{TM} II reverse transcriptase (Invitrogen), according to the manufacturer's instructions. cDNA and primers were added to SYBR Green PCR master mix (Applied Biosystems) according to the manufacturer's instructions. The quantitative analyses were carried out in triplicate on an ABI Prism 7900HT sequence detection system in the core facility of the Genomics and Proteomics Core Laboratories of the University of Pittsburgh. All data were normalized to human cyclophilin, which was used as an internal

control. Gene expression levels were analyzed using SDS 2.2 Software (ABI) and calculated based on the comparative ΔC_T method (separate tubes). Data are presented as normalized expression level (in arbitrary units). Sequences of target gene primers/probes (IDT-Integrated DNA Technologies) used in real-time qPCR and sqRT-PCR are listed below in Table 2 and Table 3 respectively.

Table 2: Primer sequences for real-time qPCR

Gene	Forward	Reverse
bFGF NM002006	ccgttacctggctatgaagg	tttccttgaccggtaagtattg
HGF NM000601	atatgtgctggggctgaaaa	cacgaccaggaacaatgaca
VEGF-A NM001025368	gcgaggcagcttgagttaaa	ctttcctggtgagagatctgg
EGF NM001963	ggtactctcgcaggaaatgg	tccaccaccaattgctcata
PDGF-β CU013138	tcccgaggagctttatgaga	gggtcatgttcaggtccaac
TGF-β1 NM000660	cgactactacgccaaggaggt	cggagctctgatgtgttgaa
Flt-1 NM002019	cttcacctggactgacagca	acagctggaatggcagaaac
Flk-1 NM002253	tgctcaagacaggaagacca	cttcgatgctttccccaata
PDGFRβ NM002609	catcagcagcaaggacaccat	gaccttggtgtctagagagtcc
IGF-1 X57025	gctggtggatgctcttcagt	aagcagcactcatccacgat
MMP-2 NM004530	gctcccggaaaagattgatgc	acctagatgagtcggtcgtg
MMP-9 BC006093	ttccctggagacctgagaac	ctacgcacctctcagcttta
Cyclophilin	catctgcactgccaagactga	gcaaagtgaaagaaggcatgaa

Table 3: Primer sequences for semi-quantitative RT-PCR

Gene	Forward	Reverse
IL-6 NM000600.3	ccacaagcgccttcggtcca	gtggctgtctgtgggggcg
LIF M63420.1	acgccaacggcacggagaag	tacccgaggtgtcagggccg
COX-2 NC000001.10	gcgagggccagctttcacca	cctgccccacagcaaaccgt
HMOX1 NM002133.2	cgtccgcaacccgacagcat	cagccttgcggtgcagctct
MCP-1 NM002982.3	agctcgcactctcgcctcca	gcatctggctgagcgagccc
IL10 NM000572.2	gctgcacccacttcccaggc	gacagcgccgtagcctcagc
iNOS NM000625.4	acccgagatggccagggtcc	ccgcactcccttgtgctggg
IL-1α NM000575.3	aatgacgccctcaatcaaag	tgggtatctcaggcatctcc
IL-4 BC067514.1	gccaccatgagaaggacact	actctggttggcttccttca
IFNγ BC070256	tgaccagagcatccaaaaga	ctcttcgacctcgaaacagc
2,3-IDO NM194294	ctggtcctgagcttcctcac	cagcaccaagtctgagtgga
HIF1α NM001530	tccatgtgaccatgaggaaa	ccaagcaggtcataggtggt
TNFα HQ201306	agcccatgttgtagcaaacc	tgaggtacaggccctctgat
Actin NM001101.3	agcgggaaatcgtgcgtg	cagggtacatggtggtgcc

3.2.12 Vascular network formation in vitro

To demonstrate the vascular cell characteristics and the supportive function of cultured pericytes, we performed cell culture and co-culture experiments using 2D and 3D Matrigel systems and observed capillary-like network formation. In brief, 350µl of Matrigel (BD) was placed in each well of a 24-well plate and incubated at 37℃ for 30 min. Fifty thousand pericytes were resuspended in 700µl of EGM2 and seeded onto the Matrigel-coated well. Experiments using $5x10^4$ HUVECs were performed as controls. A 2D co-culture system using cells pre-labeled with cell membrane dye (PKH fluorescent dye, Sigma-Aldrich) was developed to observe pericyte-

HUVEC interactions. Briefly, $5x10^4$ PKH26-labeled HUVECs (Red) and $5x10^4$ PKH67-labeled pericytes (Green) were well mixed, resuspended in 700µl of EGM2, seeded onto Matrigel in a 24-well plate, and further cultured for 24 hours. An *in vitro* 3D Matrigel culture system was used to investigate vascular support by pericytes. In short, $25x10^4$ pericytes were resuspended in EGM2 and well mixed with 350µl of Matrigel in a 3:1 ratio before being encapsulated into one well of a 24-well plate and subsequently incubated for 72 hours. A small amount of EGM2 was added after gelation and exchanged every 24-48 hours. Experiments using $25x10^4$ HUVECs were performed as controls. A 3D co-culture system using $25x10^4$ PKH26-labeled HUVECs (Red) and $25x10^4$ PKH67-labeled pericytes (Green) was performed in the same manner and subsequently cultured for 72 hours. All images were taken using an epi-fluorescence microscope (Nikon Eclipse TE 2000-U).

3.2.13 Enzyme-linked immunosorbent assay (ELISA)

The secretion of growth factors and cytokines in culture supernatant was quantified by enzyme-linked immunosorbent assay (ELISA). Vascular endothelial growth factor (VEGF) secretion by microvascular pericytes was measured by human VEGF ELISA Kit (KHG0111, Invitrogen), following the manufacturer's instructions. The secretion of angiopoietins-1 (Ang-1) and angiopoietins-2 (Ang-2) by pericytes was measured by human Ang-1 (DANG10, R&D) and Ang-2 (DANG20, R&D) ELISA Kits respectively, following the manufacturer's instructions. Data are presented as pg/ml per 100,000 cells per 24 hours.

3.2.14 Measurement of cell proliferation

Murine RAW264.7 monocyte/macrophage-like cells or primary muscle fibroblasts were quadruplicately plated (10^4 cells/well) in a 96-well plate. Four hours later, the culture media were changed to normoxic or hypoxic pericyte-culture conditioned media, or fresh serum-free media for control wells. Cells were subsequently cultured under ambient conditions for 72 hours. At this time, wells were washed and CellTiter 96® AQueous One Solution Cell Proliferation Assay (MTS Assay) Reagent (G3582, Promega) in DMEM was added. The plate was incubated in 5% CO_2 at 37 ℃ for 3 hours, at which point the absorbance at 490 nm was read with a 96-well plate reader.

3.2.15 Statistical analysis

All measured data are presented as mean ± standard error (SE). Kaplan-Meier survival curve estimation with log-rank test was performed to compare the animal survival rate between treatment groups. Statistical differences were analyzed by Student's *t*-test (two groups), one-way ANOVA (multiple groups), or two-way repeated ANOVA (repeated measures) with 95% confidence interval. Student-Newman-Keuls multiple comparison test was performed for ANOVA post-hoc analysis. Statistical analyses were performed with SigmaStat 3.5 and SPSS19 statistics software.

3.3 RESULTS

3.3.1 Transplanted human pericytes s improve survival and cardiac function

Cultured pericytes at passages 8-12 were characterized by flow cytometry (Figure 3 and Figure 4) and subsequently injected into the acutely infarcted myocardium of immunodeficient mice. Control groups received PBS injections or no injection (MI sham) following the induction of MI. The survival of animals receiving pericyte treatment (N=16) or no treatment (N=14) was monitored over the course of 8 weeks (Kaplan-Meier survival curve, Figure 5A).

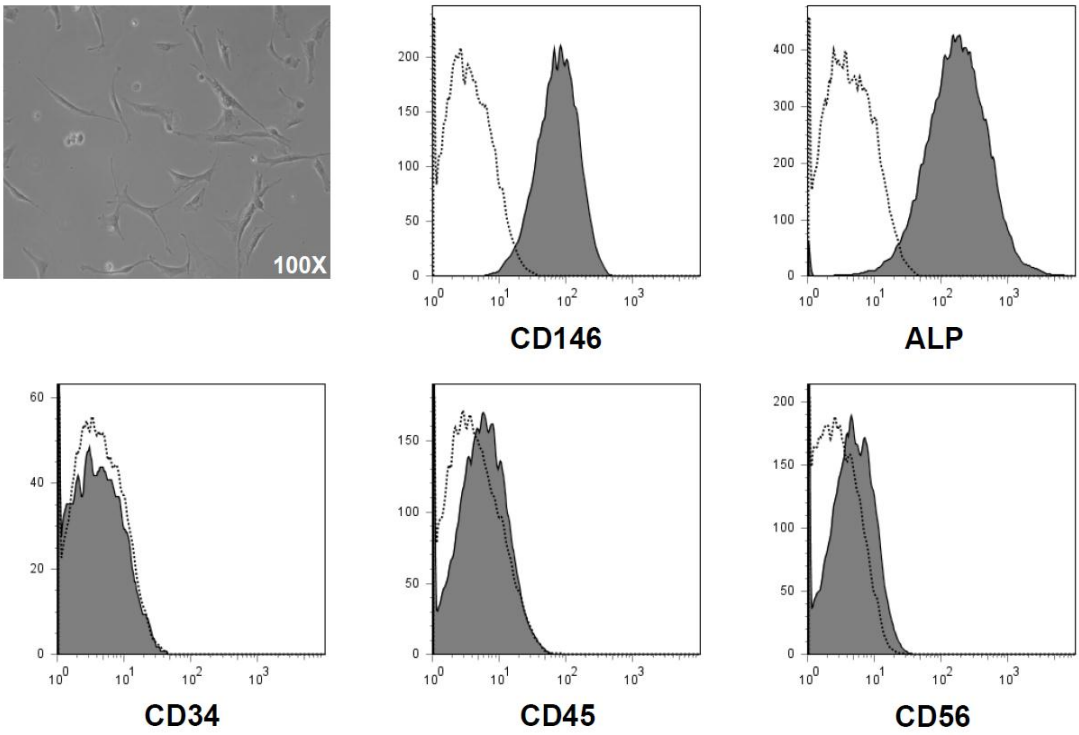

Figure 3: Morphology and characterization of purified pericytes in long-term culture

Flow cytometry analysis revealed that cultured pericytes retain original cell surface marker expression, including the robust expression of CD146 and alkaline phosphatase (ALP) with the absence of CD34, CD45, and CD56.

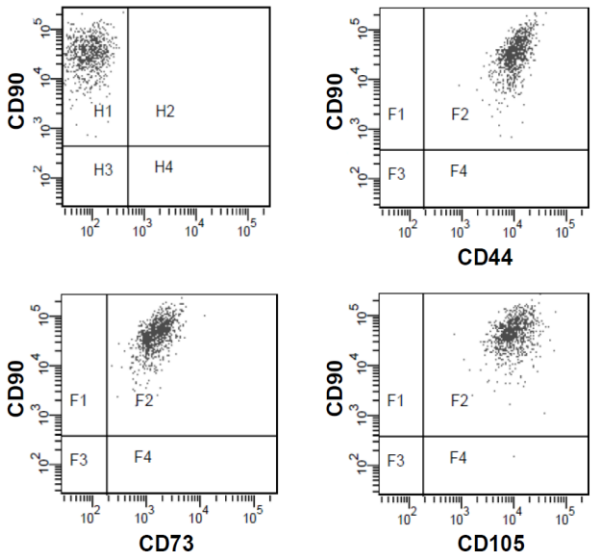

Figure 4: Flow cytometry analysis of MSC markers

The results showed that long-term cultured pericytes strongly express classic MSC markers: CD90, CD44, CD73 and CD105.

Cardiac function was assessed by echocardiography performed repeatedly before (healthy) and at 2 and 8 weeks after surgery (Figure 5B). Ischemic hearts injected with pericytes isolated from two donors (designated as P1 and P2, N=8 per donor) had significantly smaller left ventricular (LV) chamber size, as measured by LV end-diastolic area (LVEDA, C) and end-systolic area (LVESA, Figure 5D), than PBS control group (N=5) (all $p<0.05$), suggesting the reversal of progressive heart dilatation. The average LV chamber diastolic dimension after pericyte treatment (N=16) was significantly smaller when comparing to infarcted hearts without pericyte injection (N=10) (two-way repeated ANOVA, $p=0.002$). Moreover, pericyte-transplantation groups displayed significantly better LV contraction, evaluated by LV fraction shortening (LVFS, Figure 5E) and LV fractional area change (LVFAC, Figure 5F), than either PBS (N=5) or MI sham (N=5) control groups at 2 and 8 weeks post-transplantation (all $p<0.05$). Collectively, pericyte treatment (N=16) demonstrated a significant therapeutic effect on LV

contractility when compared to sham treatment (N=10) (two-way repeated ANOVA, $p<0.001$). Echocardiographic parameters are documented in Table 4.

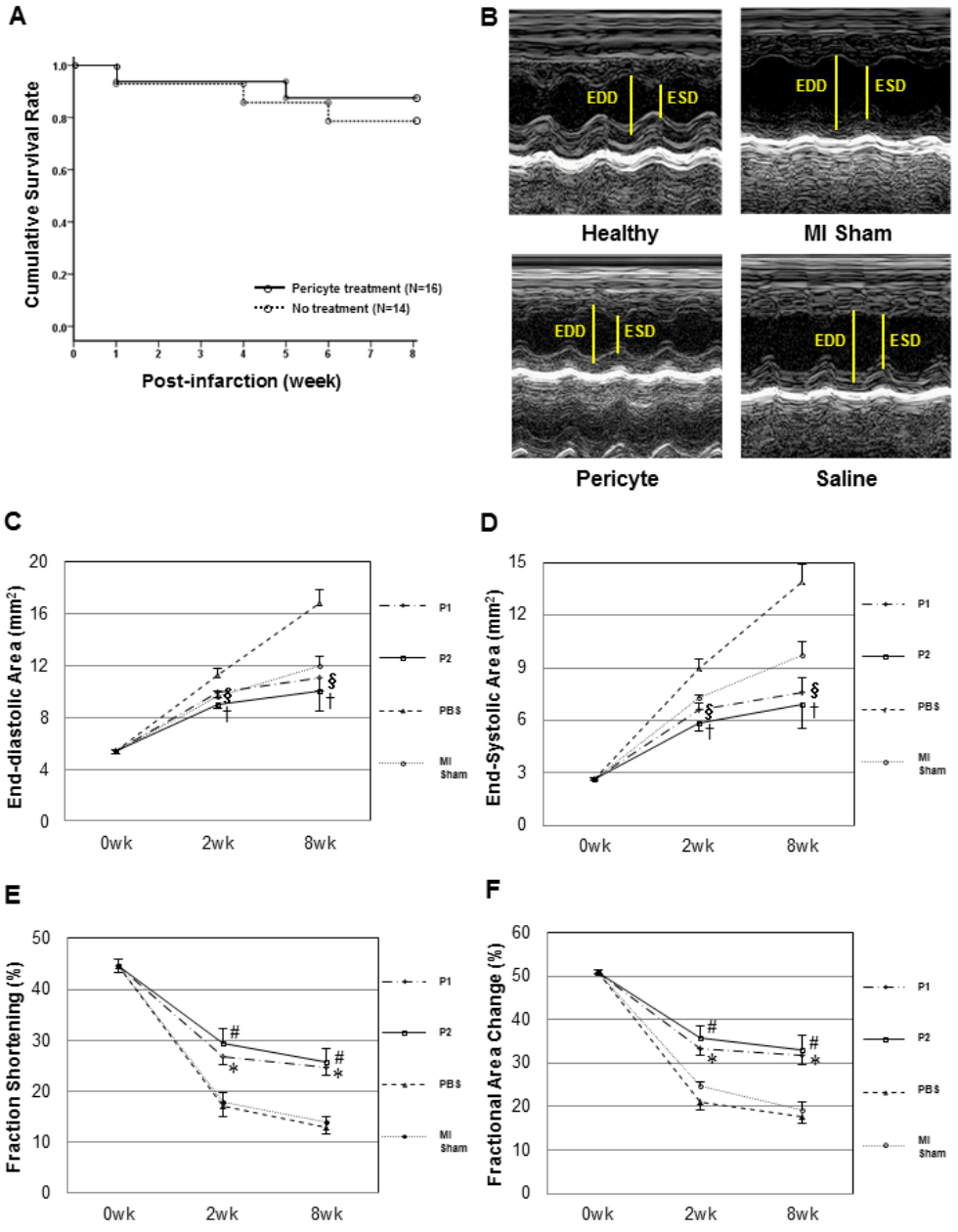

Figure 5: Survival rate and cardiac functional assessment

(A) Cumulative survival rate over 8 weeks post-surgery (Kaplan-Meier Survival Curve, log-rank test $p=0.529$). (B) Representative M-mode images of left ventricle (LV). End-systolic dimension (ESD) and end-diastolic dimension (EDD) were indicated. Echocardiographic analyses revealed a significant reduction of LV dilatation by transplantation of pericytes (P1 and P2), as shown by smaller LV areas in end-diastole (C) and end-systole (D) of hearts. Pericyte treatment also resulted in substantial improvement in LV contractility, as indicated by greater fractional shortening (E) and fractional area change (F). (†§$p<0.05$ versus PBS; *#$p<0.05$ versus PBS and MI sham)

Table 4: Echocardiographic parameters

Group	Healthy	Pericyte treatment		No treatment	
Time (Post-MI)	Pre-MI	2 weeks	8 weeks	2 weeks	8 weeks
LVESD (mm)	1.8±0.1	3.0±0.2	3.3±0.3	3.7±0.2	4.7±0.4
LVEDD (mm)	3.4±0.2	4.2±0.2	4.5±0.3	4.5±0.2	5.4±0.4
LVESA (mm^2)	2.6±0.1	6.2±0.4	7.3±1.1	8.1±0.4	11.8±0.9
LVEDA (mm^2)	5.4±0.2	9.5±0.4	10.6±1.3	10.5±0.4	14.4±0.9
LVFS (%)	44.7±1.2	28.2±2.3	25.3±2.1	17.5±2.0	13.4±1.1
LVFAC (%)	50.9±0.4	34.5±2.0	32.4±2.8	22.9±1.4	18.5±1.7

Pre- and post-MI NOD/SCID mouse hearts treated with or without pericytes. LV, left ventricle; ESD, end-systolic dimension; EDD, end-diastolic dimensions; ESA, end-systolic area; EDA, end-diastolic area; FS, fractional shortening; FAC, fractional Area Change.

3.3.2 Transplanted pericytes promote host angiogenesis

To explore the mechanisms exploited by pericytes to support functional cardiac recovery, we examined whether intramyocardial transplantation of pericytes benefits the host vascular network post-infarction. Capillaries in the peri-infarct areas (Figure 6A) and within the infarct region (Figure 6C) were revealed by anti-mouse CD31 (platelet endothelial cell adhesion molecule, PECAM-1) immunofluorescent staining. CD31-positive structures were quantified around and within the infarct region. Capillary density in the peri-infarct areas of pericyte-injected hearts (N=5) was increased by 42.8% when compared to saline-injected controls (N=5) (Figure 6B, $P<0.05$). Higher vascular density was also observed within the infarct region, with 33.2% more capillaries in the pericyte-treated hearts (Figure 6D, $P<0.001$). These findings suggest that transplanted pericytes promote host angiogenesis not only in the peri-infarct areas, where blood

vessels were generally better preserved after the ischemic injury, but also within the blood vessel-deprived infarct region.

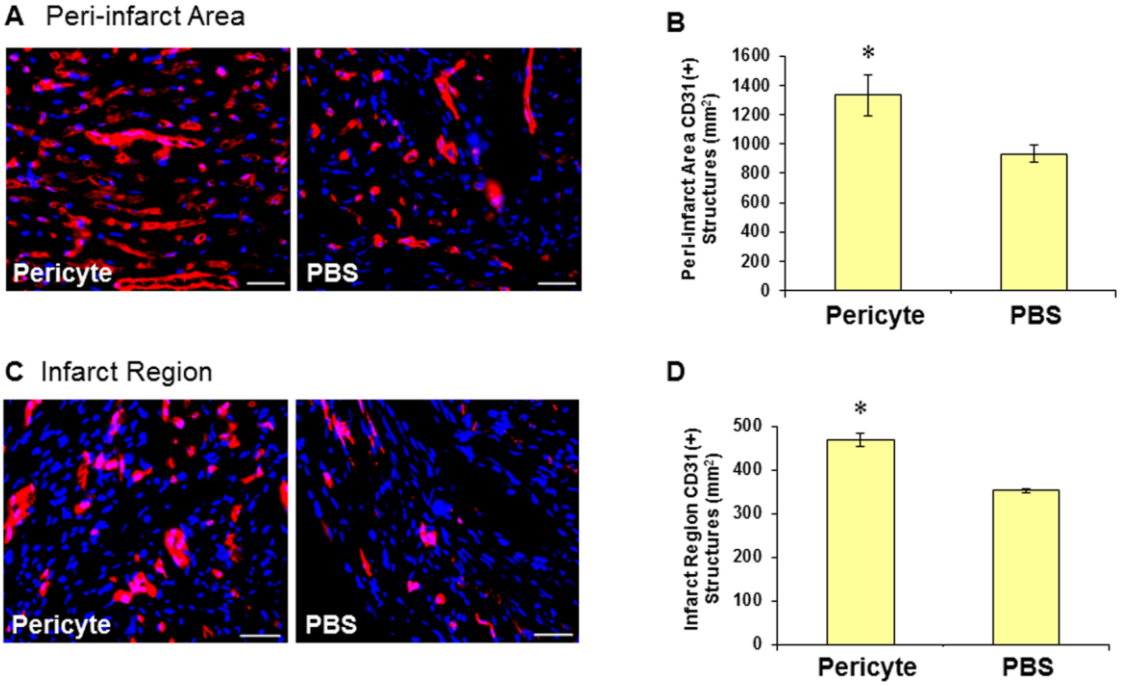

Figure 6: Promotion of host angiogenesis by pericyte treatment

(A) Representative images of anti-mouse CD31 immunostaining in the peri-infarct area of hearts injected with pericytes or PBS. (B) Pericyte-treated hearts displayed a substantially higher capillary density in the peri-infarct area ($*p<0.05$). (C) Anti-mouse CD31 immunostaining within the infarct region. (D) Significantly higher capillary density within the infarct region of pericyte-transplanted hearts ($*p<0.001$). (Scale bars=50μm)

3.3.3 Engrafted pericytes home to perivascular locations

It is not known whether transplanted pericytes home back to perivascular areas *in vivo*. To reveal their engraftment and homing pattern, cultured pericytes were transduced with a GFP reporter gene at near 100% efficiency (Figure 7A) and injected (3.0×10^5 cells) into acutely infarcted hearts. GFP-labeled pericytes extensively engrafted throughout the host ventricular myocardium (Figure 7B), particularly in the peri-infarct area (Figure 7C). Confocal microscopy showed that

GFP-positive human pericytes can engraft the interstitial space where capillaries reside (Figure 7D). A fraction of pericytes (white arrows) were identified in perivascular positions, in close contact with host CD31-positive endothelial cells (Figure 7D, inset). Indeed, pericytes were aligned with (Figure 7E) or surrounding (Figure 7E, inset) CD31-positive microvessels, suggestive of perivascular homing. The number of engrafted GFP(+) pericytes was approximately 9.1±1.3% of total injected cells at the first week and declined over time to 3.4±0.5% at 8 weeks post-infarction (N=3 per time point) (Figure 7F, black line). The perivascular homing rate instead increased from 28.6% to 40.1% over the course of 8 weeks, implicating the merit of niche-homing for long-term donor cell survival (Figure 7F, red line).

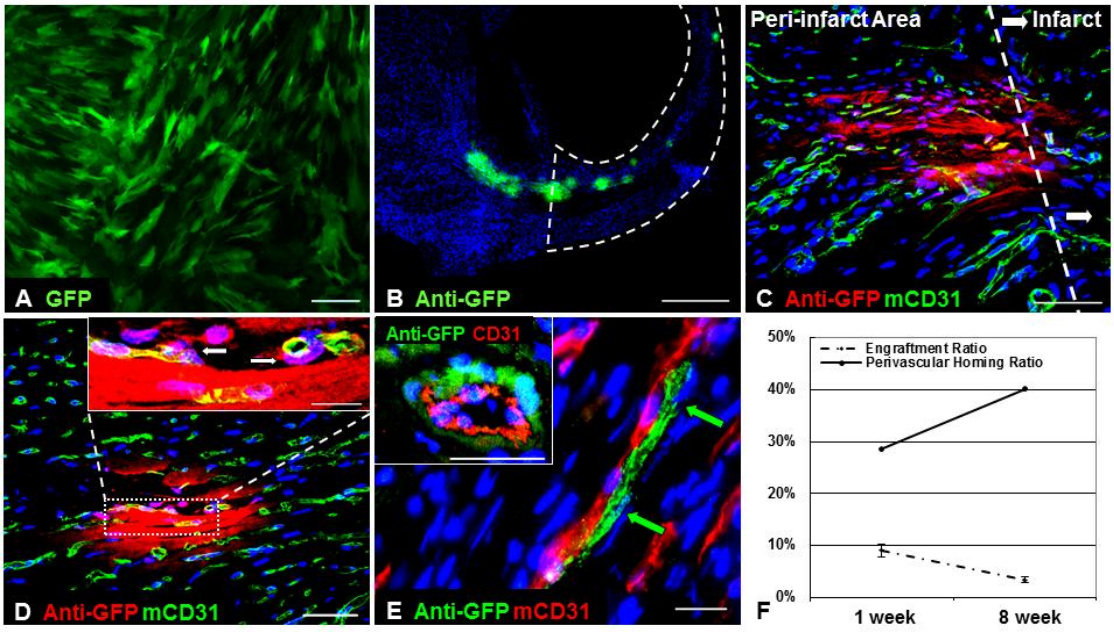

Figure 7: Transplanted pericytes home to perivascular locations

(A) Pericytes were transduced with GFP reporter at nearly 100% efficiency (scale bar=200μm). (B) Engraftment of GFP-labeled pericytes within host myocardium was revealed by anti-GFP immunostaining at 1 week post-injection (scale bar=500μm, infarct site encircled by dotted lines). (C) Donor pericytes (stained red by anti-GFP) were particularly abundant in the peri-infarct area (scale bar=50μm). (D) Confocal microscopy showed that pericytes can be located at the interstitial space where capillaries reside (scale bar=50μm) with some GFP-positive cells (white arrows) in close contact with host CD31-positive endothelial cells ([D], inset; scale bar=10μm). Pericytes were lining with (E, main) or surrounding ([E], inset) host CD31-positive microvasculature (scale bars=20μm). (F) The engraftment ratio of pericytes at 1 week (9.1±1.3%) and 8 weeks (3.4±0.5%) post-infarction was depicted (dash-dot line). The perivascular homing ratio instead increased from 28.6% to 40.1% and was delineated (solid line).

3.3.4 Pericytes support microvascular structures

To demonstrate that pericytes benefit host vascular networks through their support in microvascular structures, we developed 2D and 3D Matrigel cultures/co-cultures using pericytes and HUVECs. HUVECs seeded onto Matrigel-coated wells formed typical tubular networks after 24 hours (Figure 8A). Pericytes, however, formed similar structures within 6-12 hours of seeding (Figure 8B). To illustrate the cellular interaction between pericytes and HUVECs, dye-labeled pericytes (PKH67, green) and HUVECs (PKH26, red) were mixed and co-cultured in 2D Matrigel, which resulted in the formation within 6-12 hours of capillary-like networks that included both cell types (Figure 8C). Pericytes (green) were observed to occupy peri-endothelial positions in the co-formed three-dimensional structures after incubation for 24 hours (Figure 8C, inlet). Additionally, HUVECs (red) appeared to align with pericytes (green) (Figure 8D). To further unveil the vascular supportive properties of pericytes, an *in vitro* 3D Matrigel system designed to simulate native capillary formation was used. HUVECs evenly distributed within the 3D Matrigel were unable to form organized structures after 72 hours (Figure 8E). To the contrary, pericytes started to form capillary-like networks 24 hours after gel-casting, with structural remodeling over time (Figure 8F). The dynamic interaction between pericytes and HUVECs was best depicted by encapsulating dye-labeled pericytes (green) and HUVECs (red) in a 3D Matrigel plug. Together these two types of cells formed capillary-like networks after incubation for 72 hours (Figure 8G) with pericytes surrounding HUVECs (Figure 8H) These data suggest that pericytes retained vascular cell features and formed structures supportive of microvascular networks even after purification and long-term culture, while pericyte-EC interaction played a role in the pericyte-facilitated angiogenic process.

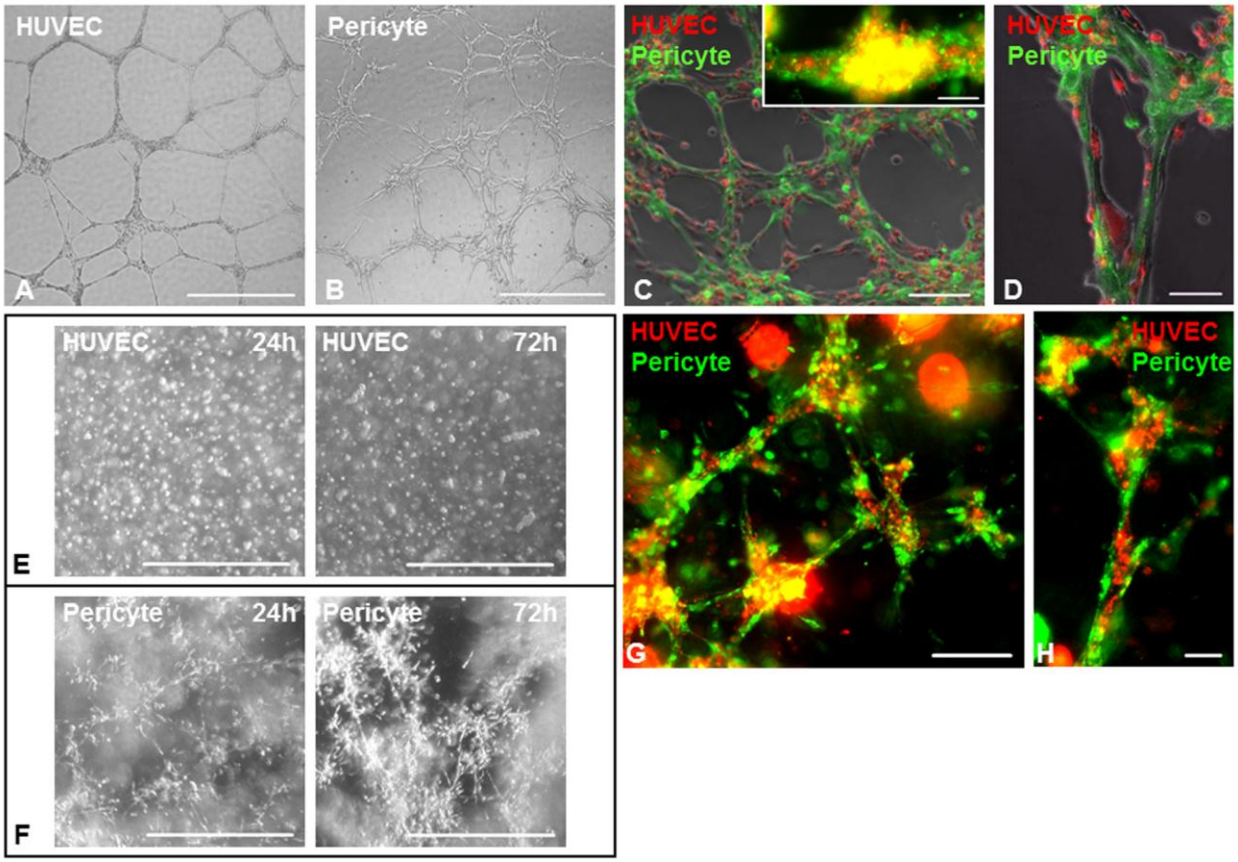

Figure 8: Pericytes support microvascular structures

(A) While HUVECs seeded onto Matrigel-coated wells formed typical capillary-like networks after 24 hours, (B) pericytes formed similar structures within 6-12 hours (scale bars=1mm). (C) When co-cultured on Matrigel, dye-labeled pericytes (green) and HUVECs (red) co-formed capillary-like networks within 6-12 hours, ([C], inset) with pericytes taking peri-endothelial positions in three-dimensional structures formed 24 hours after seeding (scale bars: main=200μm; inset=100μm). (D) HUVECs (red) appear to line and spread out on top of the pericyte-formed structures (green) (scale bar=100μm). (E) To simulate native capillary formation, HUVECs were evenly encapsulated into 3D Matrigel plug for 72 hours but unable to form any organized structure (scale bars=1mm). (F) Pericytes instead formed capillary-like networks in Matrigel plug with structural organization and maturation over time (scale bars=1mm). (G) When dye-labeled pericytes (green) and HUVECs (red) were co-casted into the 3D-gel plug, the two types of cells formed microvessel-like networks within 72 hours, (H) with pericytes surrounding HUVECs (scale bars: G=200μm; H=50μm).

3.3.5 Differential expression of pro-angiogenic factors and associated receptors by pericytes under hypoxia

We mimicked, at least in part, the hostile hypoxic microenvironment donor cells encounter in the post-infarction heart by culturing pericytes under 2.5% oxygen for 24 hours in defined, serum-free medium. Pericytes cultured under 21% oxygen (normoxia) served as controls. Expression of genes encoding pro-angiogenic factors and corresponding receptors was assessed by real-time qPCR. Vascular endothelial growth factor-A (VEGF-A), platelet-derived growth factor-β (PDGF-β), and transforming growth factor (TGF)-β1 were notably up-regulated by 307% ($p \leq 0.001$), 437% ($p = 0.067$), and 178% ($p = 0.037$) respectively in pericytes cultured under hypoxic conditions (Figure 9A). Expression of other pro-angiogenic factors, including basic fibroblast growth factor (bFGF), hepatocyte growth factor (HGF), and epidermal growth factor (EGF), was down-regulated to 44% ($p < 0.05$), 23% ($p \leq 0.001$), and 60% ($p > 0.05$) of their expression levels in normoxia (Figure 9A). On the other hand, VEGF receptor-1 (VEGFR-1/Flt-1) and -2 (VEGFR-2/KDR/Flk-1) were substantially up-regulated by 458% ($p = 0.004$) and 572% ($p \leq 0.001$) respectively under 2.5% oxygen (Figure 9B). PDGF receptor-β (PDGF-Rβ) expression was moderately increased by 161% ($p > 0.05$) (Figure 9B). VEGF secretion by pericytes significantly increased over 3-fold ($p \leq 0.001$) under hypoxic culture conditions while angiopoietins-1 (Ang-1) secretion reduced by 35% ($p > 0.05$) (Figure 9C). Very little secretion of angiopoietins-2 (Ang-2) by pericytes was detected under both conditions ($p > 0.05$) (Figure 9C). The expression of human $VEGF_{165}$ by engrafted pericytes within the infarct region was confirmed by immunohistochemistry (Figure 9D, a-c).

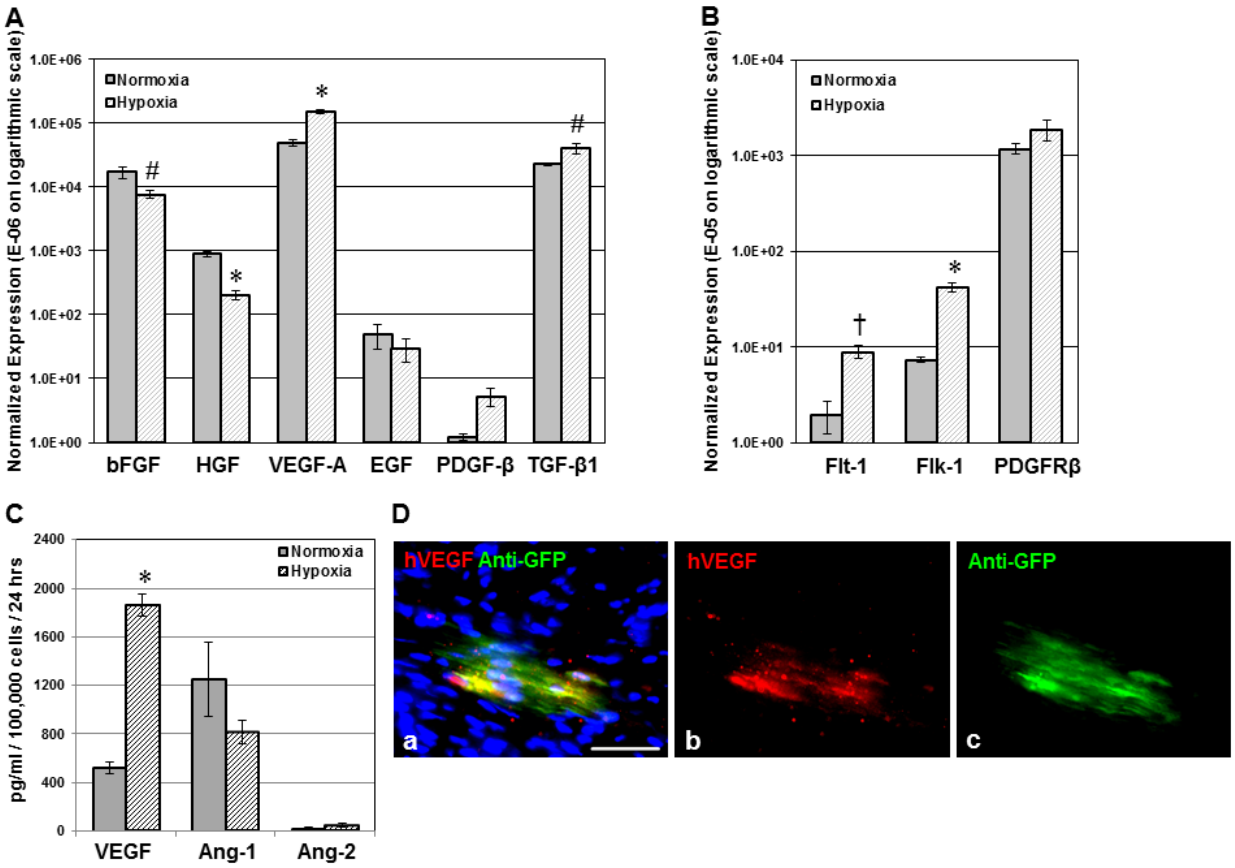

Figure 9: Expression of pro-angiogenic factors and associated receptors under hypoxia

(A) Pericytes dramatically up-regulated VEGF-A, PDGF-β, TGF-β1 gene expression under hypoxic conditions while expression of other pro-angiogenic factors, including bFGF, HGF and EGF were distinctively repressed. (B) Simultaneously, VEGFR-1 (Flt-1) and -2 (Flk-1) were substantially up-regulated, and PDGF-Rβ expression was moderately increased. All expression levels are normalized to human cyclophilin and presented in arbitrary fluorescence units on an expanded logarithmic scale (#$p<0.05$, $*p\leq0.001$, †$p<0.01$, hypoxic versus normoxic). (C) Significantly increased secretion of VEGF ($p\leq0.001$) by pericytes under hypoxic culture conditions was detected by ELISA while the secretion of Ang-1 was reduced by 35% ($p>0.05$), with very little secretion of Ang-2 under both conditions ($p>0.05$). (D) Immunohistochemistry revealed human $VEGF_{165}$ expression by the engrafted GFP-labelled pericytes within the infarct area at 2 weeks post-infarction (a) merge (b) GFP in green (c) $hVEGF_{165}$ in red (scale bar=50μm).

3.3.6 Transplantation of pericytes reduces cardiac fibrosis

To understand the influence of pericyte treatment on cardiac fibrosis, we evaluated scar tissue formation using Masson's trichrome histological staining. At 2 weeks post-infarction, pericyte-treated hearts displayed less collagen deposition (stained in blue/purple) at the ischemic area

(Figure 10A). Estimation of the total fibrotic tissue ratio unveiled a 45.3% reduction of cardiac fibrosis in the pericyte-injected myocardium (N=5, 22.03±1.81%) when comparing to saline-injected controls (N=5, 40.28±2.15%) (Figure 10B, $p \leq 0.001$), suggesting the anti-fibrotic efficacy of pericytes. Measurement of LV wall thickness at the center of the infarct indicated a 26.3% increase in the pericyte group (0.255±0.026 mm) versus the PBS group (0.202±0.040 mm), suggesting that pericytes reduce transmural infarct thinning following MI, and consequently preserve LV wall thickness (Figure 10C, $p > 0.05$).

3.3.7 Paracrine anti-fibrotic effects of pericytes under hypoxia

To elucidate the mechanism(s) involved in pericyte-mediated reduction of fibrosis, we performed a cell proliferation assay using murine primary muscle fibroblasts cultured with pericyte-conditioned medium. Fibroblast proliferation was significantly reduced when cultured in hypoxic pericyte-conditioned medium, compared to normoxic controls (Figure 10D, $p=0.011$), suggesting a paracrine anti-fibrotic effect by pericytes in hypoxia. We further proposed a fibrolytic role of pericyte-derived matrix metalloproteinases (MMPs) and examined gene expression of MMP-2 and MMP-9 by real-time qPCR. Cultured pericytes expressed more MMP-2 but nearly 10 times less MMP-9 than total skeletal muscle lysates (tissue origin control) (Figure 10E). We then explored MMP expression in hypoxia-cultured pericytes and demonstrated that MMP-2 expression in pericytes was well sustained under 2.5% oxygen, compared to normoxic culture (Figure 10F, $p > 0.05$), while MMP-9 expression remained extremely low without significant change (Figure 10F, $p > 0.05$).

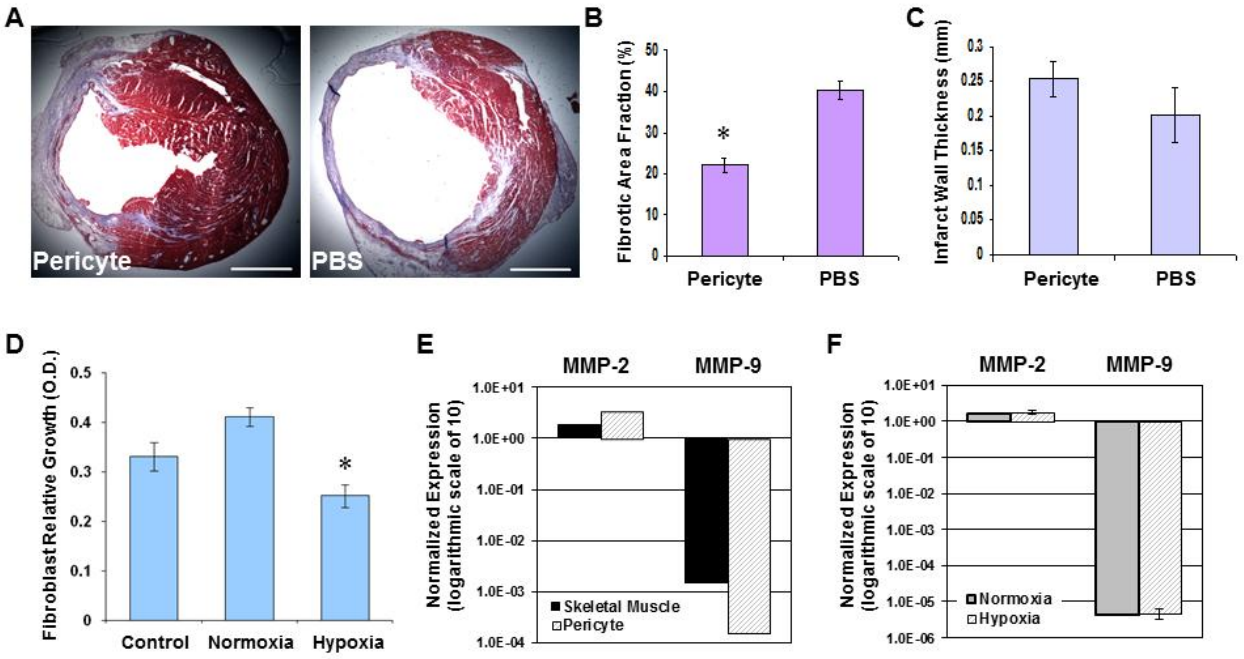

Figure 10: Attenuation of myocardial fibrosis by pericyte-treatment

(A) Masson's trichrome-stained transverse sections of hearts injected with pericytes or PBS (collagen in blue/purple, cardiac muscle in red) (scale bars=1 mm). (B) The fibrotic area fraction was dramatically decreased in pericyte-injected hearts ($p \leq 0.001$). (C) Pericyte group had a non-significant increase in the infarct wall thickness. (D) The proliferation of murine muscle fibroblasts was significantly reduced when culturing with hypoxic pericyte-conditioned medium ($_{*}p=0.011$, versus normoxic pericyte-conditioned medium). (E) Expression of MMP-2 in cultured pericytes was higher than that in skeletal muscle lysates. Conversely, MMP-9 expression in pericytes was nearly 10 times less (logarithmic scale of 10 in arbitrary fluorescence units). (F) Expression of both MMP-2 and -9 in pericytes did not change significantly under hypoxia ($p>0.05$, logarithmic scale of 10 in arbitrary fluorescence units).

3.3.8 Transplantation of pericytes inhibits chronic inflammation

Histological analysis of pericyte- and PBS-injected hearts after hematoxylin and eosin (H&E) staining indicated an increased focal infiltration of inflammatory cells (cluster of cells with dark blue-stained nuclei) within the infarct region in the latter (Figure 11A). To more precisely evaluate the immunomodulatory effect of pericyte transplantation, we detected host CD68-positive monocytes/macrophages by immunohistochemistry. Pericyte-injected hearts exhibited diminished infiltration of host phagocytic cells within the infarct region at 2 weeks post-infarction (Figure 11B). Districts of the myocardium unaffected by the ischemic insult (posterior

and septal walls) contained few CD68-positive cells in either group, similar to healthy hearts (Figure 11C). Quantitatively, injection of pericytes (N=5) resulted in a 34% reduction in infiltration of CD68-positive cells at 2 weeks post-infarction when compared to PBS controls (N=5) (Figure 11D, $p<0.001$).

3.3.9 Paracrine immunomodulation by pericytes

To understand the underlying mechanism of pericyte-induced inhibition of phagocytic cell infiltration, we analyzed the proliferation of murine monocytes/macrophages cultured with pericyte-conditioned medium. Cell proliferation assays revealed that murine monocyte/macrophage proliferation was significantly inhibited when culturing with normoxic ($p=0.018$) and hypoxic ($p<0.001$) pericyte-conditioned media, compared to control medium (Figure 11E). Furthermore, hypoxic pericyte-conditioned medium exhibited a more prominent immunomodulatory effect than the normoxic counterpart (Figure 11E, $p=0.002$). To shed light on the molecules accountable for this paracrine immunomodulation, we investigated by sqRT-PCR the differential expression by pericytes cultured under normoxia or hypoxia of genes implicated in immunoregulation. In either condition, pericytes indeed expressed a considerable array of anti-inflammatory cytokines: IL-6, LIF, cyclooxygenase-2 (COX-2/PTGS-2, prostaglandin endoperoxide synthase-2) and HMOX-1 (Figure 11F). Similarly, monocyte chemotactic protein-1 (MCP-1) and hypoxia-inducible factor-1α (HIF-1α) were highly expressed by pericytes (Figure 11F). Conversely, we detected very low to no expression by pericytes of pro-inflammatory cytokines including interleukin-1α (IL-1α), tumor necrosis factor-α (TNF-α), and interferon-γ (IFNγ) as well as no expression of interleukin-4 (IL-4), interleukin-10 (IL-10), inducible nitric oxide synthase (iNOS), or indoleamine 2,3-dioxygenase (2,3-IDO)

(Figure 11F). Quantitatively, there was no significant alteration of expression under hypoxia of immunoregulatory genes investigated, except MCP-1, whose expression was notably decreased in hypoxia-cultured pericytes (Figure 11G, all $p>0.05$; MCP-1, $p=0.027$).

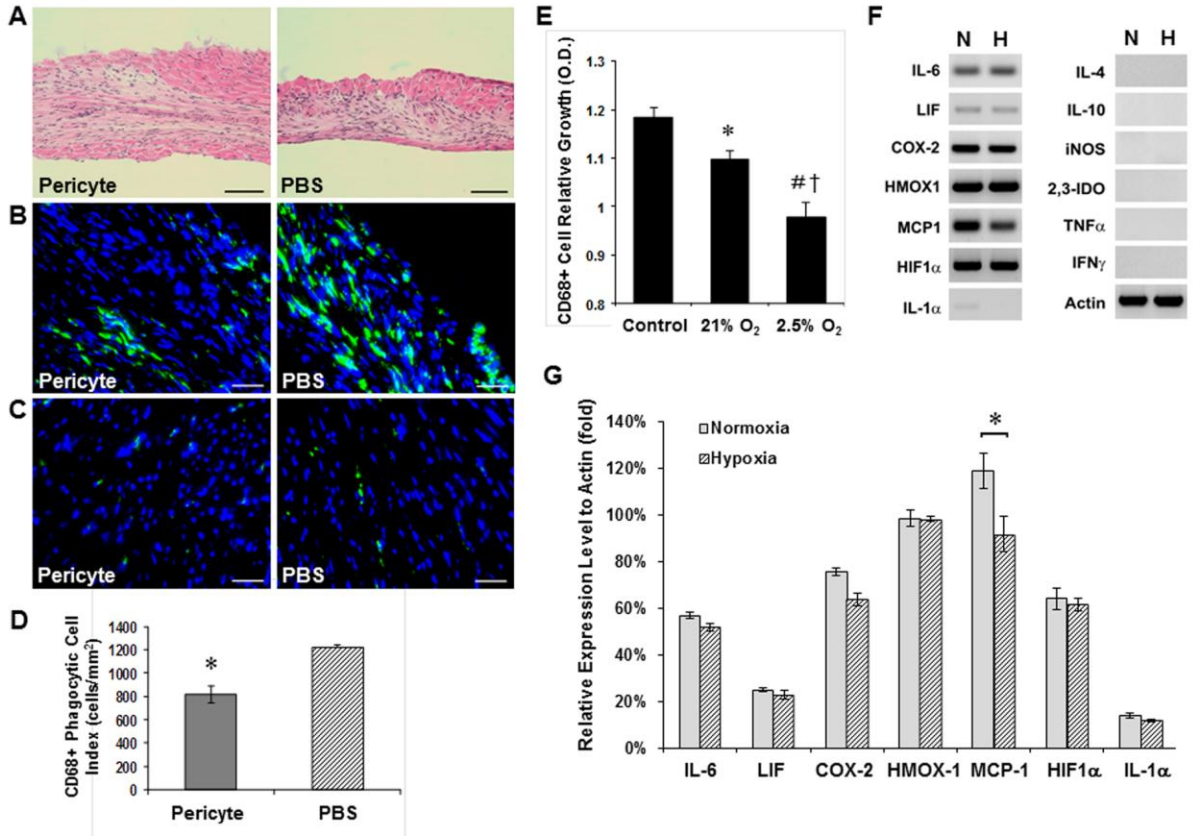

Figure 11: Reduction of host phagocytic cell infiltration by pericyte transplantation

(A) H&E staining revealed a greater focal infiltration of leukocytes (dark blue-stained nuclei) within the infarct region in PBS-injected controls at 2 weeks post-infarction (scale bars=100μm). (B) Anti-mouse CD68 immunostaining showed that the infarct region of pericyte-injected hearts contains less host phagocytic cells (scale bars=50μm). (C) Host CD68-positive cells were locally attracted to the infarct region but not to the unaffected myocardium (posterior ventricular wall) in both groups (scale bars=50μm). (D) Host monocytes/macrophage infiltration at the infarct site was significantly reduced ($p<0.001$). (E) The proliferation of murine macrophages was significantly inhibited when culturing with pericyte-conditioned media ($^{*}p=0.018$, $^{\#}p<0.001$, versus control medium), an effect more prominent with hypoxic pericyte-conditioned medium ($^{\dagger}p=0.002$, hypoxia versus normoxia). (F) Cultured pericytes exhibited sustained, high expression of genes regulating the inflammatory responses, even under 2.5% O_2 (N: normoxia; H: hypoxia). Little expression of IL-1α and no expression of IL-4, IL-10, iNOS, 2,3-IDO, TNF-α, and IFNγ were detected. (G) No statistically significant difference in expression of genes of immunoregulatory molecules between normoxic- and hypoxic-cultured pericytes except MCP-1, which notably decreased in hypoxic cultures (sqRT-PCR analysis, $p=0.027$).

3.3.10 Cell lineage fate of transplanted pericytes

GFP-labeled pericytes were employed to track cell lineages developed from engrafted pericytes and investigate the capacity of human muscle pericytes to reconstitute major cardiac cell types after injury. Immunohistochemistry was performed to simultaneously detect GFP and cell lineage markers: the cardiomyocyte marker, cardiac troponin-I (cTn-I); the smooth muscle cell (SMC) marker, smooth muscle myosin heavy chain (SM-MHC); the endothelial cell (EC) marker, CD31. Confocal microscopy revealed that in the peri-infarct area, a minor fraction of engrafted pericytes co-express GFP and cTn-I (Figure 12A), a few of which appear single-nucleated (Figure 12A, inset). Some GFP-positive cardiomyocytes were identified within the remaining myocardium (Figure 12B) with organized sarcomeric patterns (Figure 12C). A very small number of engrafted pericytes co-expressed GFP and human-specific CD31 (<1%) (Figure 12D-F). Similarly, co-expression of GFP and human-specific SM-MHC was detected in very few donor cells (<0.5%) (Figure 12G-I).

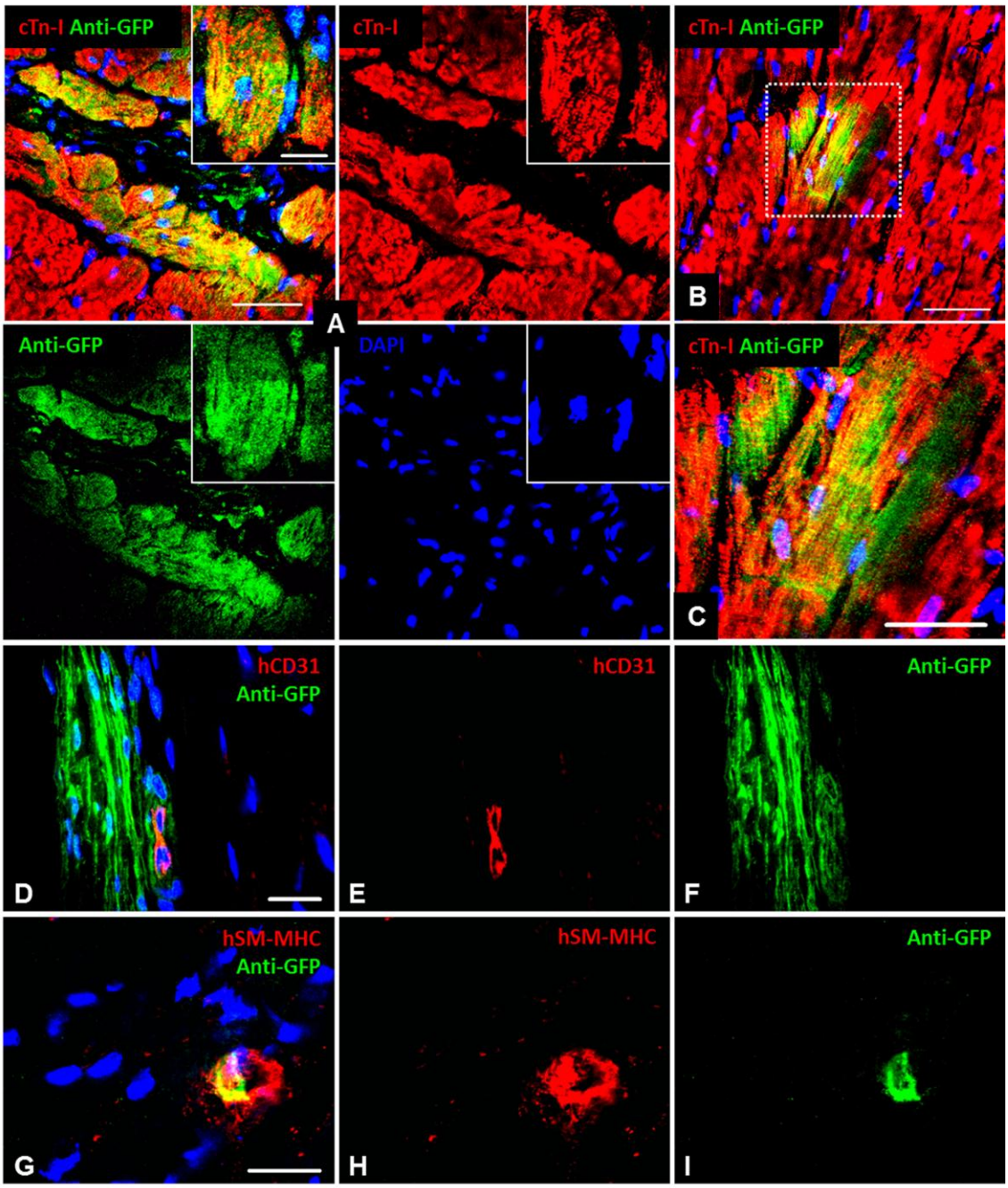

Figure 12: Tracking the cell lineage fate of engrafted pericytes

Confocal microscopy revealed that in the peri-infarct area (A) a minor fraction of GFP-labeled pericytes co-expressed a mature cardiomyocyte marker, cardiac troponin-I (cTn-I) ([A], main, scale bar=50μm); a few of them appear single-nucleated ([A], inset, scale bar=10μm) (cTn-I in red, Anti-GFP in green). (B) Immunofluorescent detection of GFP-cTn-I dual-positive cardiomyocytes integrating within the residual myocardium (scale bar=50μm) with dotted area enlarged in (C) showing sarcomeric patterns (scale bar=20μm). (D-F) A very small number of GFP(+) pericytes (<1%) co-expressed human-specific CD31 (hCD31 in red, Anti-GFP in green; scale bar=10μm). (G-I) Few donor pericytes (<0.5%) expressed human-specific SM-MHC (hSM-MHC in red, Anti-GFP in green; scale bar=10μm).

3.4 DISCUSSION

Pericytes constitute a major structural component of small blood vessels, regulating vascular development, integrity and physiology. The recent identification of microvascular pericytes as native MSC ancestors raised the possibility that these cells participate in the repair of injured/ageing organs[26, 46, 47, 53, 61-63, 112, 113]. Structural and functional regeneration of skeletal muscle involving direct pericyte differentiation into regenerative units as well as potential applications in lung repair and vascular tissue engineering indicate the therapeutic potency of pericytes[26, 46, 53, 54, 112]. Pericytes can also repair tissue via secretion of trophic and immunomodulating factors, implying a greater curative potential in clinical settings [17, 112]. The increased proliferation and migration of pericytes in response to low oxygen concentration and ECM degradation products have important implications for ischemic injury repair[114].

Recent studies indicated a possible developmental hierarchy among different stem/progenitor cell populations residing in blood vessel walls [39, 47]. Katare et al. reported that transplantation of adventitial pericyte progenitor cells repairs infarcted hearts through angiogenesis involving microRNA-132 [56]. Herein we demonstrate that transplantation of human FACS-purified microvascular pericytes contributes to the functional and structural repair of the ischemic heart, albeit unequally, through both of the aforementioned restorative pathways. A major goal of SCCT, the prevention of progressive LV dilatation and consequent heart failure, was largely achieved by pericyte treatment, implicating the attenuation of deleterious remodeling. We also observed significant improvement of cardiac contractility in an acute infarction milieu, with up to 70% of healthy contractile function consistently maintained for at least two months.

No significant difference was observed between adult and fetal pericytes in terms of heart repair. The therapeutic benefits observed could be explained, at least in part, by angiogenic, anti-fibrotic, anti-inflammatory, and to a lesser extent, cardiomyogenic properties of pericytes.

A linear correlation between secretion of pro-angiogenic factors, angiogenesis and cardiac restoration was illustrated by blocking VEGF bioactivity from administered murine muscle-derived stem cells, which not only abolished their stimulation of neovascularization but negatively influenced LV contractility and infarct size [84]. Okada et al. further delineated the superior angiogenic properties of human myoendothelial progenitor cells and secretion of VEGF in response to hypoxia [52]. Given the indigenous vascular association of pericytes, we hypothesized that pericytes are able to repair the damaged microvasculature. Indeed, upon pericyte treatment, we observed a significantly larger host microvascular network not only in the peri-infarct collateral circulation but within the infarct region itself. Cultured pericytes secrete growth factors/cytokines/chemokines related to vascular physiology and remodeling [17]; among which, only VEGF-A, PDGF-β, and TGF-β1 were substantially up-regulated under hypoxia, suggesting their role in pericyte-enhanced angiogenesis [86, 126].

Angiogenesis, and possibly vasculogenesis, may follow cell-cell contact between donor pericytes and host endothelial cells (ECs), in addition to stimulation by angiogenic factors. Recent studies reported that MSCs and vascular mural/adventitial cells support ECs in small blood vessel formation and maturation in culture and *in vivo* [40, 118]. We did observe the perivascular homing of donor pericytes in the ischemic heart. Planar Matrigel culture confirmed the vascular cell characteristics of pericytes and their capability to interact with ECs. We further demonstrated microvessel formation and vascular support by pericytes in three-dimensional cultures, indicating that interaction between pericytes and ECs may contribute to

revascularization. Altogether, these results demonstrate that the angiogenic properties of pericytes may result from both indirect paracrine effects and direct cellular interactions.

The anti-fibrotic action of mesodermal stem/progenitor cells in the injured heart has been widely reported [121-123]. MSC-conditioned medium diminished viability, proliferation, collagen synthesis and α-SMA expression in cardiac fibroblasts but stimulated MMP2/9 activities, indicating a paracrine anti-fibrotic property of MSCs [122, 123]. Our results demonstrated a near 50% reduction of myocardial fibrosis and a trend to abate thinning of the infarcted myocardial wall following pericyte injection. Along with the attenuation of progressive LV dilatation, pericyte treatment appears to result in propitious remodeling, leading to improved myocardial compliance and strengthening of ischemic cardiac tissue.

We speculated that decreased scar formation is, at least partially, associated with a reduced number of fibrotic cells resulting from the administration of pericytes. Interestingly, pericyte-treated hearts contained significantly less cells within the infarct area than saline-injected controls ($p<0.05$, Figure 13). Due to the highly fibrotic nature of MI, we were unable to quantitate fibrotic cells *in vivo*. Nevertheless, murine muscle fibroblast proliferation was notably inhibited when cultured in hypoxic pericyte-conditioned medium *in vitro*, indicating the paracrine fibrosuppressive effect of pericytes under hypoxia. Matrix metalloproteinases (MMPs)

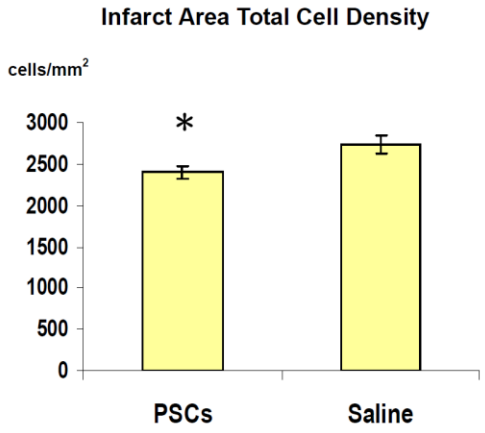

Figure 13: Comparison of total cell density within the infarct area

Pericyte-injected hearts at 2 weeks post-infarction had a significantly less number of cells within the infarct area than the saline-injected controls ($P<0.05$).

were suggested to play important roles in post-injury scar remodeling, angiogenesis, and vascular cell proliferation/migration [123, 126]. In particular, a preponderant role of MMP-2 in preventing collagen accumulation by cardiac fibroblasts was proposed [123]. Consequently, we postulated the existence of a fibrolytic activity from donor pericytes, involving MMPs, which contributes to the attenuation of cardiac fibrosis. Indeed, high expression of MMP-2, but not MMP-9, by pericytes, even under hypoxic conditions, was observed, implicating a role for MMP-2 in pericyte-mediated amelioration of fibrosis.

The immunosuppressive potential of MSCs, demonstrated by inhibiting T-lymphocyte proliferation in culture and counteracting graft-versus-host reaction in recipients of allogeneic blood stem cells, is currently exploited in clinical trials [124, 125]. In the cardiac milieu, MSC transplantation in a rat model of acute myocarditis mitigated the increase in CD68+ phagocytic cells [127]. In the present study, pericyte treatment significantly diminished host monocyte/macrophage infiltration in the infarcted myocardium, suggesting an anti-inflammatory potential which contributed to the reduction of fibrosis, amelioration of adverse remodeling, and improvement of cardiac function. Nevertheless, whether pericytes inhibit the acute-phase

inflammation occurring soon after the incidence of MI is unknown. Inhibition of murine monocyte/macrophage proliferation in culture by pericyte-conditioned medium suggests a paracrine mechanism of their immunomodulatory capacity.

The immunosuppressive and anti-inflammatory capacities of MSCs are primarily attributed to soluble factors/molecules, as IL-6, LIF, and HMOX-1 were shown to exercise beneficial immunosuppressive effects [124, 125]. The attenuation by MSCs of intense inflammation and mitigation by the same cells of multi-organ damage is dependent on monocyte/macrophage-derived cytokines and regulated via PGE_2 signaling [128]. The immunoregulatory and cardioprotective functions of these molecules appear to be similar in the cardiac milieu [119, 129]. Our data demonstrate that pericytes express high levels of IL-6, LIF, COX-2, HMOX-1, and HIF-1α, which are sustained under hypoxic conditions. MCP-1 expression, however, notably decreased under hypoxia, corresponding with reduced CD68+ cell infiltration *in vivo*. Little to no expression of pro-inflammatory cytokines including IL-1α, TNF-α and IFNγ was observed. Virtually no expression of IL-4, IL-10, iNOS, and 2,3-IDO was detected in pericytes, suggestive of an immunoregulatory cytokine secretome that is unique to human microvascular pericytes [125, 130]. Intriguingly, TGF-β1, also an anti-inflammatory yet fibrogenic cytokine, was strongly expressed by pericytes [119, 131]. Given the multiple functions each proposed growth factor/cytokine possesses, it is likely that a dynamic, interactive, and intricately orchestrated balance of trophic factors between donor and host cells holds the key to a successful ischemic tissue remodeling and regeneration.

The potential of human muscle pericytes to reconstitute major cell types in the injured myocardium, though to a small extent, was hereby demonstrated. Cell fate tracking suggests that a minor fraction of engrafted pericytes differentiated into and/or fused with cardiomyocytes.

Given the small number of GFP-cTnI dual-positive cells present, it is unlikely that these differentiated cells contributed significantly to functional recovery [85]. Pericytes, all of which were α-SMA-positive during culture expansion, lost α-SMA expression once homing to host microvasculature (data not shown), consistent with our finding that a subset of native microvascular pericytes do not express α-SMA *in situ* [26].

3.5 CONCLUSION

In summary, purified human microvascular pericytes contribute to anatomic and functional cardiac improvement post-infarction through multiple cardioprotective mechanisms: reverse of ventricular remodeling, promotion of host angiogenesis, reduction of cardiac fibrosis, and diminution of chronic inflammation. Vessel-homing and small-scale regenerative events by pericytes partially reconstitute lost cardiac cells and contribute to the structural recovery. These cardioprotective and cardioregenerative activities of a novel stem cell population that can be purified to homogeneity and expanded *in vitro* await further research and exploitation in ischemic cardiovascular diseases. Due to the extensive local inflammatory response and tissue adhesion resulted from myocardial and infarction open-chest surgery, it is technically more difficult to handle and process samples harvested at 8 weeks post-surgery for histological examination. I am currently improving my surgical techniques to overcome this deficit.

3.6 ACKNOWLEDGEMENTS

The authors wish to thank Alison Logar for technical assistance in flow cytometry, Dr. Bin Sun for expert assistance in real-time qPCR, Dr. Simon Watkins for confocal microscopy, Dr. Bing Wang for lentiviral-GFP vectors, James H. Cummins for editorial assistance, and Dr. Yun Fang for expert advice.

4.0 HUMAN HEART PERICYTES: MULTIPOTENT MESODERMAL PROGENITORS WITHIN THE MYOCARDIUM EXHIBITING TISSUE SPECIFICITY

4.1 INTRODUCTION

The human heart has long been considered a terminally differentiated organ with no regenerative capacity [108]. However, recent discoveries of resident cardiac stem/progenitor cells as well as active cardiomyocyte turnover throughout the adult human life raise the possibility that the human heart has an innate yet restricted regenerative potential [96, 132-135]. In fact, the heart is a complex organ comprising a variety of muscle and non-muscle cells, including cardiac and smooth muscle, endothelial, stromal/interstitial, valvular, and pacemaker/conduction cell types with discrete contractile, vascular, structural, and electrical roles [18, 108]. Collaborative efforts from multiple cell types operating in a temporally and spatially coordinated fashion may hold the key for successful regeneration of functional cardiac tissue [18]. It is therefore important to apprehend the significance of subpopulations of non-muscle cells in physiological and pathological cardiac regeneration.

Microvascular mural cells, i.e. pericytes, tightly surround capillaries and microvessels and play significant roles in vascular development, physiology and structural integrity [30, 136]. The essential function of pericytes to recruit and stabilize endothelial cells (ECs) is critical to the success of angiogenesis during the maturation and remodeling phase [30, 136]. We and others

have recently shown that pericytes purified from a number of human organs, such as skeletal muscle, adipose, placenta, umbilical cord, and pancreas, possess multi-lineage differentiation potential and stem/progenitor cell features [17, 26, 46, 53, 113, 137]. Pericytes regenerate injured and dystrophic skeletal muscles efficiently in murine models, showing great promise in regenerative medicine [26, 46, 53, 113]. Additionally, several populations of tissue-specific precursor cells have also been associated with the perivascular niche, indicating the important roles of vascular mural cells in tissue turnover and regeneration [9, 61, 106]. Nevertheless, it remains to be tested whether native cardiac pericytes exhibit the same phenotypes and mesodermal multipotency as their counterparts in other tissue. Furthermore, their putative roles in cardiac repair/regeneration and potential relationship to resident cardiac stem/progenitor cells await exploration.

Another important question yet to be answered is whether all pericytes are born equal. It has been shown that the pericyte population appears to be highly variable physiologically among different organs and tissues, possibly reflecting their roles in regulating hydrostatic pressures and vascular homeostasis [138]. However, due to the difficulty to purify multiple pericyte populations from different tissue sources simultaneously, it remains unknown if any tissue specificity exists in terms of multipotency and/or distinct cellular behaviors in response to pathological conditions.

In this study, we reported the identification, prospective purification, and characterization of resident heart pericytes (HPs). We described their cellular phenotypes, behaviors, and multipotency in long-term culture. By comparing HPs with skeletal muscle-derived pericytes (SkMPs), we investigated the possibility that tissue specificity and/or differential responses to

pathophysiological conditions exist among pericytes of developmentally and functionally different origins.

4.2 METHODS AND MATERIALS

4.2.1 Human tissue biopsies

In total, 4 adult and 16 fetal human heart specimens were independently used for immunohistochemistry and cell isolation. Human adult cardiac biopsies were obtained at postmortem from subjects that had died from non-cardiac causes. The usage of adult cardiac tissue was approved by Tayside Committee on Medical Research Ethics, NHS Scotland. Human fetal tissues (17 to 23 weeks of gestation) were obtained following voluntary or therapeutic pregnancy interruptions performed at Magee Womens Hospital of UPMC, in compliance with IRB protocol 0506176. Developmental age was estimated by measuring foot length. Informed consent for the use of human fetal tissues was obtained from patients in all instances.

4.2.2 Cell isolation

Fresh human adult and fetal cardiac tissues were processed for the cell isolation. Briefly, atria, heart valves, and major blood vessels were grossly removed, followed by microscopic removal of pericardium and endocardium from the ventricles. Ventricular myocardium was first cut into small pieces in Dulbecco's modified Eagle medium (DMEM, Invitrogen) containing 10% fetal bovine serum (FBS, Invitrogen), 1% penicillin-streptomycin (PS, Invitrogen), mechanically

minced, and subsequently digested with collagenases I, II and IV (1 mg/mL, Sigma) for 15-20 minutes, depending on the sample size, under agitation at 37°C. After centrifugation, pellets were washed and resuspended in erythrocyte lysis buffer (155 mM NH_4Cl, 10mM $KHCO_3$, 0,1mM EDTA) and incubated for 10 min at room temperature (RT). Cells were then washed and sequentially filtered through 100- and 70-μm cell strainers (BD Falcon) to obtain single cell suspension. Fresh human fetal muscle biopsies obtained from the same donor were processed for the cell isolation according to the previously published protocol.

4.2.3 Fluorescence-activated cell sorting (FACS) and flow cytometry analysis

4.2.3.1 Cell sorting

For cell sorting, cells ($2\text{-}5x10^6$) were incubated with all of the following fluorochrome-conjugated mouse anti-human antibodies (all with 1:100 dilutions): anti-CD34-APC (Becton-Dickinson), anti-CD45-APC-Cy7 (Santa Cruz), anti-CD56-PE-Cy7, anti-CD117-PE, and anti-CD146-FITC (all from Serotec) in DMEM supplemented with 5% FBS and 1% PS at 4℃ for 20 min in the dark. As negative controls, isotype-matched mouse IgGs conjugated with APC, PE-Cy7 (both from Becton-Dickinson), APC-Cy7 (Santa Cruz), PE and FITC (both from Chemicon), were used. After washing, all labelled cells were incubated with 7-amino-actinomycin D (7-AAD) (Becton-Dickinson, 1:100) for dead cell exclusion and then sorted on a FACSAria flow cytometer (Becton-Dickinson). Purified HPs ($CD146^{high}CD34^-CD45^-CD56^-CD117^-$) were collected for culturing. Skeletal muscle-derived pericytes (SkMPs) were sorted according to the previously published protocol.

4.2.3.2 Flow cytometry analysis

Flow cytometry was employed to examine the expression profile of cell lineage markers. Briefly, freshly sorted HPs or cultured HPs at different passages were labelled with the following fluorochrome-conjugated antibodies (all with 1:100 dilutions): anti-CD34-APC, anti-CD44-PE, anti-CD90-APC, anti-CD146-PE, anti-platelet-derived growth factor receptor-β (PDGFRβ)-PE (all from Becton-Dickinson), anti-CD73-PE, anti-CD105-PE (both from Invitrogen), anti-CD45-APC-Cy7 (Santa Cruz), anti-CD56-PE-Cy7, anti-CD117-PE, and anti-CD146-FITC (all from Serotec), for 20 min at 4℃ and subsequently analyzed on a FACSAria flow cytometer.

4.2.4 Cell culture and cell labelling

4.2.4.1 Cell culture

Freshly sorted HPs were initially seeded at $2x10^4$ cells/cm^2 in endothelial cell growth medium 2 (EGM-2™, Lonza) and cultured at 37℃ for 2 weeks in plates coated with 0.2% gelatin (Calbiochem) until confluence. HPs were then detached by 0.25% trypsin-EDTA treatment (Invitrogen) for 10 min at 37℃, split at 1:3 in uncoated plates in DMEM high glucose (Invitrogen) supplemented with 20% FBS and 1% PS. After the third passage, cells were passaged 1:5-1:6 and maintained in the same conditions with culture medium changed every 3-4 days. We calculated the population doubling time (PDT) as previously described. Sorted SkMPs were expanded and maintained in the same conditions as HPs. Single donor-derived human umbilical cord vein endothelial cells (HUVECs) were purchased from Lonza and cultured in EGM-2™, following the manufacturer's instructions.

4.2.4.2 Cell labelling

For the gene transfer of green fluorescence protein (GFP), cultured HPs at passages 5-7 were detached with trypsin-EDTA and seeded at a density of 10,000 cells/cm^2. After 24-48 hours, medium was replaced with the transduction medium (α-MEM, 10% FBS, 1% P/S, and 8 μg/mL polybrene) when the culture was reaching 60-70% confluence, and a lentivirus-based CMV-driven eGFP expression vector was added at a MOI of 10. Following incubation for 16-18 hours at 37℃, the transduction medium was removed and replenished by complete culture medium. Three days later, nearly 100% of cells expressed GFP. GFP-labeled cells were further expanded in regular culture medium for 1-2 passages without significant adverse effect. For short-term *in vitro* experiments, cells were labelled with cell membrane dye, PKH26 (Red) and PKH67 (Green) (both from Sigma-Aldrich), following the manufacturer's instructions. Dye-labelled cells were applied to experiments immediately after labelling without further expansion.

4.2.5 Immunohistochemical and immunocytochemical analyses

Sections were fixed in a pre-cooled (-20℃) mixture of methanol (Fisher Scientific) and acetone (VWR International) (1:1) for 5 min or in pre-cooled acetone for 5 min (for human spectrin) prior to staining. For immunocytochemistry, cultured HPs were washed twice with PBS and fixed in a pre-cooled methanol for 5 min. Non-specific antibody binding was blocked with 5% donkey or goat serum for 1 hour at room temperature (RT) and, if necessary, with the Mouse-on-Mouse (M.O.M.) antibody staining kit (Vector Laboratories). The following uncoupled primary antibodies were used: mouse anti-human CD31 (Santa Cruz), CD144 (Beckman Coulter), chondroitin sulphate (NG2), CD34, CD146 (all from Becton-Dickinson), and PDGFRβ (R&D Systems) (all at 1:100 dilutions); CD44, CD90 (both from Becton-Dickinson), CD73, CD105

(both from Invitrogen), and smooth muscle-myosin heavy chain (DAKO) (all at 1:50 dilutions) at 4℃ overnight. The following coupled primary antibodies were used: anti-mammalian alpha-smooth muscle actin (αSMA)-FITC (Sigma-Aldrich) and von Willebrand factor (vWF) (US Biological), biotinylated anti-human CD144 (Becton-Dickinson) (all at 1:100 dilutions), biotinylated anti-human CD146 (Miltenyi Biotec, 1:20). Skeletal muscle proteins were detected with anti- fast skeletal myosin heavy chain, anti-slow skeletal myosin heavy chain, anti-desmin (all from Sigma-Aldrich), anti-spectrin (Novocastra) (all at 1:100 dilutions). Directly biotinylated *Ulex europaeus* lectin (UEA-1) was also used as an endothelial cell marker (Vector Laboratories, 1:200).

After rinsing with PBS three times, sections were incubated for 1 hour at RT with a fluorochrome-conjugated secondary antibody at 1:400 dilutions, including anti-mouse Alexa^{TM}488 IgG, and anti-mouse-Alexa^{TM}555 IgG (both from Molecular Probes); or with biotinylated secondary antibody and then with fluorochrome-coupled streptavidin (both at 1:500 dilutions), including goat anti-mouse biotinylated IgG antibodies (DAKO and Immunotech), Streptavidin-Cy3 (Sigma-Aldrich), and Streptavidin-Cy5 (CyDye); all diluted in 5% donkey or goat serum in PBS. Nuclei were stained with DAPI (4', 6-diamino-2-phenylindole dihydrochloride, Molecular Probes, 1:2000) for 5 min at RT. An isotype-matched negative control was performed with each immunostaining. Slides were mounted in glycerol-PBS (1:1, Sigma) and observed on an epifluorescence microscope (Nikon Eclipse TE 2000-U). Alternatively, sections were analyzed on an Olympus Fluoview 1000 confocal microscope equipped with 100X oil immersion optics.

4.2.6 Multi-lineage differentiation in culture

4.2.6.1 Osteogenesis

For in vitro bone formation, cells at 70% confluence were cultivated in DMEM supplemented with 10% FBS, 0.1µM dexamethasone, 50µg/mL L-ascorbic acid, and 10mM beta-glycerophosphate. Three weeks later, cells were fixed in 4% formaldehyde for 2 min and incubated for 10 min with alizarin red, pH 4.2 for the detection of calcium deposits (all reagents from Sigma-Aldrich).

4.2.6.2 Chondrogenesis

Pellet culture was performed by spinning down $3x10^5$ cultured cells in each 15ml conical tube (BD Falcon) and grown in serum-free DMEM containing an insulin-transferrin-selenious acid mix (ITS) (Becton-Dickinson), 50µg/ml L-ascorbic acid 2-phosphate (WAKO), 100µg/ml sodium pyruvate, 40µg/ml L-proline (both from Invitrogen), 0.1µM dexamethasone (Sigma-Aldrich) and 10ng/ml transforming growth factor β1 (TGF-β1; Peprotech). Three weeks later, pellets were fixed in 10% formalin, dehydrated in ethanol and embedded in paraffin. Sections (5µm thick) were rehydrated and stained with Alcian blue and nuclear fast red for the detection of sulfated glycosaminoglycans and nuclei, respectively.

4.2.6.3 Adipogenesis

Cultured cells at 70% confluence were switched to adipogenic medium: DMEM containing 10% FBS, 1µM dexamethasone, 0.5µM isobutylmethylxanthine, 60µM indomethacine, and 170µM insulin (all from Sigma-Aldrich). Two weeks later, cells were fixed in 2% PFA at RT, washed in 60% isopropanol and incubated with Oil red O for 10 min at RT for the detection of lipids.

4.2.6.4 Skeletal myogenesis

Cells ($2x10^3$ cells/cm^2) were cultured for 7 days in muscle proliferation medium: DMEM high-glucose supplemented with 10% FBS, 10% horse serum (HS, Invitrogen), 1% chicken embryo extract (CEE, Accurate), and 1% PS, and then for additional 7 to 10 days in muscle fusion medium: DMEM high-glucose supplemented with 1% FBS, 1% HS, 0.5% CEE, and 1% PS. Half of the medium was renewed every 3-4 days. Skeletal myogenesis was induced by lowering total serum concentration from 20% to 2% until elongated, multinucleated skeletal myofibers appeared.

4.2.6.5 Cardiomyogenesis

Cultured pericytes were seeded at $2x10^3$ cells/cm^2 and further cultured for 1-2 days in pericyte medium. The medium was then replaced with cardiomyogenic induction medium: DMEM high-glucose supplemented with 5% FBS, 1% PS, and 10μM 5-azacytidine for 72 hours. After washing, cells were cultured in pericyte medium for additional 2 weeks.

4.2.7 Myogenesis in vivo

To examine myogenesis of human heart pericytes in vivo, we performed cell transplantation in an immunodeficient murine muscle injury model. The Institutional Animal Care and Use Committee at Children's Hospital of Pittsburgh of UPMC and University of Pittsburgh approved the animal usage and surgical procedures performed in this study (Protocol 15-04 and 0810310). A Total of 8 female SCID-NOD mice (4-6 weeks old) (Jackson Laboratory, Bar harbor, ME, USA) were used for this study.

Briefly, SCID-NOD mice were anaesthetized by inhalation of isoflurane/O_2. Cardiotoxin (CTX, 15 μg, Molecular Probes), diluted in 20 μL PBS, was injected into the gastrocnemius muscle three hours prior to cell transplantation. Mice were re-anaesthetized, and 5.0×10^4 cells suspended in 30 μL PBS (or the same volume of PBS as a control) were slowly injected into the injured muscle. Mice were sacrificed 2 weeks later, and muscle was flash frozen in in 2-methylbutane (Sigma-Aldrich) pre-cooled in liquid nitrogen and embedded in tissue freezing medium (Triangle Biomedical Sciences). Samples were preserved at -80℃ and cryosectioned at 8-10 μm thickness.

4.2.8 Hypoxia assay

To assess the influence of the hypoxic environment to human HPs and SkMPs, we cultured cells under 2.5% O_2 conditions *in vitro* as formerly described [52]. Concisely, HPs were seeded in 6-well culture plates and allowed the cells to reach 80-90% confluence under the ambient oxygen concentration (21% O_2). Upon the transition to low O_2 conditions, the complete culture medium was removed and cells were washed twice with PBS before defined, serum-free DMEM medium was added. Twenty-four hours later, the culture supernatant and cell lysates were collected for analysis. Cells cultured under 21% O_2 with the serum-free medium served as controls.

4.2.9 RT-PCR

Total RNA was extracted from 10^4 cells using the Absolutely RNA nanoprep kit (Stratagene). cDNA was synthesized with SuperScript™ II reverse transcriptase (Invitrogen). PCR was performed for 30 cycles at 58℃ annealing temperature with Taq polymerase (Invitrogen), and

PCR products were electrophoresed on 1% agarose gels. Each set of oligonucleotides was designed to span two different exons so that genomic DNA contamination is of no concern.

4.2.10 Matrigel culture/co-culture in vitro

Cell culture and co-culture experiments using 2D and 3D Matrigel systems were performed, and capillary-like network formation was observed. In brief, 350µl of Matrigel (Becton-Dickinson) was placed in each well of a 24-well plate and incubated at 37℃ for 30 min. Fifty thousand HPs were trypsinized, washed, and re-suspended in 700µl of EGM2^{TM} and subsequently seeded onto Matrigel-coated well. Experiments using 5x10^4 HUVECs and 5x10^4 SkMPs were performed as controls. A 2D co-culture system using cells pre-labeled with cell membrane dye (PKH26 red and PKH67 green fluorescent dye, Sigma-Aldrich) was used to observe HP-HUVEC interactions. Briefly, 5x10^4 PKH26-labeled HUVECs (red) and 5x10^4 PKH67-labeled HPs (Green) were well mixed, re-suspended in 700µl of EGM2^{TM}, seeded onto Matrigel in a 24-well plate, and further cultured for 24 hours. An *in vitro* 3D Matrigel culture/co-culture system was developed to investigate vascular support by HPs. In short, 25x10^4 PKH67-labeled HPs (green) were re-suspended in EGM2^{TM} and well mixed with 350µl of Matrigel in a 3:1 ratio before being encapsulated into one well of a 24-well plate and subsequently incubated for 72 hours. Small amount of EGM2^{TM} was added after gelation and exchanged every 24-48 hours. Experiments using 25x10^4 PKH26-labeled were performed as controls. A 3D co-culture system using 25x10^4 PKH26-labeled HUVECs (red) and 25x10^4 PKH67-labeled HPs (green) was performed in the same manner and subsequently cultured for 72 hours. Another set of Matrigel co-culture plug was simultaneously exposed to hypoxic environment (2.5% O_2) for 72 hours. The same

experiments using PKH67-labeled SkMPs (green) were performed for comparison. All images were taken using an epi-fluorescence microscope (Nikon Eclipse TE 2000-U).

4.2.11 Statistical analysis

All measured data are presented as mean ± standard deviation (SD). Statistical differences were analyzed by Student's *t*-test (two groups) or one-way ANOVA (multiple groups) with 95% confidence interval. The Student-Newman-Keuls multiple comparison test was performed for post-hoc analysis of one-way ANOVA. Statistical analyses were performed with SigmaStat statistics software.

4.3 RESULTS

4.3.1 Identification of resident human microvascular pericytes within the ventricular myocardium

To investigate whether microvascular pericytes residing in human ventricular myocardium express the previously defined combination of pericyte markers, we used immunohistochemistry to examine two adult and five fetal human ventricular biopsies. We observed consistent expression of known pericyte markers by human myocardial perivascular cells surrounding microvessels (diameter between 10-100μm) and capillaries (diameter less than 10μm), including NG2 (Figure 14A) and CD146 (Figure 14A-B and D-F), α-smooth muscle actin (αSMA) (Figure 14B), smooth muscle myosin heavy chain (SM-MHC) (Figure 14B), and PDGFRβ (Figure 14C).

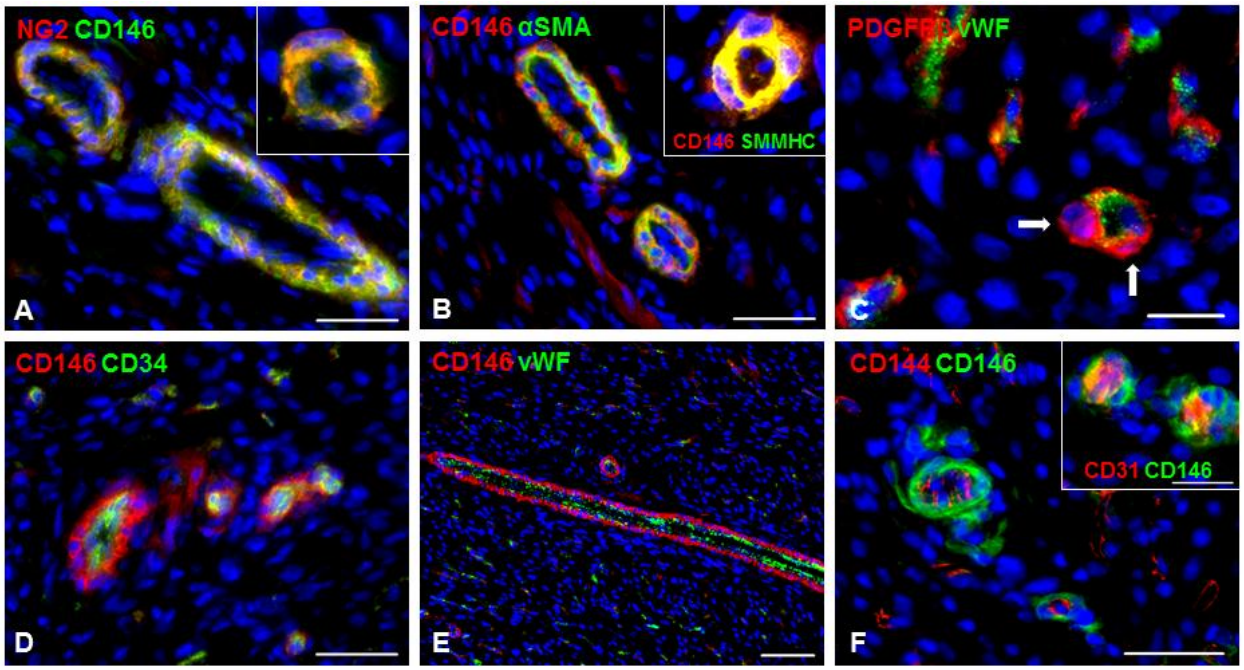

Figure 14: Identification of resident microvascular pericytes within human myocardium

Perivascular cells residing in the microvessels of various sizes are identified by (A) co-expression of CD146 (green) and NG2 (red) (main and inset both X600) and (B) co-expression of CD146 (red) and α-SMA (main, green) or SM-MHC (inset, green) (main and inset both X600). (C) Pericytes (white arrows) stained positive for PDGFR-β (red) surround vWF-positive endothelial cells (green) (X900). (D) Microvascular endothelial cells marked by CD34 expression (green) are enclosed by CD146-positive perivascular cells (red) (X600). (E) A longitudinal section of the ventricular myocardium shows that endothelial cells marked by vWF (green) are surrounded by perivascular cells detected with an antibody against CD146 (red) (X200). (F) Transverse sections of microvessels display that CD146-positive pericytes (green) surround CD144(+) (main, red, X600) and CD31(+) (inset, red, X900) endothelial cells. (scale bars = 100 μm at X200, 50 μm at X600, and 20 μm at X900)

Co-expression of NG2 and CD146 (Figure 14A main and inset), CD146 and αSMA (Figure 14B main) as well as CD146 and SM-MHC (Figure 14B inset) by myocardial perivascular cells was detected at microvessels of different sizes. PDGFRβ was also detected in all perivascular cells (Figure 14C, white arrows). Consistent with our previous reports, endothelial cell (EC) markers, including CD34 (Figure 14D), von Willebrand factor (vWF) (Figure 14C and E), CD144 (VE-cadherin) (Figure 14F main), and CD31 (Figure 14F inset), were not expressed by myocardial perivascular cells. Similar to microvascular pericytes in other tissues, expression of αSMA and SM-MHC were only noted in cells surrounding arterioles and venules but not around capillaries. Moreover, myocardial perivascular cells did not express

CD117 (c-kit) (Figure 15A-C, purple arrows) while approximately one third of CD117+ cells within the ventricular myocardium were located juxtapose to CD146+ pericytes and/or vWF+ ECs in microvessels/capillaries (Figure 15A-D, red arrows). These results indicate native cardiac heart pericytes display the same exclusive pericyte/perivascular cell surface phenotype as those found in other human organs.

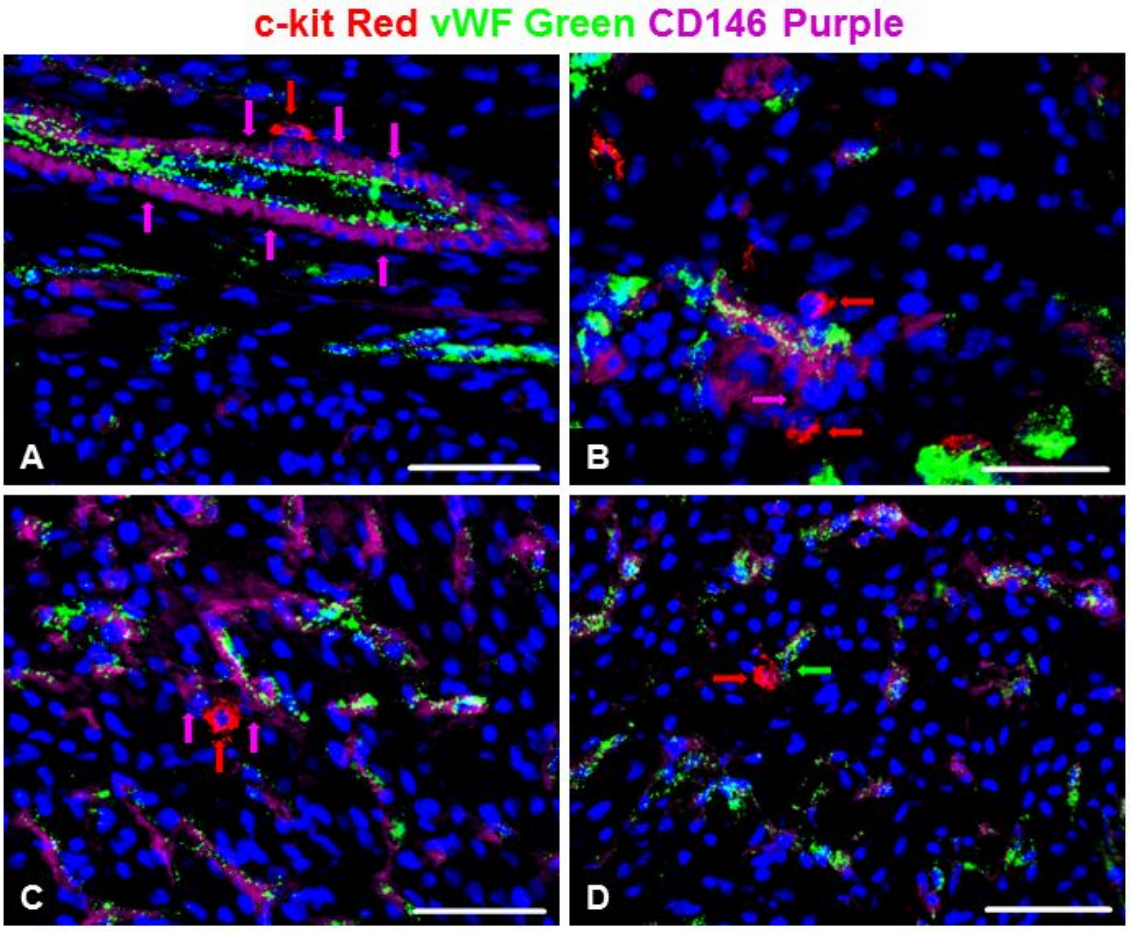

Figure 15: Human heart pericytes do not express c-kit in situ

We did not observe native co-expression of c-kit and CD146 in resident heart pericytes in all samples examined (N=5 hearts) (A-D). Nevertheless, a fraction of c-kit+ cells (red arrows) reside anatomically adjacent to capillaries/microvessels, juxtapose to CD146+ pericytes (A-C, purple arrows) and/or vWF+ endothelial cells (D, green arrows). (All pictures are taken at X400, scale bars=50μm)

4.3.2 Purification and culture of human heart pericytes

To prospectively purify human HPs using multi-color fluorescence-activated cell sorting (FACS), two adult and 12 fetal (17 to 23 weeks) heart biopsies were independently processed. Briefly, epicardium and endocardium were microscopically removed from all biopsies, and only ventricular myocardium was harvested for cell isolation, followed by mechanical dissociation and collagenase digestion. Before being subjected to fluorescence-activated cell sorting (FACS) for purification, cells were stained with fluorescence-conjugated antibodies to a panel of selective cell lineage markers, including CD34 (progenitor/endothelial cells), CD45 (leukocytes/hematopoietic cells), CD56 (neural/myogenic/NK cells), CD117 (hematopoietic/cardiac precursor cells), and CD146 (pericyte/endothelial cells). To be devoid of contamination from circulating hematopoietic and/or resident cardiac precursor cells, CD117+ cells were initially gated out of myocardial cell suspensions, followed by the exclusion of CD45+ and CD56+ cells as described in our previously published protocols (Figure 16A). Heart pericytes (HPs) were subsequently identified and gated by robust CD146 expression with the absence of CD34, the latter used to ensure the avoidance of EC contamination (Figure 16A). HPs ($CD146^{+}CD34^{-}CD45^{-}CD56^{-}CD117^{-}$) were sorted to homogeny at a frequency of 1.21 ± 0.52%, similar to the reported ratio of pericytes ($CD146^{+}CD34^{-}CD45^{-}CD56^{-}$) present in other organs.

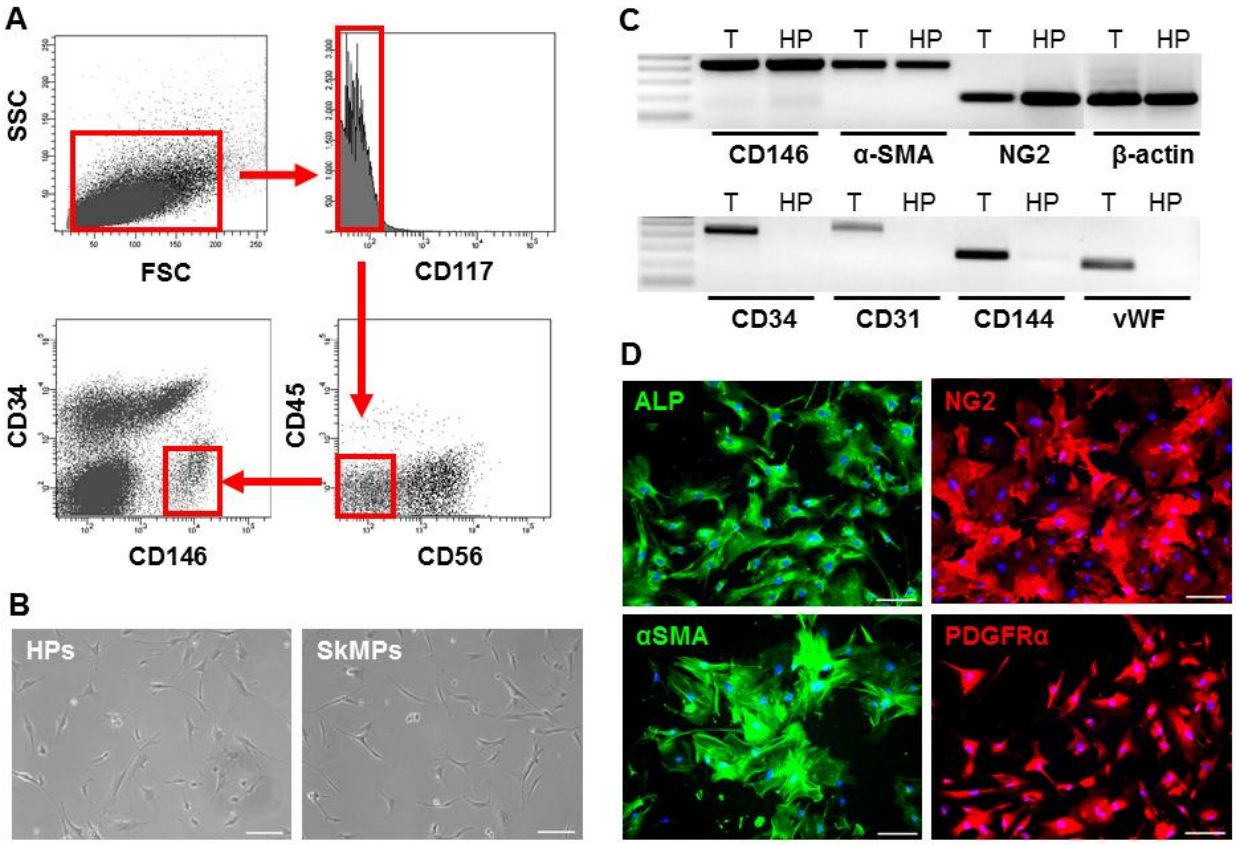

Figure 16: Purification and culture of ventricular microvascular pericytes

(A) FACS sorting of ventricular microvascular pericytes: CD117(-) fraction was first separated, followed by the selection of CD45(-)CD56(-) fraction, and finally separated by CD34(-)CD146(+) selection of heart pericytes (HPs). (B) The morphology of cultured heart pericytes (HPs, left panel) was very similar to that of skeletal muscle pericytes (SkMPs, right panel) (X100, Scale bars = 200 μm). (C) RT-PCR analysis confirmed that sorted HPs express pericyte markers: CD146, αSMA, and NG2 but not endothelial cell markers: CD34, CD31, CD144, and vWF. (D) Cultured HPs express typical pericyte markers, including ALP, NG2, αSMA as well as PDGFRα, revealed by immunocytochemistry.

Sorted HPs were cultured in typical pericyte medium, commonly exhibiting an elongated, rectangular morphology with extended arms, similar to their skeletal muscle counterparts at sub-confluence (Figure 16B). RT-PCR confirmed the homogeneity of freshly sorted HPs (Figure 16C). Purified HPs can be cultured over the long term and maintain the expression of selection marker profile (Figure 17A). The cell growth of HPs in long-term culture is comparable with skeletal muscle-derived pericytes: a population doubling time (PDT) of approximately 60 hours at passage 3-12, no apparent contact inhibition at confluence, occasional

formation of spherical structures at early passages (Figure 17B), and maximal population doublings of forty or more, except a seemingly shorter initial growth retardation (first 4 weeks after sorting). Immunocytochemistry revealed that cultured HPs express common pericyte markers such as alkaline phosphatase (ALP), NG2, αSMA as well as PDGFRα (Figure 16D). Further analyses using flow cytometry demonstrated expression of classic MSC markers by cultured HPs, including CD44, CD73, CD90, and CD105, similar to pericytes of other origins (Figure 17C).

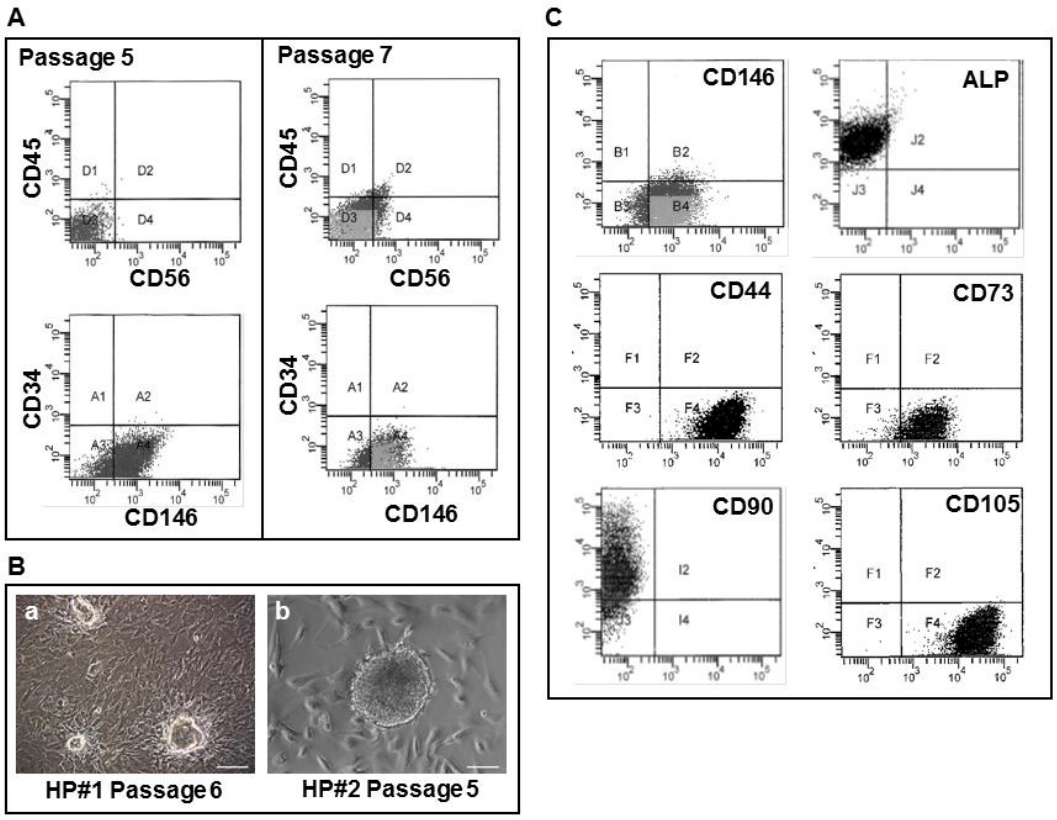

Figure 17: Heart pericytes stably express FACS-selection and MSC marker profile in long-term culture

(A) Purified heart pericytes were maintained in culture for 9 weeks and analysed by flow cytometry for FACS-selection marker expression. Cells were detached with trypsin and stained with fluorescence-conjugated antibodies: CD34-APC, CD45-APC-Cy7, CD56-PE-Cy7, and CD146-FITC. Analyses were performed with the same gating used to sort heart pericytes. (B) Representative pictures showing that cultured HPs from two donors, designated HP#1 (a) and #2 (b), occasionally form spherical structures at early passages with no obvious contact inhibition at confluence (scale bars: (a)=200μm, (b)=100μm) (C) Long-term cultured heart pericytes were also analysed for expression of pericyte/stem cell marker, CD146 and alkaline phosphatase (ALP), as well as classic MSC markers, including CD44, CD73, CD90, CD105.

4.3.3 Heart pericytes support microvascular structures yet exhibit distinctive behaviors in response to hypoxia

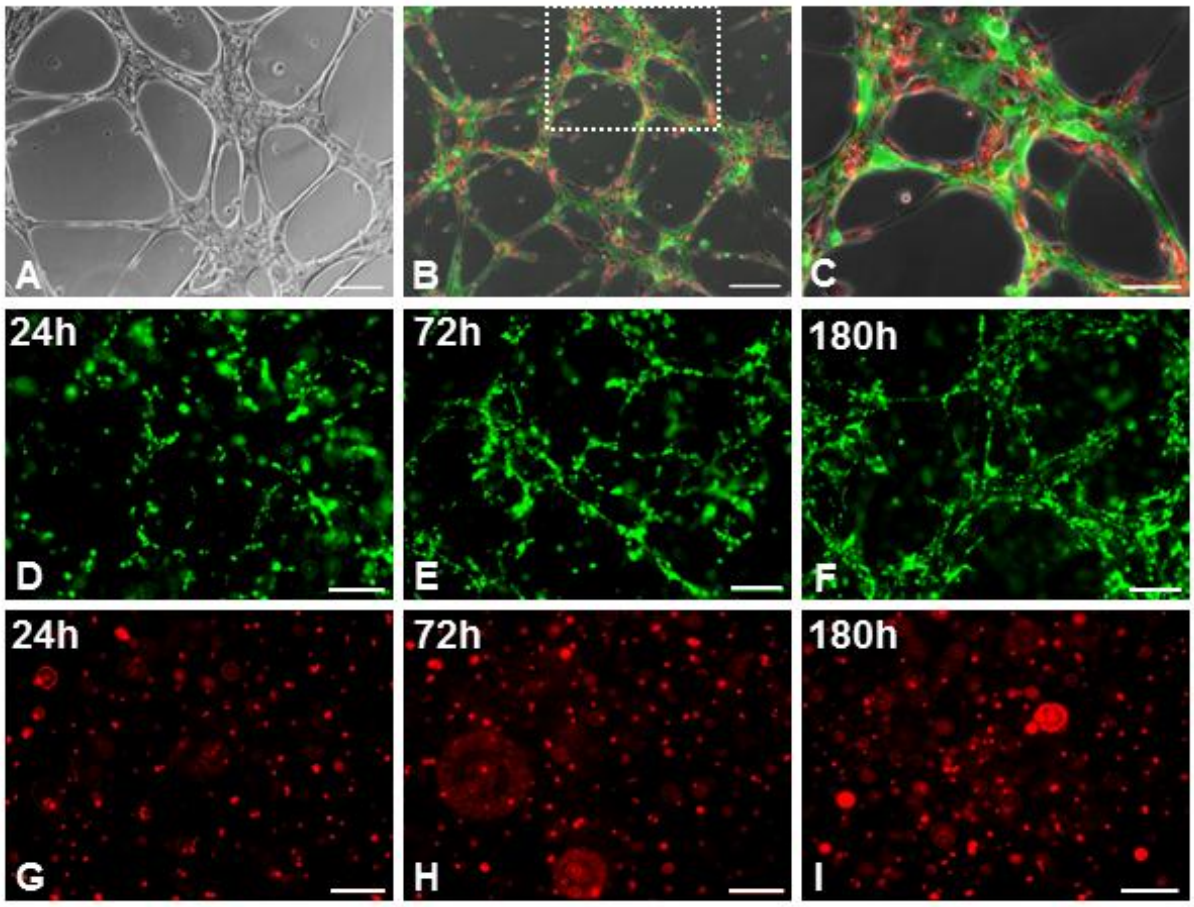

Figure 18: Heart pericytes form capillary-like networks in 2D and 3D Matrigel culture

(A) Human heart pericytes seeded onto Matrigel-coated wells formed typical capillary-like networks within 6-12 hours. (B) Dye-labeled pericytes (green) and HUVECs (red) co-formed capillary-like networks within 6-12 hours. (C) Enlargement of the dotted area in (B) showed that HUVECs (Red) appear to line and spread out on top of the pericyte-formed structures (Green). (D-F) To simulate native capillary formation, heart pericytes were evenly encapsulated into 3D Matrigel plug for up to 180 hours. Pericytes formed 3D networks with structural organization and maturation over time. (G-I) HUVECs were encapsulated into 3D Matrigel plug in the same manner but unable to form any organized structure. (All pictures are taken at X100, scale bars = 200 μm, except (C) taken at X200, scale bars = 100 μm)

To demonstrate that HPs support the integrity of microvascular structures, we used 2D and 3D Matrigel culture/co-culture systems. HPs alone seeded onto Matrigel-coated wells formed

capillary-like networks within 6-12 hours (Figure 18A), resembling those formed by HUVECs in 24 hours (not shown). Dye-labeled HPs (green) and HUVECs (red) co-formed capillary-like networks within 6-12 hours (Figure 18B), with HUVECs appearing to line and spread out on top of HP-formed structures (Figure 18C). To mimic native capillary formation, 3D Matrigel plugs encapsulating evenly distributed HPs or HUVECs were cultured. Dye-labeled HPs formed 3D capillary-like networks with structural maturation and remodeling over time (Figure 18D-F) while HUVECs did not form any organized structure in the same condition (Figure 18G-I).

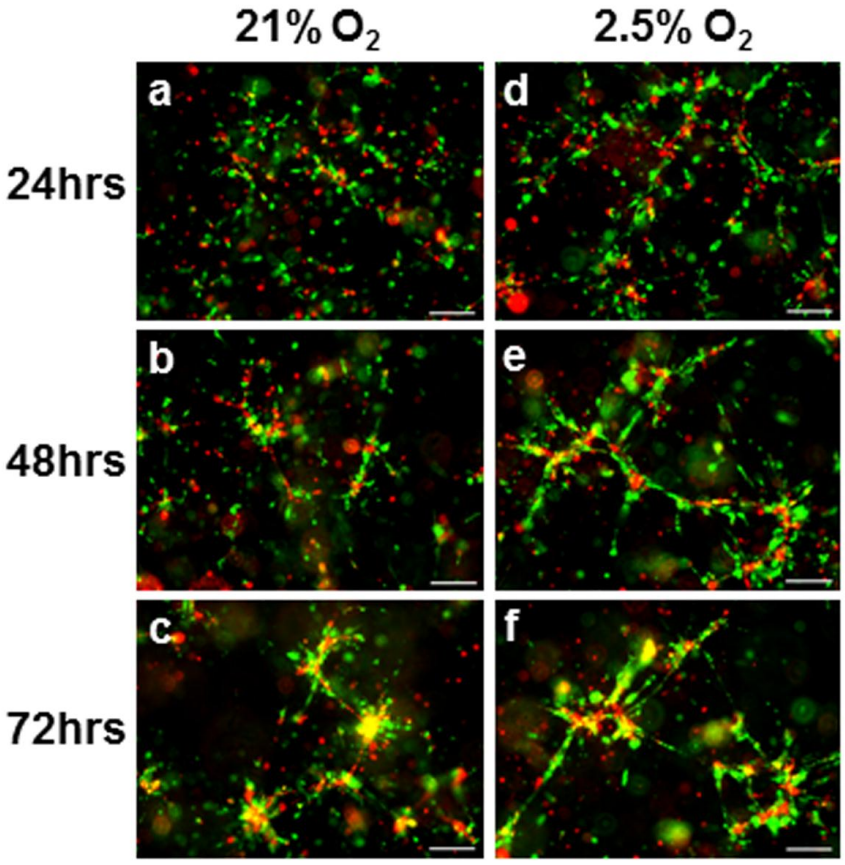

Figure 19: Vascular support function of human heart pericytes under hypoxia

When dye-labeled heart pericytes (Green) and HUVECs (Red) were evenly casted into the 3D Matrigel plug, (a-c) these two types of cells migrated and co-formed microvessel-like networks together within 72 hours under the ambient oxygen concentration (21% O_2), with pericytes assuming peri-HUVEC positions. (d-f) When the Matrigel plug was exposed to hypoxic conditions (2.5% O_2), the co-formation of microvessel-like networks was facilitated. (All pictures are taken at X100, scale bars=200μm)

The same 3D Matrigel plug culture was applied to study the interaction between HPs and HUVECs under the ambient (21%) or low (2.5%) oxygen concentration, in comparison with SkMPs isolated from the same donor. HPs (green) and HUVECs (red) gradually formed 3D capillary-like networks together within the plug in 72 hours under 21% O_2 (Figure 19A, a-c). Notably, such a process appeared to be facilitated under 2.5% O_2 (Figure 19A, d-f). Altogether these data suggest that cultured HPs not only retained mural cell features, supporting formation of microvascular networks, but also exhibiting angiogenic behaviors divergent from SkMPs under low oxygen tension.

4.3.4 Cardiomyogenic potential of human heart pericytes

To investigate the cardiomyogenic potential of HPs, we first used DNA demethylation method for induction in vitro, according to published protocols. Cultured HPs were incubated with induction medium containing 10μM 5-azacytidine for 72 hours and then back in regular medium for additional 14 days. Immunocytochemistry most HPs expressed (a) GATA4, and a fraction of them express (b) α-actinin and (c) cardiac myosin heavy chain (Figure 20, a-c).

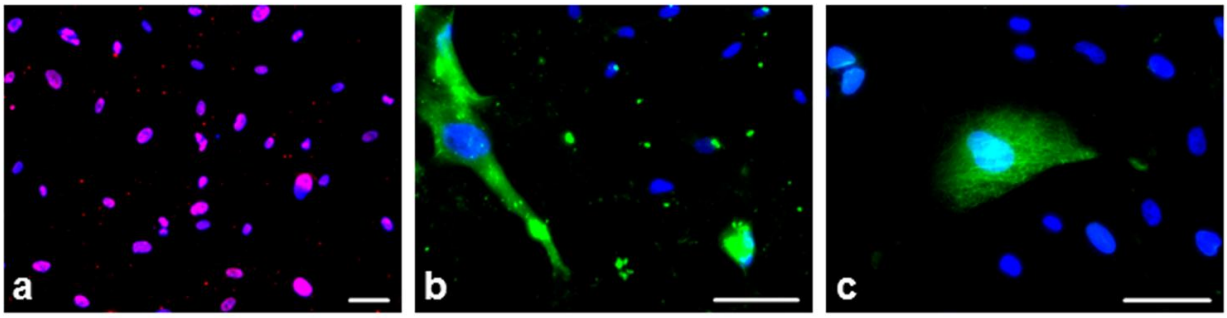

Figure 20: Cardiomyocyte differentiation of human heart pericytes

After incubation in cardiomyogenic induction medium containing 10μM 5-azacytidine for 72 hours and then in pericyte medium for additional 14 days, most HPs expressed (a) GATA4, and a fraction of them express (b) α-actinin and (c) cardiac myosin heavy chain (scale bars=100μm).

4.3.5 Heart pericytes natively express MSC markers

As we and others have previously shown that microvascular pericytes in many tissues manifest typical MSC markers in situ, we investigated if HPs shared this phenotype in the myocardium. Immunohistochemistry revealed that HPs surrounding ECs of small blood vessels in the ventricular myocardium natively express classic MSC markers, including CD44 (Figure 21A), CD73 (Figure 21B), CD90 (Figure 21C, main and inset), and CD105 (Figure 21D). Particularly, only microvascular pericytes expressed CD105 (Figure 21D enlargement, red arrows) but not perivascular cells surrounding the larger blood vessel (Figure 21D, dotted encirclement). Confocal microscopy confirmed the co-expression of CD146 and CD44 (Figure 21E) or CD90 (Figure 21F) by HPs. Flow cytometry was further employed to validate that freshly purified HPs retain the expression of MSC markers. The results showed that HPs ($CD146^{+}CD34^{-}CD45^{-}CD56^{-}CD117^{-}$) (Figure 21G, a) co-express ALP, CD44, CD73, CD90, and CD105, but not CD133 (Figure 21G, b-g).

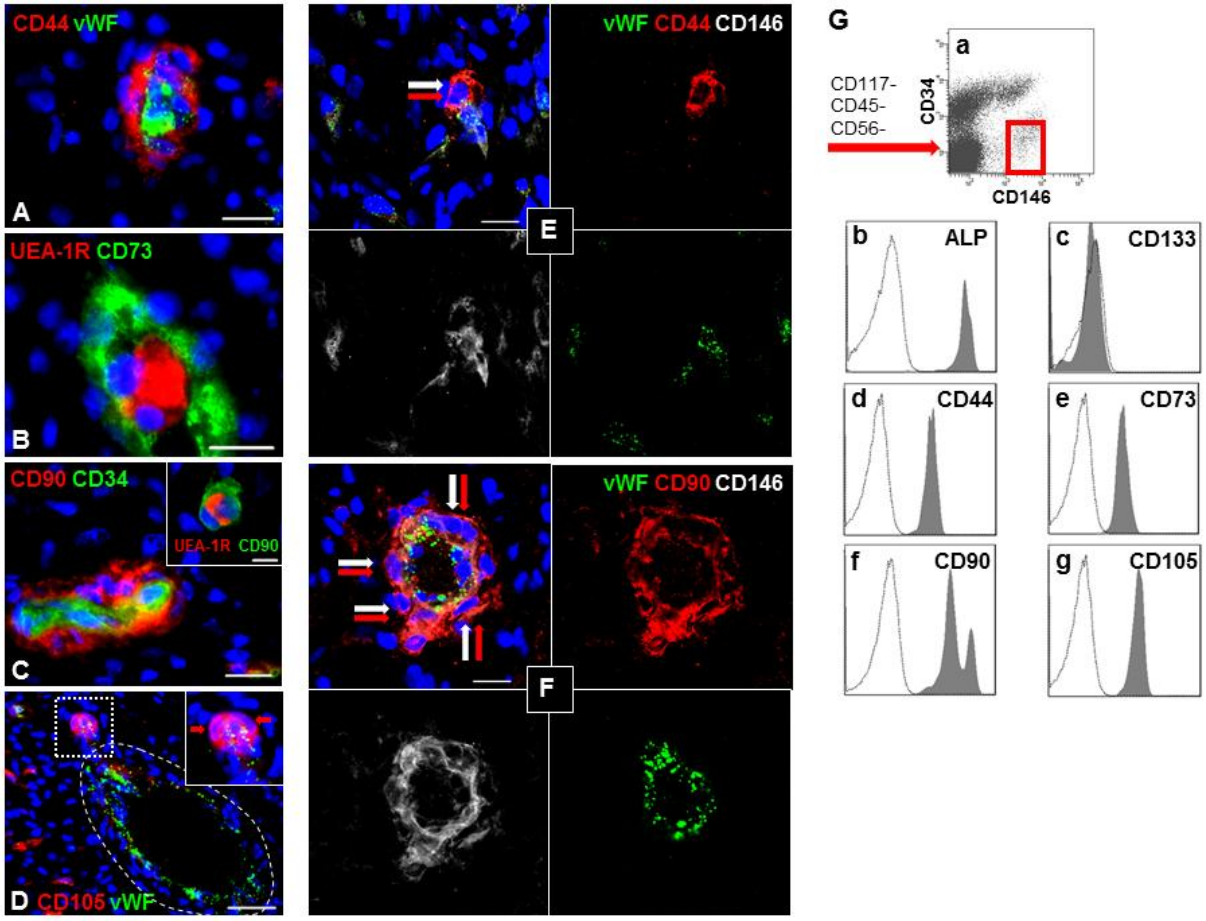

Figure 21: Heart pericytes natively express MSC markers

Left column: frozen sections of human myocardial tissue were co-stained with antibodies to classic MSC markers, including CD44 (A, red), CD73 (B, green), CD90 ([C] main, red; [C] inset, green), and CD105 (D, red) as well as endothelial cell markers: vWF (A and D, green), the *Ulex europaeus* lectin receptor (UEA-1R) (B and [C] inset, red), or CD34 ([C] main, green). Pericytes surrounding small blood vessels express CD44 (A, X900), CD73 (B, X900), CD90 ([C] main, X900), and CD105 (D, X400) (scale bars: A-[C] main=20μm; D=50μm). Pericytes encircling UEA-1R+ capillaries also strongly express CD90 ([C] inset, X900, scale bars=10μm). Notably, CD105 is only expressed by microvascular pericytes ([D] enlargement, red arrows) but not by perivascular cells surrounding the larger vWF+ vessel (D, dotted encirclement). Middle column: frozen sections of human myocardial tissue were triple-labeled with antibodies to vWF (green), CD146 (white), and either CD44 (E, red) or CD90 (F, red). Confocal microscopy revealed that pericytes encircling capillaries and microvessels express both CD44 (E, X1000) and CD90 (F, X1000) in addition to CD146 (white/red arrows) (scale bars=10μm). Right column: (G) HPs freshly isolated from human myocardium were incubated with antibodies to stem cell and MSC markers and analyzed by flow cytometry. $CD146^{high}CD34^{-}CD45^{-}CD56^{-}CD117^{-}$ population were first gated (a) and examined for co-expression of ALP (b), CD133 (c), CD44 (d), CD73 (e), CD90 (f), and CD105 (g). Clear histograms (b-g) represent negative control cells stained with non-specific isotype-matched antibodies.

4.3.6 Heart pericytes exhibit mesodermal differentiation capacity except skeletal myogenesis

After demonstrating that HPs manifest MSC markers natively and in culture, we then investigated whether HPs possess multi-lineage mesodermal differentiation potential resembling pericytes originated from other organs. Cultured HPs were incubated in inductive conditions for osteo-, chondro-, adipo-, and myo-genesis respectively. Compared with SkMPs exhibiting all four mesodermal lineage differentiations (Figure 22B, e), HPs displayed robust osteo-, chondro-, and adipo-genic differentiation, but not myotube formation, even after extended incubation for up to 3 weeks (Figure 22A, a-c and Figure 22B, d). We further examined the difference between HPs and SkMPs in skeletal myogenesis in vitro. Differentiated SkMPs expressed mature muscle proteins, including fast skeletal myosin heavy chain (FS-MHC), slow skeletal myosin heavy chain (SS-MHC), and desmin, while HPs did not display any of the three markers after culturing in muscle fusion medium for 7 days (Figure 22C). To investigate whether this tissue-specific difference in myogenesis sustains in vivo, HPs and SkMPs were isolated from the same donor, and fifty thousand cultured cells injected into cardiotoxin-injured skeletal muscles of immunodeficient mice. Immunohistochemistry with human-specific spectrin antibody showed that only SkMPs regenerated human myofibers (N=4), no human spectrin-positive myofiber was detected in HP-injected muscles (N=4) (Figure 22D).

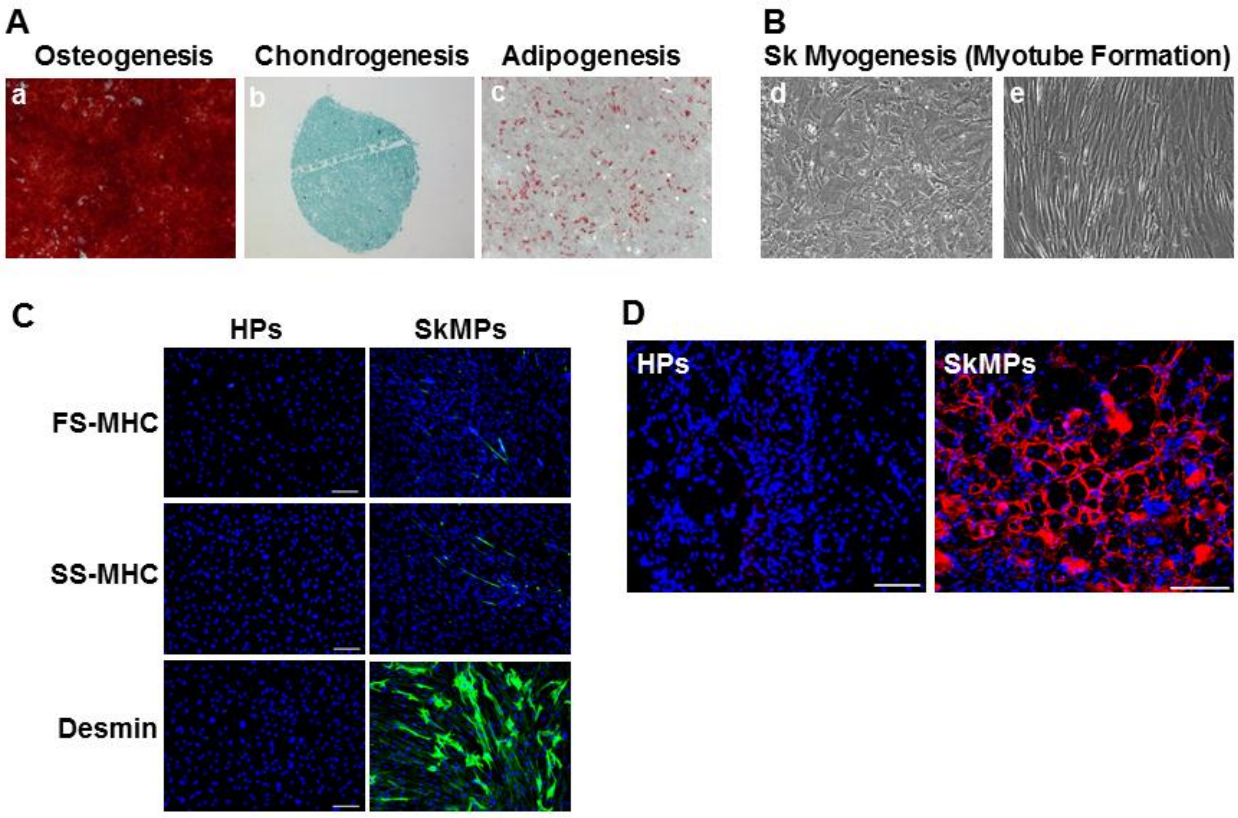

Figure 22: Heart pericytes exhibit mesodermal differentiation except skeletal myogenesis

(A) Cultured HPs were examined for mesodermal differentiation capacity in inductive conditions for osteo-, chondro-, adipo-, and myo-genesis respectively. Compared with SkMPs, which previously reported to exhibit all four mesodermal lineage differentiations after incubation, HPs displayed robust (a) osteo-, (b) chondro-, and (c) adipo-genic differentiation, revealed by alizarin red, Alcian blue, Oil red O stainings respectively. (B) But unlike SkMPs (e), HPs did not manifest myotube formation (d) even after extended incubation for up to 3 weeks. (C) Skeletal myogenesis in vitro was further evaluated by immunocytochemistry. Mature myogenic markers, including fast skeletal myosin heavy chain (FS-MHC) and slow skeletal myosin heavy chain (SS-MHC), as well as early myogenic marker, desmin, were expressed by SkMPs, but not by HPs, after culturing in muscle fusion medium for 7 days (scale bars=200 μm). (D) To investigate whether this tissue-specific difference in myogenesis sustains in vivo, fifty thousand cultured HPs or SkMPs, isolated from the same donor, were injected into cardiotoxin-injured gastrocnemius muscles of SCID-NOD mice. Two weeks later, frozen sections of recipient muscles were stained with human-specific spectrin antibody to reveal newly regenerated myofibers of human origin. In contrast to the large number of human myofibers regenerated by SkMPs in all samples (N=4), no human spectrin-positive myofiber was identified in HP-injected muscles (N=4) (scale bars=100 μm).

4.4 DISCUSSION

Recently, preliminary reports from clinical trials (SCIPIO and CADUCEUS) using resident cardiac progenitor/precursor cells (CPCs) have demonstrated encouraging results, indicating the safety of using autologous CPCs for post-infarction repair/regeneration [139, 140]. Although recent progresses in mammalian cardiac developmental and stem cell biology have greatly advanced our understanding of resident heart stem/progenitor cells, the perivascular compartment within the heart has not yet been fully studied [18, 141]. The importance of perivascular precursor cells contributing to physiological functions and participating in pathological conditions has recently been demonstrated by several groups [9, 53, 142, 143].

Despite prior studies by our and other groups have extensively characterized microvascular pericytes isolated from multiple human organs, it is not clear whether pericytes residing in the heart possess multi-lineage differentiation capacity and/or stem cell characteristics [17, 26, 113]. More importantly, despite their seemingly universal mesodermal multipotency as well as stem/progenitor cell features, whether tissue specificity and/or divergent behaviors to pathophysiological conditions exist among pericytes of different organs, notably of distinct developmental origins, remains unknown [138].

In the current study, we described that resident HPs express known pericyte markers and can be prospectively purified HPs to homogeny with a combination of cell lineage antigens. HPs natively express no CD117 and thus differ from CD117+ cardiac precursor cells. Sorted HPs ($CD146^{+}CD34^{-}CD45^{-}CD56^{-}CD117^{-}$) can be cultured long term and exhibit nearly identical phenotypes as their counterparts in other organs. HPs support formation of capillary-like network in 2D and 3D Matrigel culture, with or without endothelial cells, and further facilitate this

angiogenic process under low oxygen conditions, which is presumably attributed to the increased secretion of angiogenic factors and accelerated migration by HPs in response to decreased concentration. Coupled with their paracrine function, HPs may hold great advantage to treat ischemic heart diseases. Given the rarity and indispensability of cardiac tissue, however, future applications of HPs as a therapeutic cell source may be limited to critical conditions. Yet the therapeutic potency of HPs in cardiovascular repair and regeneration demands further investigation.

Coronary vasculature, including microvessels and capillaries, has previously been shown to arise from an epicardial origin, which differs from vasculature of other tissues, for example, skeletal muscle. Recent evidence from a transgenic murine model indicated that multipotent mesenchymal precursors residing in the heart originate from proepicardium (recent CSC paper). These data suggest that resident HPs presumably arise from proepicardium/epicardium along with coronary vasculature tree and contribute to this mesenchymal precursor pool. Whether HPs actively participate in congenital or acquired pathological conditions of the heart awaits further research.

Despite certain histological similarity as striated muscle, myocardium and skeletal muscle differ greatly in their developmental origin and physiological function. By comparing HPs with SkMPs, we observed a tissue-specific restriction of skeletal myogenic differentiation in HPs as well as their differential responses to oxygen concentrations. Nevertheless, HPs not only express MSC marker in situ and in culture but also demonstrated robust mesenchymal differentiations such as osteo-, chondro-, and adipo-genesis, comparable to pericytes from other tissues. More effort is required to elucidate if there are additional types of tissue specificity existing among this seemingly universal population of vascular mural cells throughout the body.

4.5 CONCLUSION

In summary, herein I demonstrate that resident HPs can be identified by typical pericyte markers and purified by a modified panel of selective markers. Purified HPs are multipotent mesenchymal precursors residing in human myocardium, exhibiting tissue specificity in differentiation capacity and distinct angiogenic responses to low oxygen tension. Although HPs do not express c-kit, their developmental hierarchy and relationship to other resident cardiac precursor cells remain to be elucidated. Additionally, it is worth mentioning that it has been extremely difficult to obtain healthy adult human myocardial biopsies in Pittsburgh area. The UK team, however, was able to obtain several and perform histological analyses and cell isolation.

4.6 ACKNOWLEDGEMENTS

The authors wish to thank Alison Logar and Megan Blanchard for their expert assistance with flow cytometry, Lindsay Mock for her help with the procurement of human tissues, Dr. Simon Watkins and Center for Biologic Imaging for their assistance in confocal microcopy.

5.0 PATH TO CLINICAL TRANSLATION: COMPARISON OF SKELETAL MYOGENESIS BETWEEN LINEAGES AND EXPLORATION OF ALTERNATIVE SOURCE OF BLOOD-VESSEL-DERIVED STEM CELLS

5.1 INTRODUCTION

As described in previous chapters, blood-vessel-derived stem cells (BVSCs) are composed of a number of stem cells originated from different vascular cell lineages, including myogenic endothelial cells (MECs) of endothelial cell lineage as well as pericytes and adventitial cells (ACs) of perivascular cell lineage. It is not yet clear whether all BVSC populations possess the same regenerative capacity in pathological conditions, for instance skeletal muscle injury, and how this difference of lineage origin could affect their capacity in tissue repair/regeneration. To identify optimal BVSC cell type(s) for particular organ injury/disease applications, it is deemed critical to understand the relative capacity of different BVSC populations to repair/regenerate tissue under a specific pathological condition. MECs and pericytes have only been shown to be superior to myoblasts for muscle regeneration in separate studies. Herein I used skeletal myogenesis as a model system to directly compare the efficiency of muscle repair between MECs and pericytes isolated from the same donor. Moreover, to further facilitate clinical translation of BVSCs, it is essential to investigate whether we can isolate BVSCs from any

alternative source, more convenient and clinically accessible than fresh tissue biopsies in terms of preservation and processing time.

Mammalian skeletal muscle harbors all three BVSC populations, which can repair and/or regenerate injured/defective tissues such as damaged/dystrophic skeletal muscles and ischemic hearts [1, 46, 83, 144-152]. These stem cell populations were specifically localized *in situ* within the walls of small blood vessels as described above and can be prospectively purified by fluorescence-activated cell sorting (FACS) simultaneously from fresh human skeletal muscle biopsies, through the use of a combination of positive and negative cell lineage markers [26, 45]. However, it has never been documented whether these stem cell fractions could persist and retain their high myogenic capacities after the cryopreservation of human primary skeletal muscle cell cultures (cryo-hPSMCs). Furthermore, whether MECs isolated from cryopreserved, culture-expanded hPSMCs also possessed the same superior regenerative capacity remains to be determined.

In order to identify and purify MECs and pericytes by FACS from *in vitro* expanded cryo-hPSMCs, we employed a collection of cell lineage markers reported in our previous studies, including the hematopoietic cell marker CD45, the myogenic cell marker CD56 (N-CAM), the perivascular cell marker CD146 (M-CAM/Mel-CAM/MUC18), and the endothelial cell marker UEA-1 receptor (*Ulex europaeus agglutinin I receptor*, UEA-1R) [26, 45, 153]. UEA-1R was chosen as a substitute marker for CD34 and CD144 because these two endothelial cell markers are frequently lost during long-term culture whereas UEA-1 maintains consistent reactivity within endothelial cell lineage cultures [45, 153]. We hypothesized that MECs and pericytes (with and without culture expansion), purified from cryo-hPSMCs, retain their superior

myogenic potential and exhibit greater regeneration of skeletal myofibers when compared to myoblasts.

5.2 MATERIALS AND METHODS

5.2.1 Human muscle biopsies and animal usage

In total, nine independent human skeletal muscle biopsies, from 4 female and 5 male donors (age range 4–75, mean 28), were used to obtain human primary skeletal muscle cells (hPSMCs). The procurement of human skeletal muscle biopsies from the National Disease Research Interchange (NDRI) was approved by the Institutional Review Board at the University of Pittsburgh Medical Center (UPMC). All the animal research experiments performed in this study were approved by the Animal Research and Care Committee at the Children's Hospital of Pittsburgh of UPMC (Protocol #34-05) and the University of Pittsburgh (Protocol #0810310-B2).

5.2.2 Cell isolation and cryopreservation

The human skeletal muscle biopsies were placed in Hank's balanced salt solution (HBSS, Invitrogen) and transferred to the laboratory on ice. Briefly, tissues were finely minced and serially digested with 0.2% collagenase-type XI, 0.25% dispase, and 0.1% trypsin, as previously described [45, 153]. Dispersed single cell suspensions were either labeled freshly for cell sorting or cultured in complete medium containing DMEM supplemented with 10% fetal bovine serum (FBS), 10% horse serum, 1% chicken embryo extract, and 1% penicillin/streptomycin (all from

Invitrogen). After expansion, cells were cryopreserved at passages 2-8 in medium consisting of 50% complete culture medium and 50% freezing medium (80% FBS+20% dimethylsulfoxide) and stored in liquid nitrogen [153].

5.2.3 Flow cytometry and cell sorting

FACS sorting of freshly isolated muscle cells were described in Chapter 3. To culture cryo-hPSMCs, cells were thawed and expanded for 2-6 passages. To perform flow cytometry analysis, cells were trypsinized, washed, and incubated with anti-human monoclonal antibodies/ligands: CD45-APC-Cy7, CD56-PE-Cy7, CD34-APC (all from Becton Dickinson), CD146-FITC (Serotec), UEA-1-PE (Biomeda), vWF-FITC (US Biology), KDR-APC (R&D System) and CD144-PE (Beckman Coulter). Negative control samples received equivalent amounts of isotype-matched fluorophore-conjugated antibodies. For FACS purification, cells were incubated with CD45-APC-Cy7, CD56-PE-Cy7, CD146-FITC, UEA-1-PE, and with 7-amino-actinomycin D for dead cell exclusion. Sorted subpopulations were collected for immediate transplantation or transiently expanded in appropriate conditions as previously described [26, 45].

5.2.4 Immunocytochemistry

For immunocytochemistry, cells were either directly fixed in wells with cold methanol for 5 min or cytospun onto glass slides, fixed, and incubated with 10% serum. The following primary antibodies were used to detect cell lineage markers, including myogenic cell markers, CD56 (Becton-Dickinson, 1:100), fast skeletal myosin heavy chain (FS-MHC, 1:200), slow skeletal myosin heavy chain (SS-MHC, 1:200) and desmin (1:100) (all from Sigma); perivascular cell

markers, α-smooth muscle actin (Abcam, 1:100) and CD146 (Cayman Chemical, 1:50); endothelial cell markers/ligands, CD144 (Sigma, 1:100), von Willebrand factor (vWF, 1:100) (DAKO), CD34 (Novocastra, 1:50), and biotinylated UEA-1 (Vector, 1:50), followed by incubation with biotinylated secondary antibodies plus Cy3-conjugated streptavidin (both from Sigma, 1:500) or Alexa^{TM}488-conjugated secondary antibodies (Molecular Probes, 1:400). Plates and slides were observed and photographed on epi-fluorescence microscope systems (Nikon Eclipse TE 2000U and Nikon Eclipse E800).

5.2.5 Myogenesis in vitro and in vivo

5.2.5.1 Myogenesis in vitro

Myogenesis *in vitro* has been described in Chapter 4. MECs and pericytes isolated from the same fresh muscle biopsy along with HUVECs, which represent typical endothelial cells (ECs), were cultured under the same myogenic condition.

5.2.5.2 Myogenesis *in vivo*

To investigate whether the myogenic capacities were preserved, after cryopreservation, purified MECs, pericytes, myoblasts (Myo), ECs and unpurified muscle cells, without in vitro expansion, from six independent hPSMC samples were used for intramuscular injection. The newly sorted cells, on average, $11.8\pm5.8\times10^4$ $CD56^+$ Myo, $7.3\pm4.4\times10^4$ $CD146^+$ pericytes, $4.5\pm2.6\times10^4$ UEA-$1R^+$ ECs, and $2.9\pm1.7\times10^4$ $CD56^+$UEA-$1R^+CD146^+$ MECs as well as 30×10^4 corresponding unsorted cells, were resuspended in 20µl of HBSS and used for transplantation.

To precisely measure the myogenic regenerative capacity of each stem/progenitor cell subpopulation, newly sorted MECs, pericytes and Myo were expanded in culture for 1-2

passages. Fifty-thousand cells from each subpopulation as well as 5×10^4 corresponding unsorted cells were trypsinized, washed and resuspended in 20µl of phosphate-buffered saline (PBS). Four individual animal experiments were performed, with each using cell populations purified from a single FACS sort of one independent cryo-hPSMC culture.

Cells were injected into a single site of the gastrocnemius muscles of severe combined immunodeficient (SCID) mice that were injured 24 hours before by injecting 1µg of cardiotoxin in 20µl of HBSS. The untreated group received sham injections of 20µl of HBSS or PBS only. Treated muscles were collected 2 weeks post-injection for immunohistochemical analyses. Anti-human spectrin was used to identify human cell-derived skeletal myofibers in the mouse muscles. In order to quantitatively evaluate the myogenic regenerative capacity of each subpopulation, the number of human spectrin-positive skeletal myofibers was averaged from 6 randomly selected sections at the site of the injection in each specimen and presented as the regenerative index (per section).

5.2.6 Statistical analysis

Data were summarized as average ± standard error (SE). Statistical comparison between groups (purified cells after expansion *in vitro*) was performed using one-way ANOVA with 95% confidence interval. Bonferroni pairwise multiple comparison test was performed for ANOVA post-hoc analysis. Statistical analyses were performed with SigmaStat software.

5.3 RESULTS

5.3.1 Myogenic endothelial cells exhibited the supreme myogenic capacity in culture

MECs and pericytes were simultaneously purified from a single human skeletal muscle biopsy by FACS, with a post-sort purity greater than 95 percent. Cells were expanded in culture according to previously reported conditions until confluence (Figure 23A-C). When cultured in the same myogenic condition, MECs exhibited the greatest extent of myotube formation (Figure 23F) when compared to other cell populations. Pericytes formed less and smaller myotubes (Figure 23E) while nearly all HUVECs did not survive the typical myogenic culture (Figure 23D).

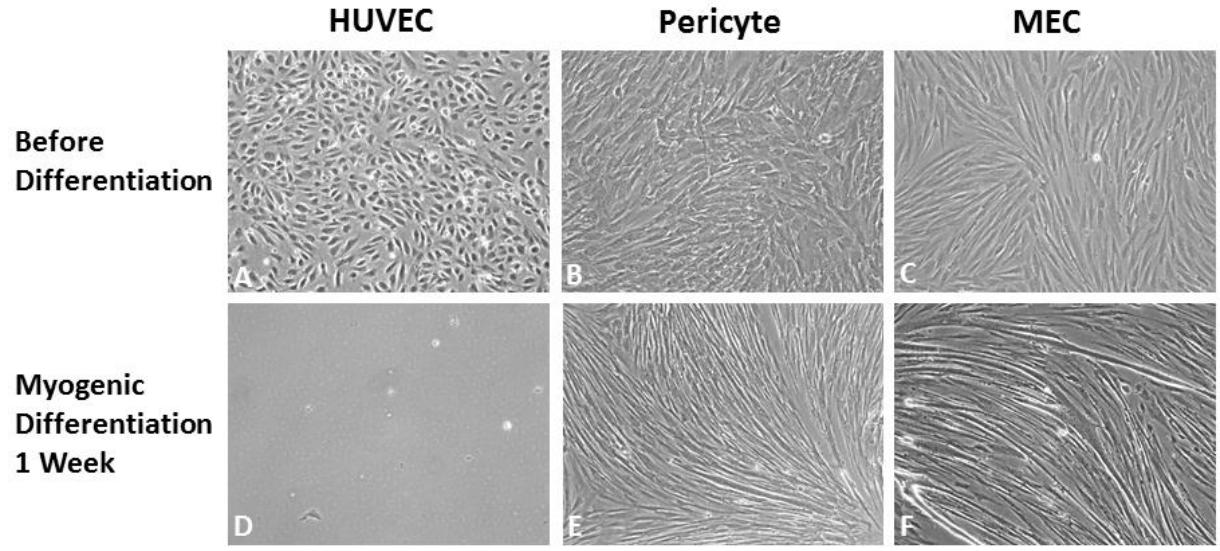

Figure 23: Myogenesis of BVSC populations in vitro

(A-C) Before switching to myogenic culture condition (2% serum), cells were expanded until confluence. After 1 week of myogenic differentiation, MECs displayed the highest extent of myotube formation (F) while pericytes formed less and smaller myotubes (E). However, nearly all HUVECs did not survive in the typical myogenic culture condition (D).

Further analyses of myogenic markers revealed that after differentiation, MECs extensively displayed mature myogenic markers, FS-MHC and SS-MHC (Figure 24G-H), while

nearly all of the MECs express early myogenic marker, desmin (Figure 24I). On the other hand, a notably smaller proportion of pericytes express FS-MHC, SS-MHC, and desmin (Figure 24D-F), indicating a smaller extent and lesser maturation of myogenesis than those of MECs. Near extinction of HUVECs in myogenic culture was confirmed by DAPI staining with no apparent myogenic marker expression (Figure 24A-C)

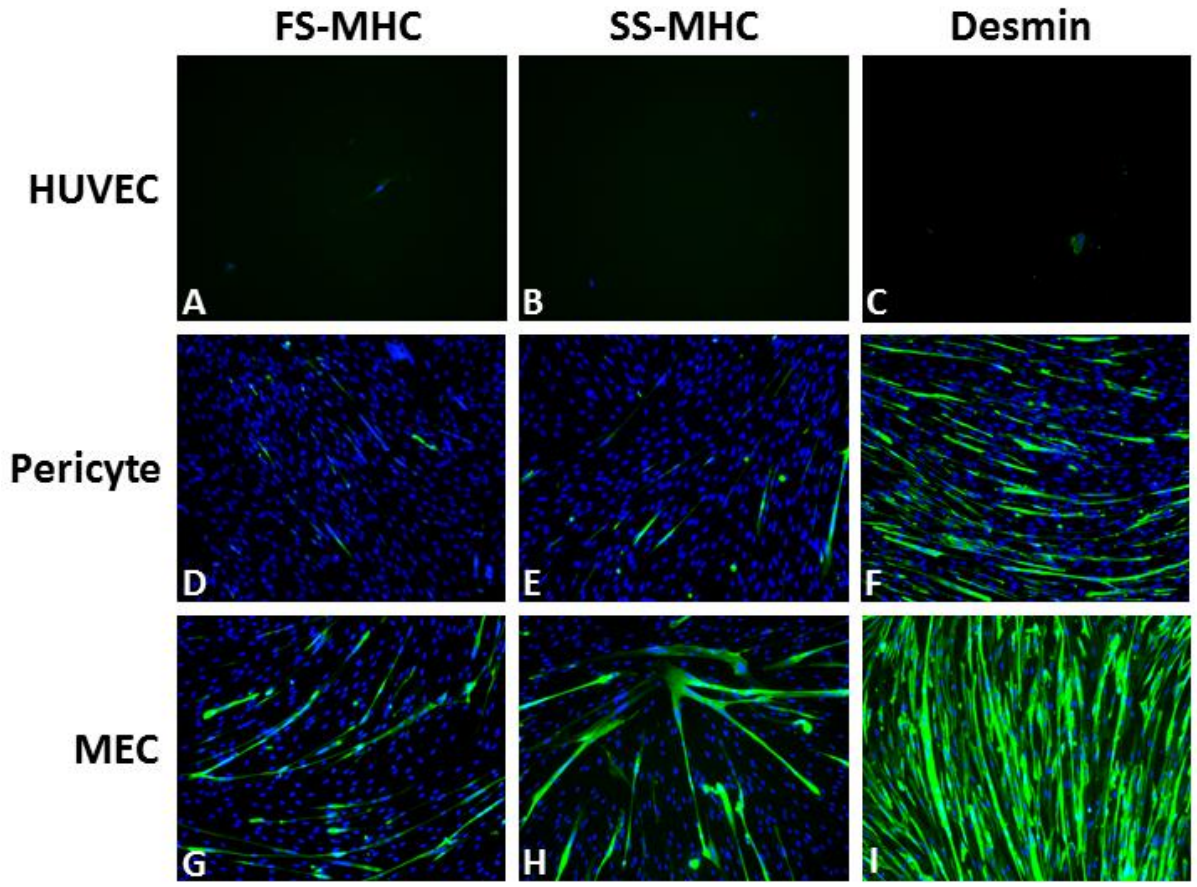

Figure 24: Immunocytochemical analyses of myogenic markers

(A-C) After myogenic differentiation for 7 days, near extinction of HUVECs in myogenic culture was confirmed by DAPI staining with no apparent myogenic marker expression. A fraction of pericytes expressed mature myogenic markers, FS-MHC (D) and SS-MHC (E), as well as early myogenic marker, desmin (F). A notably larger proportion of MECs displayed FS-MHC (G), SS-MHC (H), and desmin (I).

5.3.2 Heterogeneous cell composition of human primary skeletal muscle cell cultures (hPSMCs) after cryopreservation and long-term expansion

After expansion, the cryopreserved hPSMCs (cryo-hPSMCs) were examined by immunocytochemistry for cell surface marker expression. The majority of cryo-hPSMCs expressed desmin and CD56, and to a lesser extent, CD146 (Figure 25A). Only a fraction of cells expressed α-SMA, CD144, vWF or UEA-1R. As predicted, the cultured human cryo-hPSMCs lacked CD34 expression. After excluding $CD45^+$ hematopoietic cells (0.2±0.1%), flow cytometry analysis quantitatively confirmed the presence of cells with diverse expressions of cell lineage makers by cryo-hPSMCs: 77.1±5.7% $CD56^+$, 66.9±8.1% $CD146^+$, 11.2±2.5% $UEA\text{-}1R^+$, 0.3±0.1% $CD144^+$, 0.1% vWF^+, and null expression of CD34 and KDR (Figure 25B). The number of cryo-hPSMCs positive for CD56, CD146 or UEA-1R decreased dramatically after passage 10 (Figure 25C).

5.3.3 Isolation of myogenic stem/progenitor cells from cryo-hPSMCs

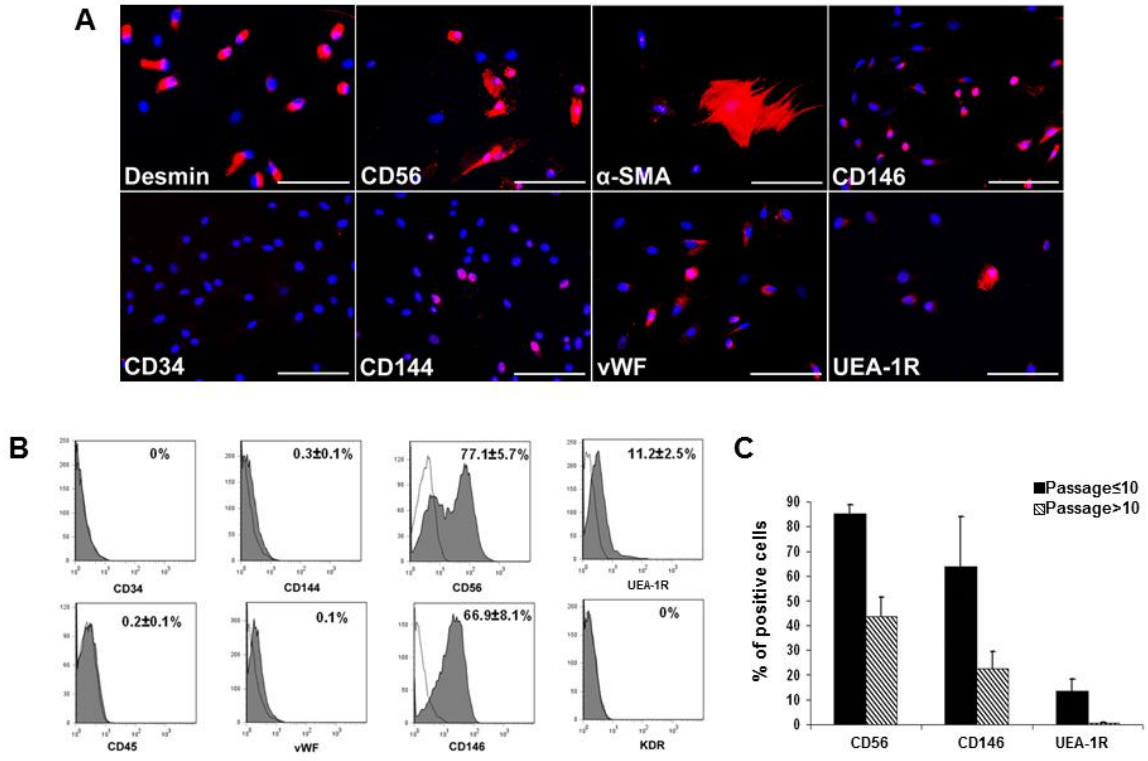

Figure 25: Expression of cell lineage markers by cryo-hPSMCs

(A) Immunocytochemistry revealed the expression of various cell lineage markers (red) by cryopreserved human primary skeletal muscle cells (cryo-hPSMCs) after expansion. Nuclei were stained blue with DAPI. (B) Flow cytometry analysis quantitatively confirmed the diverse cell composition of cryo-hPSMCs. (C) The number of cryo-hPSMCs positive for CD56, CD146, or UEA-1R decreased when cells were cultured beyond passage 10. (Scale bars = 100µm)

After revealing the heterogeneous nature of cryo-hPSMCs, we analyzed these cells for the existence of previously defined subpopulations by multi-color flow cytometry, based on their expression of hematopoietic (CD45), myogenic (CD56), endothelial (UEA-1R), and perivascular (CD146) cell lineage markers [26, 45]. After exclusion of $CD45^+$ cells, four distinct cell fractions were identified, including myoblasts (Myo) ($CD56^+/CD45^-CD146^-UEA\text{-}1R^-$), endothelial cells (ECs) ($UEA\text{-}1R^+/CD45^-CD56^-CD146^-$), pericytes ($CD146^+/CD45^-CD56^-UEA\text{-}1R^-$), and myogenic endothelial cells (MECs) which expressed all three markers ($CD56^+UEA\text{-}$

1R^{+}CD146^{+}/CD45^{-}). Long-term cultured cryo-hPSMCs included 22.58±6.32% Myo, 0.58±0.23 % ECs, 5.92±4.66% pericytes, and 1.16±0.19% MECs (Figure 26). These four cell subsets were subsequently fractionated by FACS, and on average we were able to recover the following number of each cell type: 25.61±9.16×10^{4} CD56^{+} Myo, 13.28±7.37×10^{4} UEA-1R^{+} ECs, 33.54±20.53×10^{4} CD146^{+} pericytes, and 3.84±0.96×10^{4} CD56^{+}UEA-1R^{+}CD146^{+} MECs (Figure 26).

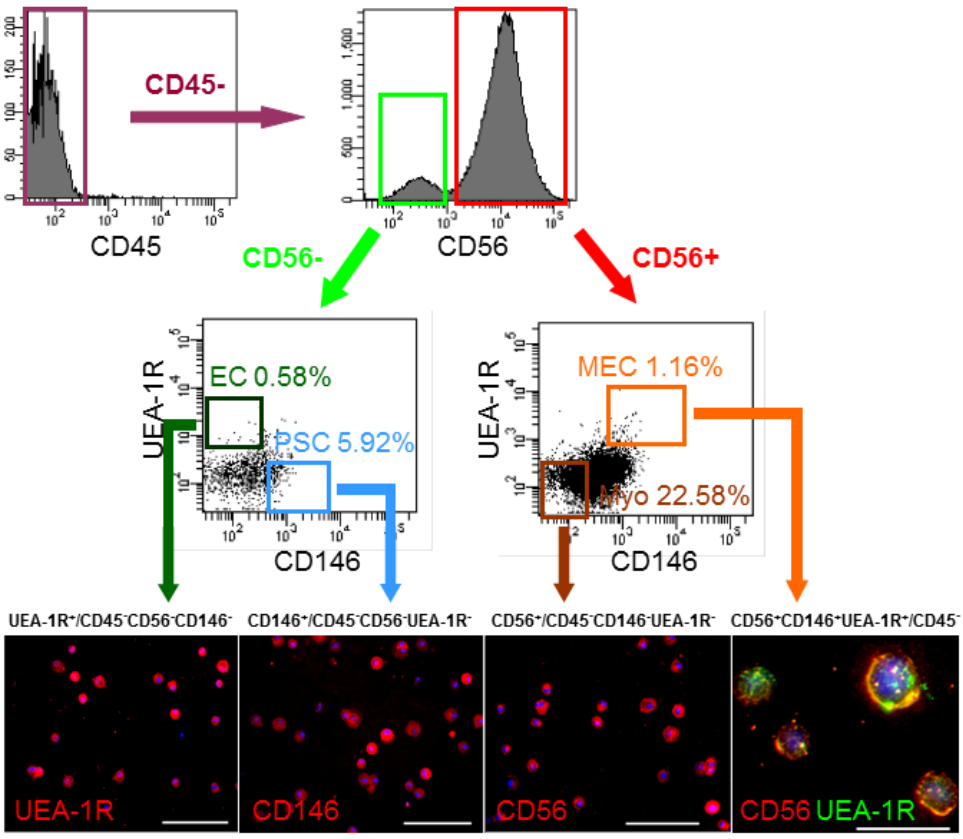

Figure 26: Identification and purification of myogenic stem cells within cryo-hPSMCs

After excluding CD45^{+} hematopoietic cells, CD45^{-} cells were separated based on CD56 expression. CD56^{+} and CD56^{-} populations were further gated on UEA-1R by CD146 to identify and/or sort four distinct cell populations: myogenic endothelial cells (MEC) (CD56^{+}UEA-1R^{+}CD146^{+}/CD45^{-}), myoblasts (Myo) (CD56^{+}/CD45^{-}CD146^{-}UEA-1R^{-}), pericytes (CD146^{+}/CD45^{-}CD56^{-}UEA-1R^{-}), and endothelial cells (EC) (UEA-1R^{+}/CD45^{-}CD56^{-}CD146^{-}). The purities of the sorted populations were 90.73±4.82%, 92.94±1.23%, 93.86±1.72, and 94.9±0.64, respectively. Immunocytochemistry confirmed the expression of key cell lineage makers by freshly sorted cells: UEA-1R, CD146, and/or CD56. Nuclei were stained blue with DAPI. (Scale bars = 100µm except in CD56/UEA-1R double staining = 20µm)

5.3.4 Purified myogenic stem/progenitor cells retain high myogenic potentials *in vivo*

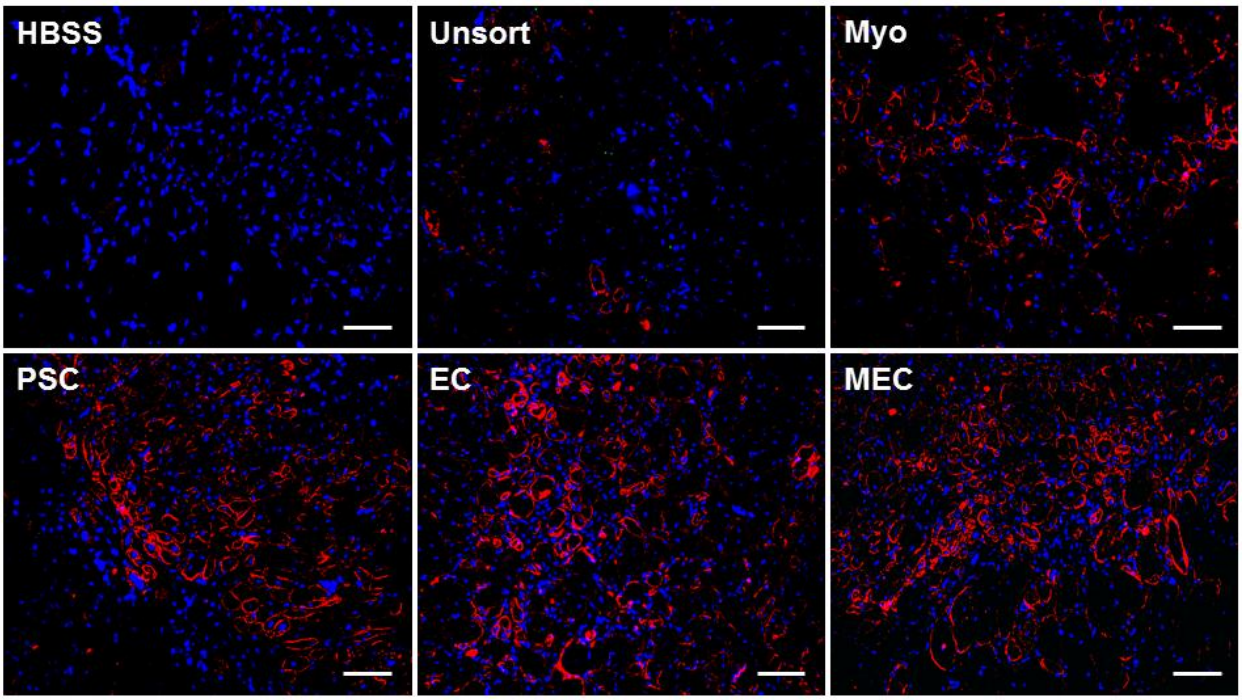

Figure 27: Myogenic capacity of cryo-hPSMC culture-derived cells in vivo

Representative pictures of regenerating human spectrin-positive myofibers in cardiotoxin-injured mouse skeletal muscles transplanted with newly sorted cell fractions from a single donor-derived cryo-hPSMC culture, including myogenic endothelial cells (MEC), pericytes, endothelial cells (EC), and myoblasts (Myo). Unsorted cryo-hPSMCs (Unsort) and HBSS were injected as treated and untreated controls respectively. (200X, scale bars = 50µm)

To evaluate whether the myogenic capacity was preserved after cryopreservation, all sorted cells were immediately transplanted (without culture expansion) into the cardiotoxin-injured gastrocnemius muscles of SCID mice (n=6 per cell fraction). Unpurified muscle cells and Hank's balanced salt solution (HBSS) injections were employed as treated and untreated controls, respectively. Mouse muscles were harvested 2 weeks post-injection, cryosectioned, and examined by immunohistochemistry to detect muscle fiber regeneration. An antibody against human spectrin, a myofiber cytoskeletal protein, was used to identify human cell-derived skeletal myofibers in the tissue sections. All of the newly purified cell fractions regenerated human spectrin-positive myofibers in injured mouse skeletal muscles, and the purified fractions appear

to be more efficient at regenerating muscle fibers than the unpurified cryo-hPSMCs (Figure 27). As expected, a lack of spectrin-expressing muscle fibers was observed in the HBSS-injected muscles (Figure 27).

To quantitatively measure the myogenic regenerative capacity of each purified stem/progenitor cell population, newly sorted MECs, pericytes and Myo were transiently expanded in culture for 1-2 passages. Fifty-thousand cells from each subpopulation as well as 5×10^4 corresponding unsorted cells were transplanted into the same muscle-injury model (n=4 per cell fraction). Phosphate-buffered saline (PBS) injections were used as negative controls. ECs were not included in this experiment due to their unstable phenotypes in culture. Quantitative analyses revealed that the myogenic regenerative index, indicated by the average number of human spectrin-positive skeletal myofibers per muscle section, was 166.3±19.2 for MECs, 90.1±8.0 for pericytes, 45.7±6.2 for myoblasts (Myo), and 28.7±8.4 for unsorted muscle cells (Unsort) (Figure 28). MECs exhibited the highest regeneration of human skeletal myofibers among all four cell fractions tested ($p<0.005$) (Figure 28). Pericytes regenerated more myofibers than the Myo ($p>0.05$) and the Unsort ($p=0.017$) (Figure 28). Although the purified myoblasts displayed a trend of higher myogenic capacity than the unsorted cells, no statistically significant difference was observed ($p>0.05$) (Figure 28).

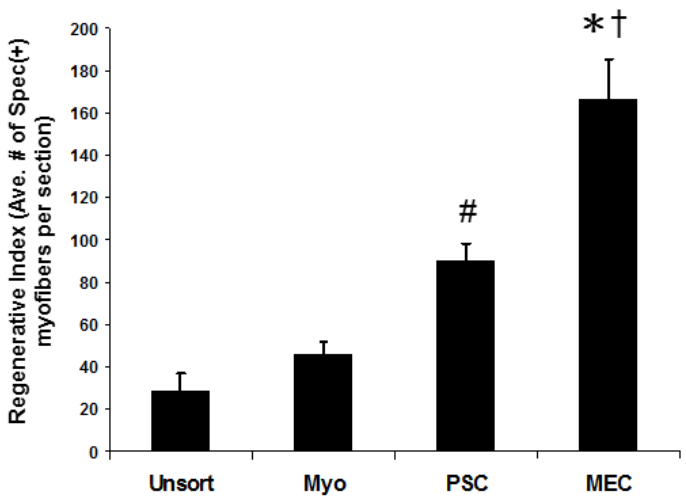

Figure 28: Comparison of myogenic regeneration in vivo

Quantitative analyses of the myogenic regenerative capacities of sorted stem/progenitor cell populations. Fifty-thousand cells from each cell fraction that was minimally expanded in culture were injected. Quantitative analyses of spectrin-positive human skeletal myofibers on tissue sections revealed that MEC mediated the highest myogenic regeneration among all four cell fractions tested (*p<0.001, vs. Myo and Unsort; †p=0.004, vs. pericytes). Injection of pericytes regenerated more human myofibers than injections of Myo (p>0.05) and Unsort (#p=0.017). Finally, Myo displayed a trend of higher myogenic capacity than Unsort, but no significant difference was observed (p>0.05).

5.4 DISCUSSION

Skeletal muscle is known to possess multiple stem/progenitor cell populations that are associated with muscle development, maintenance, and regeneration [1, 154]. Upon purification, muscle stem/progenitor cells in general display more robust myogenic regenerative capacities than unpurified muscle cells in animal disease models, suggesting the advantage of isolating stem cells for therapeutic purposes [1, 26, 45, 144]. More recent data has shown that there is a functional heterogeneity in myogenesis even among the muscle precursor cell pool [155].

In the present study, we demonstrated that even after *in vitro* expansion and cryopreservation, primary human muscle cell cultures include various subpopulations, as indicated by expression of diverse cell lineage markers. Using a modified collection of cell

lineage markers: CD45, CD56, CD146, and UEA-1R, we identified and purified to homogeneity four distinct cell populations from cryo-hPSMCs, including two stem cell subpopulations: pericytes ($CD146^{+}/CD45^{-}CD56^{-}UEA\text{-}1R^{-}$) and MECs ($CD56^{+}CD146^{+}UEA\text{-}1R^{+}/CD45^{-}$) [26, 45, 153]. Newly sorted MECs, pericytes, ECs, and Myo cells were immediately transplanted into the cardiotoxin-injured skeletal muscles of SCID mice to examine the preservation of their myogenic potential after FACS. All of which regenerated human spectrin-positive myofibers in injured mouse skeletal muscles. Quantitative analyses using sorted subpopulations that were minimally expanded in culture showed that MECs displayed the highest muscle regenerative capacity among all cell subsets tested, and pericytes were superior to myoblasts and unpurified cryo-hPSMCs.

These results were consistent with our previous observations from injections of cells isolated from fresh skeletal muscle biopsies [26, 45]. Taken together, our results suggest the presence of distinct subpopulations of highly myogenic stem/progenitor cells within culture-expanded, cryopreserved hPSMCs and support the feasibility of further purifying stem cell fractions from these unpurified cryopreserved human cells. Most importantly, these findings infer the practicability of prospective isolation of myogenic stem/progenitor cell populations from banked human skeletal muscle cells, highlighting a new technology to further enhance the availability and efficacy of cell-mediated therapies [156].

5.5 CONCLUSION

In summary, in this chapter, I demonstrate that MECs isolated from fresh human muscle biopsy possess greater myogenic capability than pericytes from the same source. Subpopulations of

BVSCs, including MECs and pericytes, can be simultaneously purified by cell sorting from cryopreserved human primary skeletal muscle cell cultures (cryo-hPSMCs). MECs isolated from cryo-hPSMCs maintained the highest regenerative capacity in the injured mouse muscles among all cell fractions tested, while pericytes remained superior to myoblasts and the unpurified primary skeletal muscle cells. This study represents a technical breakthrough for simultaneous isolation of multiple myogenic BVSC populations, from either fresh muscle biopsies or cryo-hPSMCs. It is, however, remained to be tested whether MECs and pericytes isolated from cryo-hPSMCs are functionally and developmentally identical to their freshly isolated counterparts from the same muscle biopsy. Due to the limited amount of each muscle biopsy, we were unable to obtain sufficient number of unsorted primary muscle cells for both experiments in order to perform a side-by-side comparison.

5.6 ACKNOWLEDGEMENTS

The authors also wish to thank Allison Logar for her excellent technical assistance on the flow cytometry and the cell sorting and James H. Cummins for his editorial assistance in the preparation of this manuscript.

6.0 SUMMARY AND FUTURE DIRECTIONS

Multipotent stem/progenitor cells with similar developmental potentials have been independently identified from diverse human tissue/organ cultures. The increasing recognition of the vascular/perivascular origin of mesenchymal precursors suggested blood vessels being a systemic source of adult stem/progenitor cells. Our group and other laboratories recently isolated multiple stem/progenitor cell subsets from blood vessels of adult human tissues. Each of the three structural layers of blood vessels: intima, media, and adventitia, has been found to include at least one precursor population, i.e. myogenic endothelial cells (MECs), pericytes, and adventitial cells (ACs), respectively. MECs and pericytes efficiently regenerate myofibers in injured and dystrophic skeletal muscles. MECs also improve cardiac function after myocardial infarction. The applications of ACs in vascular remodeling and angiogenesis/vasculogenesis have been examined. These findings suggest that blood vessels play a critical role in tissue repair, resulting from the regenerative power of blood-vessel-derived stem cells (BVSCs).

Despite decades of research, cardiovascular diseases remain the leading cause of morbidity and mortality worldwide and a daunting challenge for mankind to overcome. Stem cell therapy has gained an increasing attention in the past decade and is deemed promising as the future alternatives for tissue/organ transplantation. Multipotent mesodermal precursor cells, including mesenchymal stem cells (MSCs) and MSC-like cells, are by far the most accessible sources for autologous transplantation. In the cardiovascular milieu, MSCs have been

extensively tested for their therapeutic efficacy in pre-clinical and clinical trials, with many mechanisms of action being proposed, for example, paracrine secretion of trophic factors, regulation of post-injury tissue remodeling, immunoregulation, activation of endogenous repair/regeneration mechanisms, vasculogenesis and cardiomyogenesis. Enhancement of MSC cellular function and improvement of delivery modality are currently under intensive investigation. Nevertheless, the retrospective identification and heterogeneous nature of MSCs in culture hindered further research progress. The recent discovery of the likely perivascular origin of MSCs represents a new chapter in stem cell research and a giant leap to understand pathophysiological roles of mesodermal precursors in the adult human body. BVSC populations, including MECs, pericytes, and ACs, are well defined cells subsets that are presumably contributing to such a multipotent mesodermal precursor pool. With purified BVSC populations, we will be able to harness progresses made with MSCs in order to systematically understand the regenerative capacity associated with these precursor cells in each organ. Nonetheless, whether there exists a hierarchy between these subsets of BVSCs remains unclear to date. Further research is required to investigate their potential relationship, developmentally and functionally, as well as the regulation of these multipotent precursors during tissue repair/regeneration.

Despite microvascular pericytes purified from multiple human organs have been shown to possess multipotency and repair/regenerate defective tissues, notably skeletal muscle, their ability to repair the ischemic heart remains unknown. In Chapter 3, I have investigated and documented the therapeutic potential and associated repair mechanisms of human skeletal muscle-derived microvascular pericytes in a murine model of myocardial infarction. Briefly, echocardiographic analysis of acutely infarcted mouse myocardium injected with human pericytes revealed reduced left ventricular dilatation and significant improvement in cardiac

contractility for up to 2 months. Host angiogenesis was significantly increased around and within the infarct area. Vascular support by pericytes was illustrated by their perivascular homing *in vivo* and the formation of capillary networks with/without endothelial cells in two- and 3-dimensional co-cultures. Under hypoxia, pericytes dramatically increased expression of VEGF-A, PDGF-β, TGF-β1 and corresponding receptors while expression of bFGF, HGF, EGF, and Ang-1 was repressed. High expression of MMP-2, but not MMP-9, by pericytes was observed in hypoxic cultures. Pericyte treatment substantially reduced myocardial fibrosis and significantly diminished infiltration of host inflammatory cells at the infarct site. Furthermore, hypoxic pericyte-conditioned medium suppressed fibroblast proliferation and inhibited monocyte/macrophage proliferation *in vitro.* High expression of immunoregulatory molecules by pericytes, including IL-6, LIF, COX-2 and HMOX-1, was sustained under hypoxia, except MCP-1. Finally, GFP-based cell tracking revealed that pericytes differentiate into and/or fuse with cardiomyocytes, endothelial and smooth muscle cells, though to a minor extent. These findings suggest that intramyocardial transplantation of pericytes post-infarction promotes functional and structural recovery, presumably attributable to multiple restorative mechanisms involving paracrine effects and cellular interactions.

Based on the work described in Chapter 3, I am currently extending the research to the following directions in order to further understand the regenerative capacity of pericytes in the ischemic heart. First, to investigate the significance of donor cell-derived VEGF during pericyte-mediated cardiac repair, I am using lentiviral anti-VEGF shRNA to block the secretion of VEGF from pericytes, in collaboration with Dr. Bing Wang (Department of Orthopedic Surgery, University of Pittsburgh). Second, in order to understand the mechanism of anti-inflammatory effect by donor pericytes, I am collaborating with Dr. Stephen Badylak (Department of Surgery,

University of Pittsburgh) to investigate the immunoregulation during the regenerative response, including the regulation of M1/M2 phenotype switching in host macrophages. Finally, it is important to investigate the efficacy of treatment with pericytes and/or other BVSC subsets in a chronic MI model, which is more clinically relevant.

It is not clear whether pericytes residing in human heart possess multipotency and stem/progenitor cell characteristics similar to their developmentally distinct counterparts in other organs. In Chapter 4, I explored the hypothesis that pericytes are present within the human myocardium as multi-lineage mesodermal progenitors with tissue specificity. Immunohistochemistry showed that human adult and fetal cardiac microvascular pericytes express known pericyte markers *in situ*, including CD146, NG2, PDGFR-β, αSMA, and SM-MHC, but not CD117, CD133, and endothelial cell markers. Human heart cells were isolated from ventricular myocardial biopsies by mechanical dissociation and collagenase digestion and subsequently subjected to fluorescence-activated cell sorting (FACS) for purification. Using a combination of selective cell surface markers, including positive selection marker CD146 and negative selection markers: CD34, CD45, CD56, and CD117, we prospectively purified human heart pericytes (HPs) to homogeny. Sorted HPs ($CD146^{+}CD34^{-}CD45^{-}CD56^{-}CD117^{-}$) can be cultured in the long term and displayed morphological and proliferative profiles similar to skeletal muscle-derived pericytes (SkMPs). Cultured HPs consistently expressed CD146, NG2, αSMA, alkaline phosphatase (ALP), and notably PDGFR-α. When seeded in Matrigel cultures, HPs not only formed capillary-like networks alone but also tightly interact with endothelial cells in co-cultures to facilitate angiogenic network formation under ambient and low oxygen conditions, showing functional discreteness from SkMPs under hypoxia. HPs natively express classic MSC markers, including CD44, CD73, CD90, and CD105 and exhibited robust osteo-,

chondro-, and adipogenesis, but not skeletal myogenesis, in culture. No myotube formation or expression of fast skeletal myosin heavy chain was observed, suggesting tissue specificity of HPs, distinct from pericytes of other origins, in myogenesis.

Currently we are investigating the differential activation of myogenic genes in HPs after induction as well as the engraftment and cardiomyocyte differentiation of transplanted GFP-labeled HPs within the healthy and ischemic myocardium in immunodeficient mouse models. Further investigation of their differentiation into all cardiac cell lineages has been planned. Whether there exists a potential hierarchical relationship between heart pericytes and resident c-kit+ or Isl1+ cardiac stem cells remains unknown. It is also important to investigate the role of heart pericytes in supporting resident cardiac stem/progenitor cells.

To facilitate clinical translation of BVSCs for tissue repair and regeneration, I compared the myogenic efficiency of BVSC populations of different lineage, namely MECs and pericytes. MECs isolated from fresh human muscle biopsy exhibited the highest myogenic capacity in culture. In addition, I demonstrated that populations of BVSCs, such as MECs and pericytes, can be simultaneously purified by cell sorting from cryopreserved human primary skeletal muscle cell cultures (cryo-hPSMCs), a more clinically accessible cell source. MECs ($CD56^{+}$UEA-$1R^{+}CD146^{+}/CD45^{-}$) and pericytes ($CD146^{+}/CD45^{-}CD56^{-}$UEA-$1R^{-}$) retained their superior myogenic capacity in the injured mouse muscles. My findings suggest that long-term cryopreserved primary tissue/cell cultures can serve as a source of stem cells in the clinical setting. This new approach can be used to readily extract therapeutic stem cells from human muscle cells cryogenically banked for clinical purposes.

Currently I am expanding the research work described in Chapter 5 in to the following directions. First, I am investigating the difference(s) in the mechanisms, other than direct

myogenesis, which different BVSCs subsets utilize to promote repair/regeneration of the damaged skeletal muscle. Second, it is important to evaluate the efficiency of BVSCs subsets differentiating into other mesenchymal lineages such as osteogenesis and chondrogenesis. To facilitate the translational use of cryo-BVSCs subsets, we have planned to examine their repair/regenerative capacity in other animal disease models such as myocardial infarction and skull defect models.

BIBLIOGRAPHY

1. Peault, B., et al., *Stem and Progenitor Cells in Skeletal Muscle Development, Maintenance, and Therapy.* Mol Ther, 2007. **15**(5): p. 867-877.

2. Zuk, P.A., et al., *Human Adipose Tissue Is a Source of Multipotent Stem Cells.* Mol. Biol. Cell, 2002. **13**(12): p. 4279-4295.

3. Toma, J.G., et al., *Isolation of multipotent adult stem cells from the dermis of mammalian skin.* Nat Cell Biol, 2001. **3**(9): p. 778-84.

4. Choi, Y., et al., *Adult pancreas generates multipotent stem cells and pancreatic and nonpancreatic progeny.* Stem Cells, 2004. **22**(6): p. 1070-84.

5. Messina, E., et al., *Isolation and Expansion of Adult Cardiac Stem Cells From Human and Murine Heart.* Circulation Research, 2004. **95**(9): p. 911-921.

6. Hsu, Y.-C., Lee, D.-C., and Chiu, I.-M., *Neural Stem Cells, Neural Progenitors, and Neurotrophic Factors.* Cell Transplantation, 2007. **16**: p. 133-150.

7. Ballas, C.B., Zielske, S.P., and Gerson, S.L., *Adult bone marrow stem cells for cell and gene therapies: Implications for greater use.* Journal of Cellular Biochemistry, 2002. **85**(S38): p. 20-28.

8. Chao, H. and Hirschi, K.K., *Hemato-vascular origins of endothelial progenitor cells?* Microvascular Research, 2010. **79**(3): p. 169-173.

9. Tang, W., et al., *White Fat Progenitor Cells Reside in the Adipose Vasculature.* Science, 2008. **322**(5901): p. 583-586.

10. Gimble, J.M., Katz, A.J., and Bunnell, B.A., *Adipose-Derived Stem Cells for Regenerative Medicine.* Circulation Research, 2007. **100**(9): p. 1249-1260.

11. Jiang, Y., et al., *Pluripotency of mesenchymal stem cells derived from adult marrow.* Nature, 2002. **418**(6893): p. 41-49.

12. Minasi, M.G., et al., *The meso-angioblast: a multipotent, self-renewing cell that originates from the dorsal aorta and differentiates into most mesodermal tissues.* Development, 2002. **129**(11): p. 2773-2783.

13. Barry, F.P. and Murphy, J.M., *Mesenchymal stem cells: clinical applications and biological characterization.* Int J Biochem Cell Biol, 2004. **36**(4): p. 568-84.

14. Akar, A.R., et al., *Regenerative Medicine for Cardiovascular Disorders-New Milestones: Adult Stem Cells.* Artificial Organs, 2006. **30**(4): p. 213-232.

15. Segers, V.F.M. and Lee, R.T., *Stem-cell therapy for cardiac disease.* Nature, 2008. **451**(7181): p. 937-942.

16. Joggerst, S.J. and Hatzopoulos, A.K., *Stem cell therapy for cardiac repair: benefits and barriers.* Expert Reviews in Molecular Medicine, 2009. **11**: p. e20.

17. Chen, C.-W., et al., *Perivascular multi-lineage progenitor cells in human organs: Regenerative units, cytokine sources or both?* Cytokine & Growth Factor Reviews, 2009. **20**(5-6): p. 429-434.

18. Chien, K.R., Domian, I.J., and Parker, K.K., *Cardiogenesis and the complex biology of regenerative cardiovascular medicine.* Science, 2008. **322**(5907): p. 1494-7.

19. Salem, H.K. and Thiemermann, C., *Mesenchymal Stromal Cells: Current Understanding and Clinical Status.* Stem Cells, 2010. **28**(3): p. 585-596.

20. Karussis, D., et al., *Safety and Immunological Effects of Mesenchymal Stem Cell Transplantation in Patients With Multiple Sclerosis and Amyotrophic Lateral Sclerosis.* Arch Neurol, 2010. **67**(10): p. 1187-1194.

21. Locatelli, F., et al., *Stem cell therapy in stroke.* Cellular and Molecular Life Sciences, 2009. **66**(5): p. 757-772.

22. Ott, H.C., Davis, B.H., and Taylor, D.A., *Cell Therapy for Heart Failure—Muscle, Bone Marrow, Blood, and Cardiac-Derived Stem Cells.* Seminars in thoracic and cardiovascular surgery, 2005. **17**(4): p. 348-360.

23. Piepoli, M.F., *Transplantation of progenitor cells and regeneration of damaged myocardium: more facts or doubts? Insights from experimental and clinical studies.* Journal of Cardiovascular Medicine, 2009. **10**(8): p. 624-634 10.2459/JCM.0b013e328329ac77.

24. Sieveking, D.P. and Ng, M.K., *Cell therapies for therapeutic angiogenesis: back to the bench.* Vascular Medicine, 2009. **14**(2): p. 153-166.

25. Tavian, M., et al., *The Vascular Wall as a Source of Stem Cells.* Annals of the New York Academy of Sciences, 2005. **1044**(1): p. 41-50.

26. Crisan, M., et al., *A Perivascular Origin for Mesenchymal Stem Cells in Multiple Human Organs.* Cell Stem Cell, 2008. **3**(3): p. 301-313.

27. Kumar, V., Fausto, N., and Abbas, A., *Robbins & Cotran Pathologic Basis of Disease*. 7th ed. Blood Vessels2004, Philadelphia, PA: Saunders. Ch.11.

28. Tilki, D., et al., *Emerging biology of vascular wall progenitor cells in health and disease.* Trends in Molecular Medicine, 2009. **15**(11): p. 501-509.

29. Zengin, E., et al., *Vascular wall resident progenitor cells: a source for postnatal vasculogenesis.* Development, 2006. **133**(8): p. 1543-1551.

30. Armulik, A., Abramsson, A., and Betsholtz, C., *Endothelial/Pericyte Interactions.* Circ Res, 2005. **97**(6): p. 512-523.

31. Crocker, D.J., Murad, T.M., and Geer, J.C., *Role of the pericyte in wound healing - an ultrastructural study.* Experimental and Molecular Pathology, 1970(13): p. 51-65.

32. Andreeva, E.R., et al., *Continuous subendothelial network formed by pericyte-like cells in human vascular bed.* Tissue and Cell, 1998. **30**(1): p. 127-135.

33. von Tell, D., Armulik, A., and Betsholtz, C., *Pericytes and vascular stability.* Experimental Cell Research, 2006. **312**(5): p. 623-629.

34. Rucker, H.K., Wynder, H.J., and Thomas, W.E., *Cellular mechanisms of CNS pericytes.* Brain Research Bulletin, 2000. **51**(5): p. 363-369.

35. Dore-Duffy, P. and La Manna, J.C., *Physiologic Angiodynamics in the Brain.* Antioxidants & Redox Signaling, 2007. **9**(9): p. 1363-1372.

36. Kuhnert, F., et al., *Soluble receptor-mediated selective inhibition of VEGFR and PDGFRβ signaling during physiologic and tumor angiogenesis.* Proceedings of the National Academy of Sciences, 2008. **105**(29): p. 10185-10190.

37. Lindahl, P., et al., *Pericyte Loss and Microaneurysm Formation in PDGF-B-Deficient Mice.* Science, 1997. **277**(5323): p. 242-245.

38. Majesky, M.W., et al., *The adventitia: a dynamic interface containing resident progenitor cells.* Arteriosclerosis, Thrombosis, and Vascular Biology, 2011. **31**(7): p. 1530-1539.

39. Zimmerlin, L., et al., *Stromal vascular progenitors in adult human adipose tissue.* Cytometry A, 2010. **77**(1): p. 22-30.

40. Campagnolo, P., et al., *Human Adult Vena Saphena Contains Perivascular Progenitor Cells Endowed With Clonogenic and Proangiogenic Potential.* Circulation, 2010. **121**(15): p. 1735-1745.

41. Hu, Y., et al., *Abundant progenitor cells in the adventitia contribute to atherosclerosis of vein grafts in ApoE-deficient mice.* The Journal of Clinical Investigation, 2004. **113**(9): p. 1258-1265.

42. Hoshino, A., et al., *Human vascular adventitial fibroblasts contain mesenchymal stem/progenitor cells.* Biochemical and Biophysical Research Communications, 2008. **368**(2): p. 305-310.

43. Shi, Y., et al., *Adventitial Myofibroblasts Contribute to Neointimal Formation in Injured Porcine Coronary Arteries.* Circulation, 1996. **94**(7): p. 1655-1664.

44. Oparil, S., et al., *Estrogen attenuates the adventitial contribution to neointima formation in injured rat carotid arteries.* Cardiovascular Research, 1999. **44**(3): p. 608-614.

45. Zheng, B., et al., *Prospective identification of myogenic endothelial cells in human skeletal muscle.* Nat Biotech, 2007. **25**(9): p. 1025-1034.

46. Dellavalle, A., et al., *Pericytes of human skeletal muscle are myogenic precursors distinct from satellite cells.* Nat Cell Biol, 2007. **9**(3): p. 255-267.

47. Corselli, M., et al., *The tunica adventitia of human arteries and veins as a source of mesenchymal stem cells.* Stem Cells and Development, 2011. **21**(8): p. 1299-308.

48. Brighton, C.T., et al., *The pericyte as a possible osteoblast progenitor cell.* Clin Orthop Relat Res., 1992(275): p. 287-99.

49. Doherty, M.J., et al., *Vascular Pericytes Express Osteogenic Potential In Vitro and In Vivo.* Journal of Bone and Mineral Research, 1998. **13**(5): p. 828-838.

50. Farrington-Rock, C., et al., *Chondrogenic and Adipogenic Potential of Microvascular Pericytes.* Circulation, 2004. **110**(15): p. 2226-2232.

51. Hu, Y. and Xu, Q., *Adventitial Biology: Differentiation and Function.* Arteriosclerosis, Thrombosis, and Vascular Biology, 2011. **31**(7): p. 1523-1529.

52. Okada, M., et al., *Myogenic Endothelial Cells Purified From Human Skeletal Muscle Improve Cardiac Function After Transplantation Into Infarcted Myocardium.* Journal of the American College of Cardiology, 2008. **52**(23): p. 1869-1880.

53. Dellavalle, A., et al., *Pericytes resident in postnatal skeletal muscle differentiate into muscle fibres and generate satellite cells.* Nat Commun, 2011. **2**: p. 499.

54. He, W., et al., *Pericyte-based human tissue engineered vascular grafts.* Biomaterials, 2010. **31**(32): p. 8235-8244.

55. Chen, C.-W., et al., *Purified Human Muscle-derived Pericytes Support Formation of Vascular Structures and Promote Angiogenesis After Myocardial Infarction.* Circulation, 2009. **120**: p. S1053.

56. Katare, R., et al., *Transplantation of Human Pericyte Progenitor Cells Improves the Repair of Infarcted Heart Through Activation of an Angiogenic Program Involving*

Micro-RNA-132 / Novelty and Significance. Circulation Research, 2011. **109**(8): p. 894-906.

57. Gauvin, R., et al., *Mechanical Properties of Tissue-Engineered Vascular Constructs Produced Using Arterial or Venous Cells.* Tissue Engineering Part A, 2011. **0**(0): p. null.

58. Pevsner-Fischer, M., Levin, S., and Zipori, D., *The Origins of Mesenchymal Stromal Cell Heterogeneity.* Stem Cell Reviews and Reports, 2011: p. 1-9.

59. Guilak, F., et al., *Clonal analysis of the differentiation potential of human adipose-derived adult stem cells.* Journal of Cellular Physiology, 2006. **206**(1): p. 229-237.

60. Caplan, A.I., *All MSCs Are Pericytes?* Cell Stem Cell, 2008. **3**(3): p. 229-230.

61. Sacchetti, B., et al., *Self-Renewing Osteoprogenitors in Bone Marrow Sinusoids Can Organize a Hematopoietic Microenvironment.* Cell, 2007. **131**(2): p. 324-336.

62. Tormin, A., et al., *CD146 expression on primary nonhematopoietic bone marrow stem cells is correlated with in situ localization.* Blood, 2011. **117**(19): p. 5067-5077.

63. Feng, J., et al., *Dual origin of mesenchymal stem cells contributing to organ growth and repair.* Proceedings of the National Academy of Sciences, 2011. **108**(16): p. 6503-6508.

64. Tedesco, F.S., et al., *Repairing skeletal muscle: regenerative potential of skeletal muscle stem cells.* The Journal of Clinical Investigation, 2010. **120**(1): p. 11-19.

65. American Heart Association, *Heart Disease and Stroke Statistics - 2010 Update.* Circulation, 2010. **121**: p. e1-e170.

66. Kumar, V., Fausto, N., and Abbas, A., *Robbins & Cotran Pathologic Basis of Disease*. 7th ed. Peripheral Nerve and Skeletal Muscle2004, Philadelphia, PA: Saunders. Ch.27.

67. Tsonis, P.A., *Regenerative biology: the emerging field of tissue repair and restoration.* Differentiation, 2002. **70**(8): p. 397-409.

68. Orlic, D., Hill, J.M., and Arai, A.E., *Stem Cells for Myocardial Regeneration.* Circ Res, 2002. **91**(12): p. 1092-1102.

69. Sakai, T., et al., *The Use of Ex Vivo Gene Transfer Based on Muscle-Derived Stem Cells for Cardiovascular Medicine.* Trends in Cardiovascular Medicine, 2002. **12**(3): p. 115-120.

70. Paul, D., Samuel, S.M., and Maulik, N., *Mesenchymal Stem Cell: Present Challenges and Prospective Cellular Cardiomyoplasty Approaches for Myocardial Regeneration.* Antioxidants & Redox Signaling, 2009. **11**(8): p. 1841-1855.

71. Drowley, L., et al., *Cellular Antioxidant Levels Influence Muscle Stem Cell Therapy.* Mol Ther, 2010. **18**(10): p. 1865-1873.

72. Caplan, A.I. and Dennis, J.E., *Mesenchymal stem cells as trophic mediators.* Journal of Cellular Biochemistry, 2006. **98**(5): p. 1076-1084.

73. Fraser, J.K., et al., *Adult stem cell therapy for the heart.* Int J Biochem Cell Biol., 2004. **36**(4): p. 658-66.

74. Mazhari, R. and Hare, J.M., *Mechanisms of action of mesenchymal stem cells in cardiac repair: potential influences on the cardiac stem cell niche.* Nat Clin Pract Cardiovasc Med, 2007. **4**(SUPPLEMENT 1): p. S21-6.

75. Mazhari, R. and Hare, J.M., *Advances in Cell-Based Therapy for Structural Heart Disease* Progress in Cardiovascular Diseases 2007. **49**(6): p. 387-95.

76. Ohnishi, S. and Nagaya, N., *Prepare Cells to Repair the Heart: Mesenchymal Stem Cells for the Treatment of Heart Failure.* Am J Nephrol., 2007. **27**(3): p. 301-7.

77. Madonna, R. and De Caterina, R., *Adipose tissue: a new source for cardiovascular repair.* Journal of Cardiovascular Medicine, 2010. **11**(2): p. 71-80 10.2459/JCM.0b013e328330e9be.

78. Orlic, D., et al., *Bone marrow cells regenerate infarcted myocardium.* Nature, 2001. **410**(6829): p. 701-705.

79. Wang, F. and Guan, J., *Cellular cardiomyoplasty and cardiac tissue engineering for myocardial therapy.* Advanced Drug Delivery Reviews, 2010. **62**(7-8): p. 784-797.

80. Song, H., et al., *Modification of mesenchymal stem cells for cardiac regeneration.* Expert Opin Biol Ther, 2010. **10**(3): p. 309-19.

81. Davani, S., et al., *Can stem cells mend a broken heart?* Cardiovascular Research, 2005. **65**(2): p. 305-316.

82. Matsuura K, Wada H, Nagai T, Iijima Y, Minamino T, Sano M, Akazawa H, Molkentin JD, Kasanuki H, Komuro I, *Cardiomyocytes fuse with surrounding noncardiomyocytes and reenter the cell cycle.* J Cell Biol., 2004. **167**(2): p. 351-63.

83. Oshima, H., et al., *Differential myocardial infarct repair with muscle stem cells compared to myoblasts.* Mol Ther, 2005. **12**(6): p. 1130-41.

84. Payne, T.R., et al., *A Relationship Between Vascular Endothelial Growth Factor, Angiogenesis, and Cardiac Repair After Muscle Stem Cell Transplantation Into Ischemic Hearts.* Journal of the American College of Cardiology, 2007. **50**(17): p. 1677-1684.

85. Gnecchi, M., et al., *Paracrine Mechanisms in Adult Stem Cell Signaling and Therapy.* Circ Res, 2008. **103**(11): p. 1204-1219.

86. Ohnishi, S., et al., *Effect of Hypoxia on Gene Expression of Bone Marrow-Derived Mesenchymal Stem Cells and Mononuclear Cells.* Stem Cells, 2007. **25**(5): p. 1166-1177.

87. Chen, S.-l., et al., *Effect on left ventricular function of intracoronary transplantation of autologous bone marrow mesenchymal stem cell in patients with acute myocardial infarction.* The American Journal of Cardiology, 2004. **94**(1): p. 92-95.

88. Hare, J.M., et al., *A Randomized, Double-Blind, Placebo-Controlled, Dose-Escalation Study of Intravenous Adult Human Mesenchymal Stem Cells (Prochymal) After Acute Myocardial Infarction.* J Am Coll Cardiol, 2009. **54**(24): p. 2277-2286.

89. Lee, J.S., et al., *A Long-Term Follow-Up Study of Intravenous Autologous Mesenchymal Stem Cell Transplantation in Patients With Ischemic Stroke.* STEM CELLS, 2010. **28**(6): p. 1099-1106.

90. Vanikar, A.V., et al., *Cotransplantation of Adipose Tissue-Derived Insulin-Secreting Mesenchymal Stem Cells and Hematopoietic Stem Cells: A Novel Therapy for Insulin-Dependent Diabetes Mellitus.* Stem Cells Int., 2010. **2010: 582382**.

91. Matthay, M.A., et al., *Therapeutic Potential of Mesenchymal Stem Cells for Severe Acute Lung Injury*. Chest, 2010. **138**(4): p. 965-972.

92. Chavakis, E., Koyanagi, M., and Dimmeler, S., *Enhancing the Outcome of Cell Therapy for Cardiac Repair: Progress From Bench to Bedside and Back.* Circulation, 2010. **121**(2): p. 325-335.

93. Heeschen, C., et al., *Profoundly Reduced Neovascularization Capacity of Bone Marrow Mononuclear Cells Derived From Patients With Chronic Ischemic Heart Disease.* Circulation, 2004. **109**(13): p. 1615-1622.

94. Dimmeler, S., Zeiher, A.M., and Schneider, M.D., *Unchain my heart: the scientific foundations of cardiac repair*. The Journal of Clinical Investigation, 2005. **115**(3): p. 572-583.

95. Ballard VLT, Edelberg JM, *Stem Cells and the Regeneration of the Aging Cardiovascular System.* Circ. Res., 2007(100): p. 1116-27.

96. Bergmann, O., et al., *Evidence for Cardiomyocyte Renewal in Humans.* Science, 2009. **324**(5923): p. 98-102.

97. Xiang, G., et al., *Lentivirus-mediated Wnt11 Gene Transfer Enhances Cardiomyogenic Differentiation of Skeletal Muscle-derived Stem Cells.* Mol Ther, 2011.

98. Shimizu, T., et al., *Fabrication of Pulsatile Cardiac Tissue Grafts Using a Novel 3-Dimensional Cell Sheet Manipulation Technique and Temperature-Responsive Cell Culture Surfaces.* Circ Res, 2002. **90**(3): p. e40-48.

99. Bonaros, N., et al., *Enhanced Cell Therapy for Ischemic Heart Disease.* Transplantation, 2008. **86**(9): p. 1151-1160 10.1097/TP.0b013e3181880f9e.

100. Chavakis, E., Urbich, C., and Dimmeler, S., *Homing and engraftment of progenitor cells: A prerequisite for cell therapy.* Journal of Molecular and Cellular Cardiology, 2008. **45**(4): p. 514-522.

101. Pittenger, M.F., et al., *Multilineage potential of adult human mesenchymal stem cells.* Science, 1999. **284**(5411): p. 143-7.

102. Jiang, Y., et al., *Multipotent progenitor cells can be isolated from postnatal murine bone marrow, muscle, and brain.* Experimental Hematology, 2002. **30**(8): p. 896-904.

103. Zuk, P.A., et al., *Multilineage Cells from Human Adipose Tissue: Implications for Cell-Based Therapies.* Tissue Engineering, 2001. **7**(2): p. 211-228.

104. Oberlin, E., et al., *Blood-forming potential of vascular endothelium in the human embryo.* Development, 2002. **129**(17): p. 4147-57.

105. Kokkalis, Z.T., Jain, S., and Sotereanos, D.G., *Vein wrapping at cubital tunnel for ulnar nerve problems.* Journal of Shoulder and Elbow Surgery, 2010. **19**(2, Supplement 1): p. 91-97.

106. Shi S, Gronthos S, *Perivascular niche of postnatal mesenchymal stem cells in human bone marrow and dental pulp.* J Bone Miner Res., 2003. **18**(4): p. 696-704.

107. Roger, V.L., et al., *Heart Disease and Stroke Statistics—2012 Update.* Circulation, 2012. **125**(1): p. e2-e220.

108. Kumar, V., Fausto, N., and Abbas, A., *Robbins & Cotran Pathologic Basis of Disease*. 7th ed. Ch.12 The Heart2004, Philadelphia, PA: Saunders.

109. Hansson, E.M., Lindsay, M.E., and Chien, K.R., *Regeneration Next: Toward Heart Stem Cell Therapeutics.* Cell Stem Cell, 2009. **5**(4): p. 364-377.

110. Menasche, P., *Cardiac cell therapy: Lessons from clinical trials.* Journal of Molecular and Cellular Cardiology, 2011. **50**(2): p. 258-265.

111. Janssens, S., *Stem Cells in the Treatment of Heart Disease.* Annual Review of Medicine, 2010. **61**(1): p. 287-300.

112. Montemurro, T., et al., *Differentiation and migration properties of human foetal umbilical cord perivascular cells: potential for lung repair.* Journal of Cellular and Molecular Medicine, 2011. **15**(4): p. 796-808.

113. Park, T.S., et al., *Placental Perivascular Cells for Human Muscle Regeneration.* Stem Cells and Development, 2011. **20**(3): p. 451-463.

114. Tottey, S., et al., *Extracellular Matrix Degradation Products and Low-Oxygen Conditions Enhance the Regenerative Potential of Perivascular Stem Cells.* Tissue Engineering Part A, 2011. **17**(1-2): p. 37-44.

115. Corselli, M., et al., *Perivascular ancestors of adult multipotent stem cells.* Arterioscler Thromb Vasc Biol, 2010. **30**(6): p. 1104-9.

116. Renault, M.-A. and Losordo, D.W., *Therapeutic myocardial angiogenesis.* Microvascular Research, 2007. **74**(2-3): p. 159-171.

117. Saunders, W.B., et al., *Coregulation of vascular tube stabilization by endothelial cell TIMP-2 and pericyte TIMP-3.* The Journal of Cell Biology, 2006. **175**(1): p. 179-191.

118. Au, P., et al., *Bone marrow–derived mesenchymal stem cells facilitate engineering of long-lasting functional vasculature.* Blood, 2008. **111**(9): p. 4551-4558.

119. Frangogiannis, N.G., *The immune system and cardiac repair.* Pharmacological Research, 2008. **58**(2): p. 88-111.

120. Berry, M.F., et al., *Mesenchymal stem cell injection after myocardial infarction improves myocardial compliance.* Am J Physiol Heart Circ Physiol, 2006. **290**(6): p. H2196-2203.

121. Pittenger, M.F. and Martin, B.J., *Mesenchymal Stem Cells and Their Potential as Cardiac Therapeutics.* Circ Res, 2004. **95**(1): p. 9-20.

122. Ohnishi, S., et al., *Mesenchymal stem cells attenuate cardiac fibroblast proliferation and collagen synthesis through paracrine actions.* FEBS Letters, 2007. **581**(21): p. 3961-3966.

123. Mias, C., et al., *Mesenchymal stem cells promote matrix metalloproteinase secretion by cardiac fibroblasts and reduce cardiac ventricular fibrosis after myocardial infarction.* Stem Cells, 2009. **27**(11): p. 2734-43.

124. Ghannam, S., et al., *Immunosuppression by mesenchymal stem cells: mechanisms and clinical applications.* Stem Cell Res Ther, 2010. **1**(1): p. 2.

125. Shi, Y., et al., *Mesenchymal stem cells: a new strategy for immunosuppression and tissue repair.* Cell Res, 2010. **20**(5): p. 510-8.

126. Enciso, J.M. and Hirschi, K.K., *Understanding Abnormalities in Vascular Specification and Remodeling.* Pediatrics, 2005. **116**(1): p. 228-230.

127. Ohnishi, S., et al., *Transplantation of mesenchymal stem cells attenuates myocardial injury and dysfunction in a rat model of acute myocarditis.* Journal of Molecular and Cellular Cardiology, 2007. **42**(1): p. 88-97.

128. Nemeth, K., et al., *Bone marrow stromal cells attenuate sepsis via prostaglandin E(2)-dependent reprogramming of host macrophages to increase their interleukin-10 production.* Nat Med, 2009. **15**(1): p. 42-9.

129. Liu, X., et al., *Heme oxygenase-1 (HO-1) inhibits postmyocardial infarct remodeling and restores ventricular function.* Faseb J, 2006. **20**(2): p. 207-16.

130. Ren, G., et al., *Species variation in the mechanisms of mesenchymal stem cell-mediated immunosuppression.* Stem Cells, 2009. **27**(8): p. 1954-62.

131. Abarbanell, A.M., et al., *Proinflammatory cytokine effects on mesenchymal stem cell therapy for the ischemic heart.* Ann Thorac Surg, 2009. **88**(3): p. 1036-43.

132. Beltrami, A.P., et al., *Adult Cardiac Stem Cells Are Multipotent and Support Myocardial Regeneration.* Cell, 2003. **114**(6): p. 763-776.

133. Urbanek, K., et al., *Myocardial regeneration by activation of multipotent cardiac stem cells in ischemic heart failure.* Proceedings of the National Academy of Sciences of the United States of America, 2005. **102**(24): p. 8692-8697.

134. Kajstura, J., et al., *Cardiomyogenesis in the Adult Human Heart.* Circulation Research, 2010. **107**(2): p. 305-315.

135. Parmacek, M.S. and Epstein, J.A., *Cardiomyocyte Renewal.* New England Journal of Medicine, 2009. **361**(1): p. 86-88.

136. Gaengel, K., et al., *Endothelial-Mural Cell Signaling in Vascular Development and Angiogenesis.* Arterioscler Thromb Vasc Biol, 2009. **29**(5): p. 630-638.

137. Montemurro, T., et al., *Differentiation and migration properties of human fetal umbilical cord perivascular cells: potential for lung repair.* J Cell Mol Med, 2010.

138. Sims, D.E., *Diversity within pericytes.* Clin Exp Pharmacol Physiol., 2000. **27**(10): p. 842-6.

139. Bolli, R., et al., *Cardiac stem cells in patients with ischaemic cardiomyopathy (SCIPIO): initial results of a randomised phase 1 trial.* The Lancet, 2011. **378**(9806): p. 1847-1857.

140. Makkar, R.R., et al., *Intracoronary cardiosphere-derived cells for heart regeneration after myocardial infarction (CADUCEUS): a prospective, randomised phase 1 trial.* The Lancet, 2012. **379**(9819): p. 895-904.

141. Ptaszek, L.M., et al., *Towards regenerative therapy for cardiac disease.* The Lancet, 2012. **379**(9819): p. 933-942.

142. Krautler, Nike J., et al., *Follicular Dendritic Cells Emerge from Ubiquitous Perivascular Precursors.* Cell, 2012. **150**(1): p. 194-206.

143. Dar, A., et al., *Multipotent Vasculogenic Pericytes from Human Pluripotent Stem Cells Promote Recovery of Murine Ischemic Limb.* Circulation, 2011.

144. Jankowski, R.J., Deasy, B.M., and Huard, J., *Muscle-derived stem cells.* Gene Ther., 2002. **9**(10): p. 642-7.

145. Collins, C.A., et al., *A Population of Myogenic Stem Cells That Survives Skeletal Muscle Aging.* STEM CELLS, 2007. **25**(4): p. 885-894.

146. Pisani, D.F., et al., *Isolation of a highly myogenic CD34-negative subset of human skeletal muscle cells free of adipogenic potential.* Stem Cells, 2010. **28**(4): p. 753-64.

147. Torrente, Y., et al., *Autologous Transplantation of Muscle-Derived CD133 Stem Cells in Duchenne Muscle Patients.* Cell Transplantation, 2007. **16**: p. 563-577.

148. Carr LK, Steele D, Steele S, Wagner D, Pruchnic R, Jankowski R, Erickson J, Huard J, Chancellor MB, *1-year follow-up of autologous muscle-derived stem cell injection pilot study to treat stress urinary incontinence.* Int Urogynecol J Pelvic Floor Dysfunct., 2008. **19**(6): p. 881-3.

149. Rousseau, J., et al., *Dystrophin Expression Following the Transplantation of Normal Muscle Precursor Cells Protects mdx Muscle From Contraction-Induced Damage.* Cell Transplantation, 2010. **19**(5): p. 589-596.

150. Seidel M, et al., *Cell-based therapy for heart failure: skeletal myoblasts.* Cell Transplant., 2009. **18**(7): p. 695-707.

151. Sherman W, et al., *Myoblast transfer in ischemic heart failure: effects on rhythm stability.* Cell Transplant., 2009. **18**(3): p. 333-41.

152. Drowley L, et al., *Sex of muscle stem cells does not influence potency for cardiac cell therapy.* Cell Transplant., 2009. **18**(10): p. 1137-46.

153. Zheng, B.L., G., et al., *Identification of CD56+CD146+UEA-1+ Cell Population within Cryopreserved Human Skeletal Muscle Cells which Endowed with a High Myogenic Potential in vivo*, in *The Orthopaedic Research Society (ORS) 54th Annual Meeting*2008: San Francisco, CA.

154. Sherwood, R.I., et al., *Isolation of Adult Mouse Myogenic Progenitors: Functional Heterogeneity of Cells within and Engrafting Skeletal Muscle.* Cell, 2004. **119**(4): p. 543-554.

155. Cerletti, M., et al., *Highly Efficient, Functional Engraftment of Skeletal Muscle Stem Cells in Dystrophic Muscles.* Cell, 2008. **134**(1): p. 37-47.

156. Hirt-Burri, N., et al., *Human muscular fetal cells: a potential cell source for muscular therapies* Pediatric Surgery International, 2008. **24**(1): p. 37-47.